# Development of a Quantitative Health Index and Diagnostic Method for Efficient Asset Management of Power Transformers

Md Mominul Islam

This thesis is presented for the degree of
Doctor of Philosophy at the
School of Engineering and Information Technology


Murdoch University

**August 2017**

Perth, Australia

# Copyrights

# Abstract

Power transformers play a very important role in electrical power networks and are frequently operated longer than their expected design life. Therefore, to ensure their best operating performance in a transmission network, the fault condition of each transformer must be assessed regularly. For an accurate fault diagnosis, it is important to have maximum information about an individual transformer based on unbiased measurements. This can best be achieved using artificial intelligence (AI) that can systematically analyse the complex features of diagnostic measurements.

Clustering techniques are a form of AI that is particularly well suited to fault diagnosis. To provide an assessment of transformers, a hybrid k-means algorithm, and probabilistic Parzen window estimation are used in this research. The clusters they form are representative of a single or multiple fault categories. The proposed technique computes the maximum probability of transformers in each cluster to determine their fault categories.

The main focus of this research is to determine a quantitative health index (HI) to characterize the operating condition of transformers. Condition assessment tries to detect incipient faults before they become too serious, which requires a sensitive and quantified approach. Therefore, the HI needs to come from a proportionate system that can estimate health condition of transformers over time. To quantify this condition, the General Regression Neural Network (GRNN), a type of AI, has been chosen in this research. The GRNN works well with small sets of training data and avoids the needs to estimate large sets of model parameters, following a largely non-parametric approach. The methodology used here regards transformers as a collection of subsystems and summarizes their individual condition into a quantified HI based on the existing agreed benchmarks drawn from IEEE and CIGRE standards. To better calibrate the HI, it may be mapped to a failure probability estimate for each transformer over the coming year. Experimental results of the research show that the proposed methods are more effective than previously published approaches when

diagnosing critical faults. Moreover, this novel HI approach can provide a comprehensive assessment of transformers based on the actual condition of their individual subsystems.

## Declaration

*I declare that this thesis is my own account of research and contains as its main content work which has not previously been submitted for a degree at any other university or institution.*

.....

**(Md Mominul Islam)**

# Table of Contents

## Chapter 2: A Review of Condition Monitoring and Diagnostic Tests for Life Time Estimation of Power Transformers

## Chapter 3: A Nearest Neighbour Clustering Approach for Incipient Fault Diagnosis of Power Transformers

## Chapter 4: Application of Parzen Window Estimation for Incipient Fault Diagnosis in Power Transformers



## Chapter 5: Missing Measurement Estimation of Power Transformers Using a GRNN.

## Chapter 6: Application of a General Regression Neural Network for Health Index Calculation of Power Transformers

## Chapter 7: Calculating a Health Index for Power Transformers Using a Subsystem-based GRNN Approach

## Chapter 8: Summary and Future Directions.

# List of Tables

# List of Figures

# List of Abbreviations and Symbols

| | |
|---|---|
| AC | Alternating Current |
| AE | Acoustic Emission |
| AHED | Arcing-High-Energy Discharge |
| AI | Artificial Intelligence |
| AMHA | Asset-management and Health Assessment Consulting Company |
| ANNs | Artificial Neural Networks |
| BLR | Binary Logistic Regression |
| CIGRE | International Council on Large Electric Systems |
| DBS | Dibenzyl-disulfide |
| DBV | Dielectric Breakdown Voltage |
| DC | Direct Current |
| DDF | Dielectric Dissipation Factor |
| DGA | Dissolved Gas Analysis |
| DP | Degree of Polymerization |
| DRA | Dielectric Response Analysis |
| DTM | Duval's Triangle Method |
| ELM | Extreme Learning Machines |
| EM | Expectation Maximization |
| FDR | Frequency Dielectric Response |
| GC | Gas Chromatography |
| GPC | Gel Permeation Chromatography |
| GRNN | General Regression Neural Network |

| | |
|---|---|
| HFCT | High Frequency Current Transformer |
| HI | Health Index |
| HPLC | High Performance Liquid Chromatography |
| HST | Hot Spot Temperature |
| HV | High Voltage |
| IEC | International Electrotechnical Commission |
| IEEE | Institute of Electrical and Electronics Engineers |
| IFT | Interfacial Tension |
| IGRNN | Incremental General Regression Neural Network |
| IR | Insulation Resistance |
| KFT | Karl Fischer Titration |
| KGA | Key Gas Analysis |
| KMA | k-Means Algorithm |
| KMC | k-Means Clustering |
| KNN | k-Nearest Neighbour |
| kV | kilo Volts |
| LEDA | Low-Energy Density Arcing |
| LBG | Linde-Buzo-Gray Algorithm |
| LTC | Load Tap Changer |
| LTT | Low Temperature Thermal |
| LV | Low Voltage |
| MAR | Missing at Random |
| MC | Mass Chromatography |
| NNCA | Nearest Neighbour Clustering Approach |
| PD | Partial Discharge |

| | |
|---|---|
| PDC | Polarization and Depolarization Current |
| PDF | Probability Density Function |
| PF | Power Factor |
| PI | Polarization Index |
| ppm | Parts per million |
| PW | Parzen Windows |
| OLTC | On Load Tap Changer |
| FDR | Frequency Dielectric Response |
| RRM | Roger's Ratios Method |
| RS | Rough Sets |
| RV | Recovery Voltage |
| RVM | Recovery Voltage Measurement |
| SaE-ELM | Self-Adaptive Evolutionary Extreme Learning Machine |
| SCI | Short Circuit Impedance |
| SFRA | Sweep Frequency Response Analysis |
| SVMs | Support Vector Machines |
| TCG | Total Combustible Gases |
| TDCG | Total Dissolved Combustible Gas |
| TF | Transfer Function |
| TTR | Turn Ratio of Transformers |
| UHF | Ultra-High Frequency |
| $C_0$ | Geometric Capacitance |
| $\Sigma$ | Multivariate Covariance |
| $\sigma$ | Composite Conductivity |
| $\epsilon_0$ | Vacuum Permittivity |

# List of Publications

## Journal Papers

- M.M. Islam, G. Lee and S.N. Hettiwatte, A nearest neighbour clustering approach for incipient fault diagnosis of power transformers, Electrical Engineering, vol. 99, pp. 1109-1119, 2016.
- M.M. Islam, G. Lee, S.N. Hettiwatte, A Review of Condition Monitoring Techniques and Diagnostic Tests for Life Time Estimation of Power Transformers, Electrical Engineering, **DOI:**10.1007/s00202-017-0532-4, pp. 1-25, 2017.
- M.M. Islam, G. Lee and S.N. Hettiwatte, Application of a GRNN for Health Index Calculation of Power Transformers- International Journal of Electrical Power and Energy Systems, vol. 93, pp. 308-315, 2017.
- M.M. Islam, G. Lee and S.N. Hettiwatte, Calculating a Health Index for Power Transformers Using a Subsystem-based GRNN Approach, IEEE Transactions on Power Delivery**, DOI:** 10.1109/TPWRD. 2017.2770166.
- M.M. Islam, G. Lee and S.N. Hettiwatte, Application of Parzen Window Estimation for Incipient Fault Diagnosis in Power Transformers, Electric Power Components and Systems - **Under Review**.

## Conference Papers

- M.M.Islam, G. Lee, and S.N. Hettiwatte, Incipient fault diagnosis in power transformers by clustering and adapted KNN, Australasian Universities Power Engineering Conference (AUPEC), **DOI:** 10.1109/AUPEC.2016.7749387.
- M.M. Islam, G. Lee and S.N. Hettiwatte, Missing Measurement Estimation of Power Transformers using a General Regression Neural Network , Australasian Universities Power Engineering Conference (AUPEC), 2017- **Accepted.**

# Acknowledgements

I am very grateful to my lovely wife Farhana, son Faiyaz and daughter Manha for their encouragement and inspiration throughout my journey towards achieving my Ph.D. degree. This research presented in this thesis would not have been possible without your sacrifice and continuous support.

I would like to express my sincere gratitude to my principal supervisor Dr Gareth Lee for his ongoing support, guidance, and inspiration throughout my research project. You have given me the opportunity to experience the new field of research that I am interested in by providing the clues and assistance to realize the concept. Thank you for guiding me to pursue the alternative ways. I would also like to thank my secondary supervisor Dr Sujeewa Hettiwatte for his continuous technical support and constructive feedback throughout my Ph.D. program.

I would like to acknowledge the contribution of Kerry Williams and Emanuel Santos for their continuous technical support, giving access and permission to use their transformers data in this research work.

Also, I would like to thank Murdoch University for the Maintenance Funds for the Conference Travel. I would also like to give special thanks to my colleagues and friends Dr Mohammad Mahbubur Rahman, Dr Mohammad Kabir Uddin, Brother Khalil Ibrahim, Ehsan, and Muktadir, for their support in different aspects of my candidature, especially in the thesis writing.

Finally, I would like to extend special thanks to my parents-in-law for their encouragement and the support of my family.

# Chapter 1: General Introduction and Overview of Thesis

## 1.1 Introduction

Power transformers are the most expensive and strategic devices in a power transmission and distribution network. They play a significant role in the transmission of power from generation points to the end users [1-2]. It is expected that asset managers will keep these expensive devices functional continuously throughout their service life without any unscheduled outages. Maintenance of a power transformer can be costly and time-consuming. Moreover, a sudden failure can make the maintenance expense even greater than the allocated budget due to associated repair and replacement costs. Therefore, to ensure uninterrupted power supply and avoid catastrophic failure of a power transformer, both fault diagnosis, and condition monitoring are very important to utilities. A number of different off-line and on-line techniques are currently used to detect faults in transformers and to monitor the progressive degradation of their insulation, core, windings, tap changer and bushings [2]. Most of them are based on the concentration of dissolved gases and various by-products produced from the degradation of insulation. As the opening of transformers is mostly impractical, the gas concentrations and other byproducts are used as a secondary evidence to diagnose the faults without disconnecting them from service. Each of the available methods has some limitations to diagnose faults. Therefore, utility experts are dependent on multiple parallel approaches to classify the actual faulty category of a transformer. To overcome the shortcomings of existing techniques, it becomes necessary to develop a reliable fault diagnostic and condition monitoring method. This project is concerned with the limitation of existing fault diagnosis, condition monitoring and failure probability estimation techniques of transformers. Therefore, the fundamental research question of the thesis is chosen as: *Can the application of artificial intelligence and machine learning techniques estimate the missing measurements of transformers, improve their fault diagnosis*

*techniques, quantify actual operating state and estimate the failure probability based on their condition as a function of time?* It is expected that improvements to existing methods can help to setup an appropriate maintenance strategy that can minimize the operational risk while maximizing operating efficiency and service life [2-3].

## 1.2 Objectives of the Study

Current fault diagnostic techniques are mostly dependent on the ratio and proportion of different gases that dissolve in the transformer oil. One of the widely accepted diagnostic methods is the family of Duval triangles where combustible hydrocarbon gases represent the three axes of a triangular graph. Each triangle is sub-divided into different regions, associated with a specific transformer fault. However, the boundaries of the graphical Duval triangles and the ranges of different ratio approach for fault diagnosis are not absolute. They are all changing over time based on the accumulated evidence and practical experience [4]. There are also growing concerns from transformer experts' regarding the quantification process of various routine and diagnostic tests of transformers into a measurable index so that maintenance decision can be made by looking at the single index value. Therefore, a detailed, comprehensive study was required to improve the accuracy of condition monitoring and fault diagnostic techniques.

Given the research questions in the previous section, a framework was developed with six objectives that will answer all of them. To achieve the goals, measurements from more than 350 power transformers operated by a utility company in Australia are used in this research. A comprehensive study and analysis will be seen in this report based on the collected field measurements. The main objectives of this research can be summarized as follows:

i. Identify the limitations of existing condition monitoring techniques and diagnostic tests of power transformers.

ii. Develop a fault diagnostic method to improve the fault classification accuracy of power transformers.
iii. Investigate the correlation between different routine and diagnostic measurement.
iv. Estimate missing values in multidimensional vectors based on the complete set of correlated vector measurements of transformers.
v. Develop a quantitative health index for condition assessment of power transformers.
vi. Estimate the failure probability of an individual transformer over time based on its calculated health index.

In this thesis, a comprehensive literature review was conducted to understand the limitations of existing diagnostic and condition monitoring techniques of transformers using relevant international standards and common industrial practices. In this project, a hybrid clustering and a probabilistic Parzen window function were used to improve the diagnostic techniques and faults classification. If transformer health is to be quantified, it is essential to evaluate the operating condition of its subsystems and explore the correlation of different measurements. The quantified condition index, based on diagnostic tests, tries to detect incipient faults in transformers before they became too severe and may be used to estimate its failure probability as a function of operating age. Moreover, a General Regression Neural Network was also adapted to estimate the missing measurements of transformers that are critical to making a decision on asset management and scheduling their maintenance.

## 1.3 Fault Diagnosis

The dielectric properties of insulating oil and paper used in a transformer changes with the increase of its operating age. Therefore, ageing of this insulation over time is inevitable. However, a proper maintenance plan can reduce the degradation rate and

help to increase the service life of these valuable assets. A transformer may need to handle several faults and variable stresses throughout its service life that may degrade its insulation and other ancillary components. The degraded insulation reacts with moisture and polar contaminants to produce different gases and chemical compounds such as acid and the derivatives of furan. At higher operating temperatures, and in the presence of moisture, the production rate of these by-products is increases. Over time, most of them are partially dissolved in the insulating oil, and they carry valuable information about a transformer's internal condition. Therefore, oil samples from the main tank of transformers are periodically collected to measure the concentrations of the dissolved materials as evidence for diagnosing fault classes.

The concentration of dissolved gases in a transformer's oil increases over time. The relative percentages of the dissolved combustible gases are directly correlated with different fault conditions. Therefore, to analyze the concentration of the gases, several standard techniques such as the family of Duval triangles and ratio approaches like Key Gas, Roger's Ratios, Doernenburg and the IEC method are currently available [4-6]. All the ratio methods are based on the practical experience of experts, and there is no direct way to express them using a mathematical formula. They can only give a valid diagnosis if some of the gas concentrations exceed certain thresholds [5]. Moreover, in some cases, the gas ratios may fall outside the boundaries of predefined ranges and remain unclassified. To overcome the shortcomings of these existing methods, a novel hybrid clustering approach with the combination of k-means, k-nearest neighbors, and the Linde-Buzo-Gray (LBG) algorithm was developed during this research. The method forms the clusters with multidimensional measured vectors in a high dimensional space in such a way that each group may contain a single or multiple types of faulty transformers with different distinguishable percentages. To take the opinion of neighbors, the measured vectors are indexed based on distances from the center of three closest clusters. Therefore, each of them could vote for a single or multiple faulty classes. The cumulative votes are added together to make the decision on the fault category of

transformers. In a later stage, another fault diagnostic technique is introduced using a probabilistic Parzen window (PW) estimation [7-8]. The window function of PW method is implemented using a multivariate Gaussian kernel. The approach measures the probability of a vector measured from an unknown transformer into different faulty groups to identify its fault category. It makes a decision based on the highest probability of a measured vector in any group.

## 1.4 Missing Data Estimation

To monitor the performance and health condition of transformers, besides secondary evidence (oil test results) a set of electrical and dielectric tests are regularly performed on in-service transformers. However, due to technical problems and limited maintenance budgets, different types of measurements may be made at different rates or occasionally omitted. Therefore, some measured vectors remain incomplete or may contain outdated proxy data. Moreover, due to the improper oil sampling and wrong experimental setup in electrical and dielectric tests, some ambiguity may be found in measurement. If the dimensions of measured vectors are correlated, then their missing elements can be estimated using a finite set of complete measurements [9]. To verify the measured data and determine the missing values in the vectors, a General Regression Neural Networks (GRNN) based artificial intelligence approach has been adopted in this research. The method estimates the missing data based on the correlated set of other measurements. Although not a new method, it has not previously been applied to industrial fault detection problems. The performance of the method is compared against a deliberately omitted value in some complete vectors. Although the estimation of missing value does not offer any new information to the model, the remaining dimensions of an incomplete vector, comprised of actual measurements, can be used to improve the accuracy of model parameters estimation. After estimating the missing values, the complete vector may help transformer experts to take appropriate maintenance decisions by looking at the

full set of necessary information. A paper dealing with missing data estimation procedure has been included as one chapter of this thesis.

## 1.5 Condition Monitoring

Generally, manufacturers of power transformers expect their products to operate in a network for 50 years [10]. To manage the growing demand for electricity, many transformers in the utility systems are already beyond their expected design life. Moreover, a large population of them are approaching this age without clear evidence of their imminent failure. Occasionally, they are required to endure over loading conditions to manage the peak demand for electricity. During these peaks, they experience higher thermal, dielectric, chemical and mechanical stresses that can potentially damage the dielectric and mechanical properties of their solid and liquid insulation [11]. When an aged transformer faces regular over loading and repetitive short circuit incidents, these can cause severe degradation of its insulation that may even lead to an imminent breakdown. To manage the growing number of older assets in the utility networks, the effective approach is to either continuously monitor their condition or replace them from the existing system. However, the decision to replace a transformer is not easy, as it is associated with the huge capital investment. Therefore, to justify the decision of a rigorous maintenance or replacement, a high standard of evidence is necessary [10]. A quantitative health index can help to take the trade-off decision between the cases.

A power transformer is made from different subsystems such as insulation, bushings, tap changer, a core, windings and ancillary components. For proper functioning, each of them needs to simultaneously operate correctly. A fault in any subsystem may lead to catastrophic failure of a transformer. Therefore, to summarize the operating condition of the various subsystems in a transformer, beside online condition monitoring, health index (HI) calculation of a transformer received more attention to the utilities. In a HI calculation, the measurements from different subsystem are

combined into a quantitative index based on the knowledge of experts and application of relevant industrial standards [10]. However, most of the available techniques are based on the linear combination of using a weighted average and require a significant number of measurements. Therefore, they are not sensitive enough to the condition of an individual subsystem. Moreover, a level of quantization is applied to the measured vectors at a very early stage that throws away valuable information and treats wide ranges of measurements equally. Only a few limited nonlinear approaches, based on artificial intelligence have been published in recent years [12-14]. They all rely on heavily parametric models and use only oil test measurements to compute the HI of a transformer. Therefore, a complete assessment of a transformer is not possible. Moreover, the accuracy of these approaches is dependent on the correct estimation of their large number of model parameters. According to the recent statistical surveys [15], it is evident that most of the transformer failure occurred due to the malfunction of their tap changer and bushings. Therefore, it is important to include their performance in a HI calculation. To assess the overall health condition of transformers, a novel artificially intelligent algorithm based on a multiple General Regression Neural Networks (GRNN) has been developed in the research. The GRNN combined the condition of individual subsystems into a quantified health index that summarizes the overall state of each transformer. Moreover, the technique also shows the relation of failure probability of individual transformer over time, based on their calculated health index. A comparative performance of the newly developed approach with expert's classifications based on 345 transformers measurement is provided in this report.

## 1.6 Outline of the Thesis

The chapters of the report are a collection of six manuscripts, of which four have already been published in reputed journals and one was presented in a peer-reviewed conference. One other manuscript (Chapter 4) is currently undergoing review by a journal. As each chapter was published separately, readers should expect a degree of

repetition in the introduction to each new topic. Papers have received minor reedits during the review of this thesis, but there have been no significant changes compared with the published versions.

In Chapter 2, a comprehensive review of the condition monitoring and diagnostic tests is presented. This includes both the fundamental properties of transformers' insulation and as well as condition monitoring, diagnostic tests and lifetime estimation principles. Chapter 3 introduces the reader to a multidimensional clustering approach for fault diagnosis of transformers. Another fault diagnosis technique based on a probabilistic approach is presented in Chapter 4. Chapter 5 describes the missing data estimation problem in the context of power transformers. In Chapter 6 and 7, the main work is presented in the context of a quantitative health index based on the diagnostic tests and the combination of different subsystem condition measurements respectively. Moreover, a correlation between health index and the probability of failure of each transformer is also present in Chapter 7. Finally, Chapter 8 represents the summary of the research along with suggestions about future work in this area.

## References

[1] A. Jahromi, R. Piercy, S. Cress and W. Fan, An approach to power transformer asset management using health index, IEEE Electr Insul Mag,Vol. 2, pp. 20-34, 2009.
[2] A. Setayeshmehr, A. Akbari, H. Borsi and E. Gockenbach, On-line monitoring and diagnoses of power transformer bushings, IEEE Transactions on Dielectrics and Electrical Insulation, Vol. 13, pp. 608-615, 2006.
[3] C. Bengtsson, Status and trends in transformer monitoring, IEEE Trans DielectrElectrInsul, Vol. 11, pp. 1379-1384, 1996.
[4] G.K. Irungu, A.O. Akumu and J.L. Munda, A new fault diagnostic technique in oil-filled electrical equipment; the dual of Duval triangle, IEEE Trans DielectrElectrInsul, Vol. 23, pp. 3405-3410, 2016.

[5] IEEE guide for the interpretation of gases generated in oil-immersed transformers, IEEE Std. C57.104. 2008.

[6] A. Akbari, A. Setayeshmehr, H. Borsi and E. Gockenbach, A Software Implementation of the Duval Triangle Method, In: Conference Record of the IEEE International Symposium on Electrical Insulation (ISEI), 2008, pp. 124-127.

[7] Z. Hu, M. Xiao and L. Zhang, Mahalanobis Distance Based Approach for Anomaly Detection of Analog Filters Using Frequency Features and Parzen Window Density Estimation, Journal of Electronic Testing, Vol. 24, pp. 901-907, 2008.

[8] E. Parzen, On Estimation of a Probability Density Function and Mode, Annals of Math Statistics, Vol.33, pp.1065-1076, 1962.

[9] A.R. Abas, Using incremental general regression neural network for learning mixture models from incomplete data, Egyptian Informatics Journal, Vol. 12, pp.185-196, 2011.

[10] A. Jahromi, R. Piercy, S. Cress and W. Fan, An approach to power transformer asset management using health index, IEEE ElectrInsul Mag, Vol. 2, pp. 20-34, 2009.

[11] X. Zhang, E. Gockenbach, Asset-management of transformers based on condition monitoring and standard diagnosis [feature article], IEEE Electrical Insulation Magazine, Vol. 24, pp. 26-40, 2008.

[12] A.E.B. Abu-Elanien, M.M.A. Salama and M. Ibrahim, Calculation of a Health Index for Oil-Immersed Transformers Rated Under 69 kV Using Fuzzy Logic, IEEE Transactions on Power Delivery, Vol. 27, pp. 2029-2036, 2012.

[13] A.D. Ashkezari, H. Ma, T.K. Saha and C. Ekanayake, Application of fuzzy support vector machine for determining the health index of the insulation system of in-service power transformers, IEEE Trans DielectrElectrInsul, Vol. 20, pp. 965-973, 2013.

[14] W. Zuo, H. Yuan, Y. Shang, Y. Liu and T. Chen, Calculation of a Health Index of Oil-Paper Transformers Insulation with Binary Logistic Regression, Mathematical Problems in Engineering, Vol. 9. 2016.

[15] I.A. Metwally, Failures Monitoring and New Trends of Power Transformers, IEEE Potentials, Vol. 30, pp. 36-43, 2011.

# Chapter 2: A Review of Condition Monitoring and Diagnostic Tests for Life Time Estimation of Power Transformers

## Abstract

Power transformers are a key component of electrical networks, and they are both expensive and difficult to upgrade in a live network. Many utilities monitor the condition of the components that make up a power transformer and use this information to minimize the outage and extend the service life. Routine and diagnostic tests are currently used for condition monitoring and appraising the ageing and defects of the core, windings, bushings and tap changers of power transformers. To accurately assess the remaining life and failure probability, methods have been developed to correlate results from different routine and diagnostic tests. This paper reviews established tests such as dissolved gas analysis, oil characteristic tests, dielectric response, frequency response analysis, partial discharge, infrared thermograph test, turns ratio, power factor, transformer contact resistance, and insulation resistance measurements. It also considers the methods widely used for health index, lifetime estimation, and probability of failure. The authors also highlight the strengths and limitations of currently available methods. This paper summarizes a wide range of techniques drawn from industry and academic sources and contrasts them in a unified frame work.

## 2.1 Introduction

In electric power systems, power transformers are usually considered the most costly item and comprise about 60 % investment of high voltage substations [1]. The huge investment and growing demand of electricity motivate utilities to accurately assess the condition of transformer assets. During operation, transformers regularly experience electrical, thermal, chemical and environmental stresses. Over time, due to these stresses, faults and chemical reactions, different types of catalytic ageing by-products like moisture, acids and gases are produced in transformer oil. The ageing products gradually reduce the dielectric and mechanical strength of insulation. Consequently, as transformers approach the end of their service life, their probability of failure increases. Additionally, regular overloading and short circuit incidents on aged transformers may lead to unexpected premature failures, resulting in damage to customer relationships due to interruption of power supply. Moreover, failure of transformers can damage the environment through oil leakages and could be dangerous to utility personal by creating fire and explosions, resulting in costly repairs and significant revenue losses.

This paper reviews established routine and diagnostic tests for condition monitoring and life time estimation and underlines the limitations of individual methods. Routine tests are periodically conducted after a certain interval to assess the overall condition and check the performance of transformers. If any degraded performance is detected in routine tests, diagnostic tests may need to be performed. Moreover, after any fault, commissioning and transportation, some diagnostic tests are always performed to check the integrity of a transformer. The measurements produced by these tests are used by most utilities to produce health indices that indicate the operating condition and estimate the remaining lifetime. This paper would be useful for new maintenance engineers taking responsibility for managing electrical power assets to help them setup a strategy for maintenance.

However, in scheduled maintenance, a fault can develop in the time between inspections and can be catastrophic. This limitation promotes utilities to move away from scheduled to condition-based maintenance [2-3]. Condition based monitoring means that the schedule for conducting tests reflects the best current knowledge about the condition of a transformer based on the results of previous tests. This implies a transformer that is considered as being in poor condition is monitored more frequently than the scheduled maintenance rate. Condition based monitoring can help to avoid unexpected failures through improved assessment of insulation and can save both down time and money wasted by scheduled maintenance. Condition based monitoring does not imply online monitoring, where remote sensing is used to monitor the transformer in real time, but online monitoring has become established for important assets. This paper has been organized as follows: In section 2.2, statistical failure rate and standard diagnosis have been discussed. Section 2.3 provides a short review of different routine and diagnostic tests. In section 2.4, remaining service life calculation methods have been discussed. Section 2.5 concludes the paper.

## 2.2 Transformer Failure Statistics

The insulation of transformers loses its dielectric and mechanical strength with increasing service time. This increases the probability of failure and decreases the residual life. According to industry standards, the average expected working life of a power transformer is about 40 years [1]. After this time, it is widely accepted that the probability of catastrophic failure is very high. To improve the service quality and reduce the operating cost of an aged transformer, different condition monitoring and diagnostic techniques are currently in use. The age profile of power transformers of a leading utility company in Australia is shown in Figure 2.1.

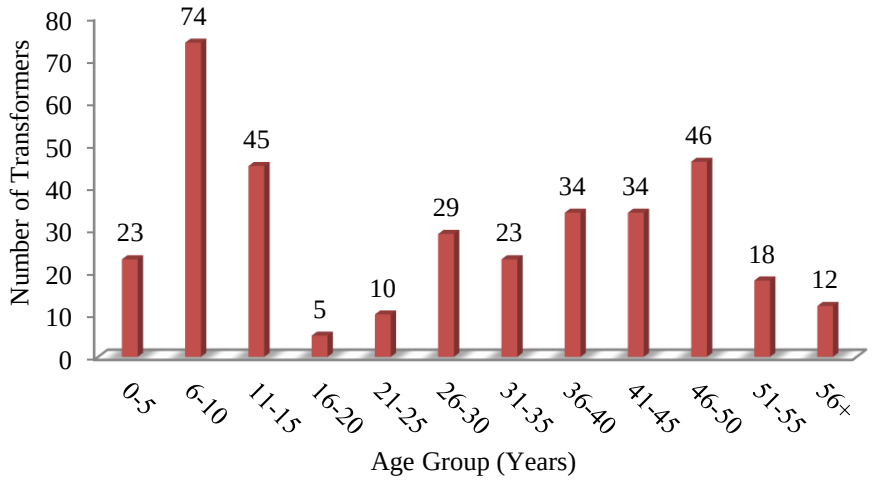


**Figure 2.1:** Power transformers age profile.

According to the age profile, a large population of transformers (110), out of 360 has already crossed the average service life and increasing to 167 within the next decade. So, around 31% of these transformers, based on their service length have already exceeded the operator's expected lifetime and an additional 16% will lapse within a decade. Nevertheless, the rate of failure among transformers beyond their projected lifetime is less than expected by the utilities and they are performing well. In order to avoid unpredicted failures of these transformers in the near future, instead increasing time based maintenance; continuous condition monitoring is highly desirable.

Transformer failure rate and life expectancy are affected by a range of external and internal mechanisms such as electrical, thermal and mechanical causes. Electrical stresses like switching surges, lightning impulses or frequent over loading gradually reduce the dielectric strength of insulation that ultimately leads to transformer failure. The increased contact resistance, partial discharge (PD) and problems with the cooling system increase operating temperature, while mechanical deformation can arise from short circuit current and transportation. Thermal stresses and mechanical defects, when combined with moisture and contamination, will increase the ageing rate of insulation and hasten the electrical failure. Statistics about the common causes of transformer failure are shown in Figure 2.2 [4].

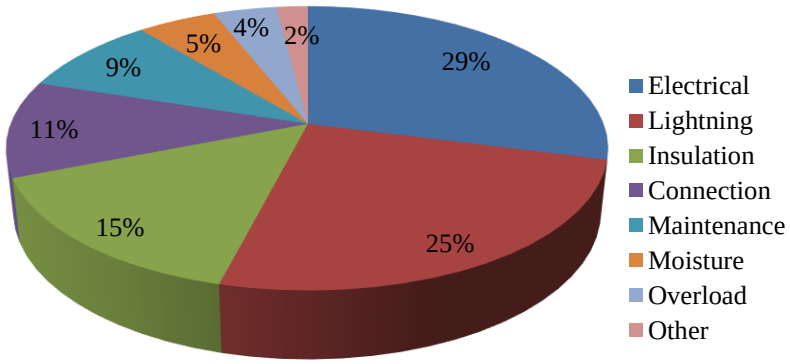


**Figure 2.2:** Causes of failure [4].

Although the main tank accessories are the primary contributors to transformers failure, there is also a significant contribution from bushings, tap changers and other accessories. According to a recent survey conducted by CIGRE work group WGA2.37 on 364 failures (>100 kV) [5], the statistics of typical failure location has been illustrated in Figure 2.3.

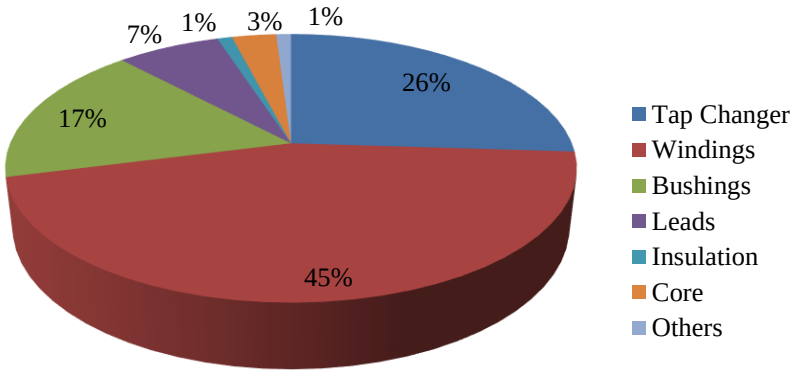


**Figure 2.3:** Failure locations of transformers [5].

Additionally, their study on Europe shows that 80% of bushing failure occurs in mid service age (12-20 years) and initiate 30% of transformer failures. Given this statistic, it is apparent that the integrity of a transformer is dependent on multiple factors. It is also essential to prioritize the diagnostic tests based on the degree of influence each

component has on transformer health. A taxonomy of important diagnostic methods for condition assessment of transformers is provided by Figure 2.4.

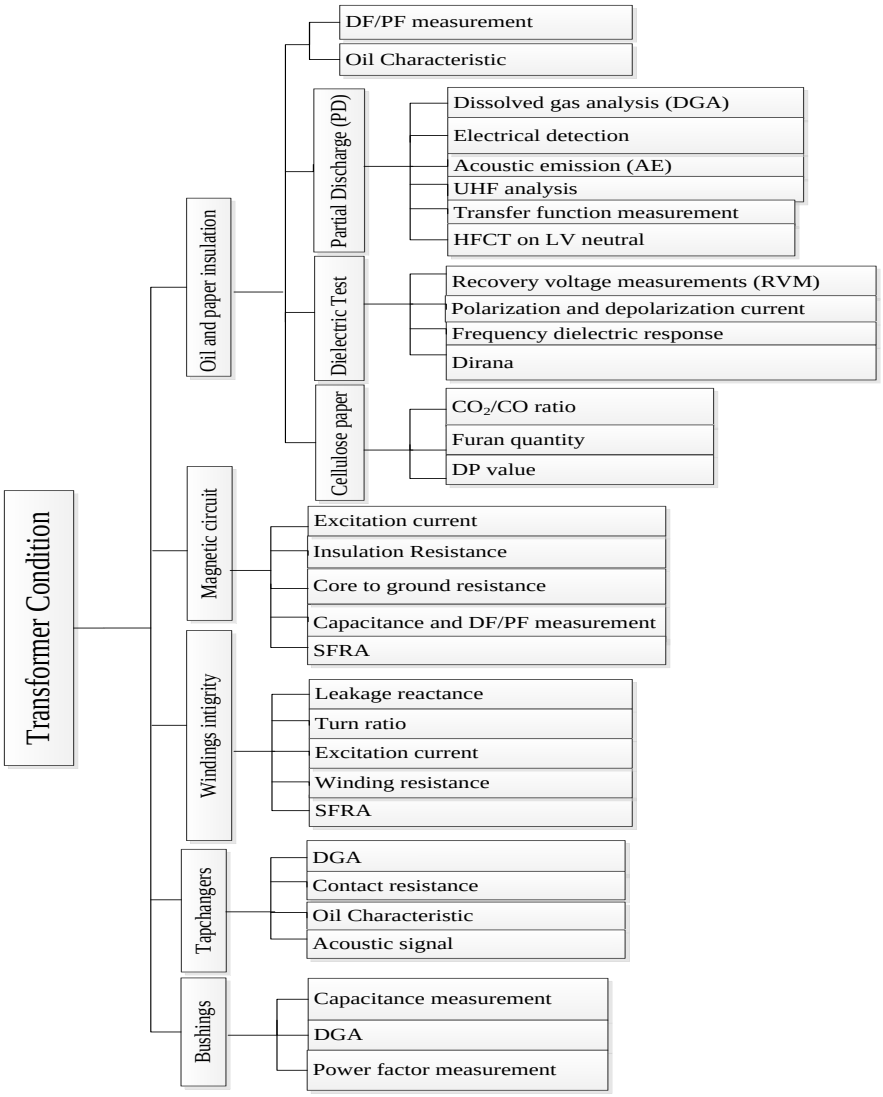


**Figure 2.4:** Condition monitoring and diagnostic techniques.

## 2.3 Condition Monitoring and Diagnostic Tests

After installing and commissioning power transformers, utilities always expect to operate them continuously throughout their service life with a minimum of casual

maintenance. To reduce unplanned outages and minimize operational cost, a number of routine and diagnostic tests are regularly conducted by utilities to assess the insulation condition and mechanical integrity of each transformer. A review on conventional and sophisticated routine and diagnostic tests has briefly been discussed in the following sections.

### 2.3.1 Dissolved Gas Analysis

Dissolved gas analysis (DGA) is a widely accepted and established method for condition monitoring of power transformers. It can identify faults such as arcing, partial discharge, low-energy sparking, overheating and detect hot spots at an early stage without interrupting the service [6]. This approach is accompanied by analysing combustible and non-combustible gases dissolved in transformer oil. During their working life, transformers regularly have to face faults and stresses (thermal, electrical, chemical and mechanical) that produce various fragments, ageing and polar oxidative products. Over time, due to interaction between fragments or interaction among ageing products, various chemical reactions start that change the molecular properties of oil-paper insulation [7]. Additionally, the catalytic behaviour of oxygen and moisture produced in oil-paper insulation along with thermal dynamic increases the reaction rate. Eventually, different type of gases such as Hydrogen ($H_2$), Oxygen ($O_2$), Nitrogen ($N_2$), Carbon dioxide ($CO_2$), Carbon monoxide (CO), Methane ($CH_4$), Ethylene ($C_2H_4$), Ethane ($C_2H_6$), Acetylene ($C_2H_2$), Propane ($C_3H_8$) and Propylene ($C_3H_6$) are produced and dissolved in transformer oil. To assess the condition of oil and paper insulation and detect faults indirectly from the gases, a number of DGA methods like Key Gas, Roger's Ratios, Duval Triangle, Doernenburg, IEC ratio and single gas ratio are currently in use [6]. According to [8], 70% of power transformer common faults can be detected by DGA. An integrated gas monitoring system is helping operators to continuously monitor the trends and production of gases produced by operating transformers. However, comparison of

results from different methods on the same sample may lead to contradiction and there is no clear way to prioritise one result over another. An integrated gas monitoring system along with supplemental tests might help to overcome this limitation by cross-checking the faults. Although, DGA can detect and classify faults, in most cases, it cannot identify the fault location. Consequently, operators need to supplement the results with other diagnosis methods. A review of the various DGA methods follows.

#### 2.3.1.1 Key Gas Analysis (KGA) Method

The Key gas method diagnoses faults based on the proportion of combustible gases. It provides a series of "templates" associated with standard fault conditions. For instance, 63% of Ethylene with some Ethane (19%) and Methane (16%) indicates that transformer oil is overheated [9]. If the majority of gas is Carbon monoxide (92%) then it indicates that the cellulose is overheating. A high percentage of Hydrogen (85%) with some proportion of Methane (13%) indicates partial discharge, while a high percentage of Hydrogen (60%) with some percentage of Acetylene (30%) indicates arcing in oil. In practice, it is almost impossible to obtain exact proportions of gases that perfectly match these templates. Often the percentages are lower but experience can see a trend and intervene early before a critical stage is reaches. As a result, the accuracy of KGA is highly dependent on the investigator's experience and correlation skills.

#### 2.3.1.2 Roger's Ratios Method

Roger's Ratios method (RRM) uses the ratios of gas concentration to identify and classify faults in a transformer. The ratios of $C_2H_2/C_2H_4$, $CH_4/H_2$ and $C_2H_4/C_2H_6$ are used in this method. According to RRM, the classification of different electrical and thermal faults is shown in Table 2.1. In some cases, the calculated ratios may not fall

any of the classes shown in Table 2.1. Additionally, over time, gases are normally produced in transformer without any fault. Consequently, the chance of misclassification is a major limitation of the Roger's Ratios method.

**Table 2.1:** Roger's Ratios [9].

| Case | R2=$C_2H_2/C_2H_4$ | R1= $CH_4/H_2$ | R5=$C_2H_4/C_2H_6$ | Suggested Fault Diagnosis |
|---|---|---|---|---|
| 0 | <0.1 | >0.1 to <1.0 | <1.0 | Unit normal |
| 1 | <0.1 | <0.1 | <1.0 | Low-energy density arcing – PD |
| 2 | 0.1 to 3.0 | 0.1 to 1.0 | >3.0 | Arcing-high-energy discharge |
| 3 | <0.1 | >0.1 to <1.0 | 1.0 to 3.0 | Low temperature thermal |
| 4 | <0.1 | >1.0 | 1.0 to 3.0 | Thermal <700 ˚C |
| 5 | <0.1 | >1.0 | >3.0 | Thermal >700 ˚C |

#### 2.3.1.3 Gas Patterns Method

According to the gas patterns method, ethylene ($C_2H_4$) and methane ($CH_4$) are the key gases that are used to detect poor connection between conductors [10] . Over time, due to vibration of the transformer, the contact between conductors may become weaken and increase the series resistance. As a result, with the flow of current, the contacts get over heat and the hot metal gases such as ($C_2H_4$) and ($CH_4$) are produced. Additionally, a small proportion of catalytic metals for instance iron, copper, zinc, aluminium and dibenzyldisulfide (DBS) are inherently present in a transformer [10]. The normal proportion of dibenzyldisulfide (DBS) in transformer oil is between 40 to 65 mg/kg. The concentration of DBS decreases with an increase of temperature. At high temperature, the sulfur of DBS starts reacting with copper and produces copper sulfide [10]. As this reaction is completely temperature dependent, the concentration of copper sulfide and DBS can be used to assess the quality of internal contacts of transformers.

### 2.3.1.4 Doernenburg Method

Doernenburg is a four gas ratios method based on five individual key gases ($H_2$, $CH_4$, $C_2H_2$, $C_2H_4$ and $C_2H_6$) that can detect faults and PD activity in a transformer. The accuracy of this method is high, but only if significant amount of key gases are produced. The correlation summary between faults and four gas ratios is shown in Table 2.2.

**Table 2.2:** Gas ratios for Doernenburg method [11].

| Ratio 1 $CH_4/H_2$ | Ratio 2 $C_2H_2/C_2H_4$ | Ratio 3 $C_2H_2/CH_4$ | Ratio 4 $C_2H_6/C_2H_2$ | Suggested Fault Diagnosis |
|---|---|---|---|---|
| 0.1-1.1 | 0.75-1.0 | 0.3-1.0 | 0.2-0.4 | Thermal Decomposition |
| 0.01-0.1 | Not Significant | 0.1-0.3 | 0.2-0.4 | Corona (Low Intensity PD) |
| 0.01-0.1 | 0.75-1.0 | 0.1 -0.03 | 0.2-0.4 | Arcing (High Intensity PD) |

### 2.3.1.5 Duval Triangle Method

The Duval triangle (DTM) is a three-axis coordinated graphical method, where the axes represent $CH_4$, $C_2H_4$ or $C_2H_2$ percentages from 0% to 100% [12]. Due to its accuracy and capability of detecting large number of faults, it is widely used by the utilities. In DTM, the entire triangular area has been subdivided into 7 fault regions labelled PD, D1, D2, T1, T2, T3 and DT, as shown in Figure 2.5 [13].

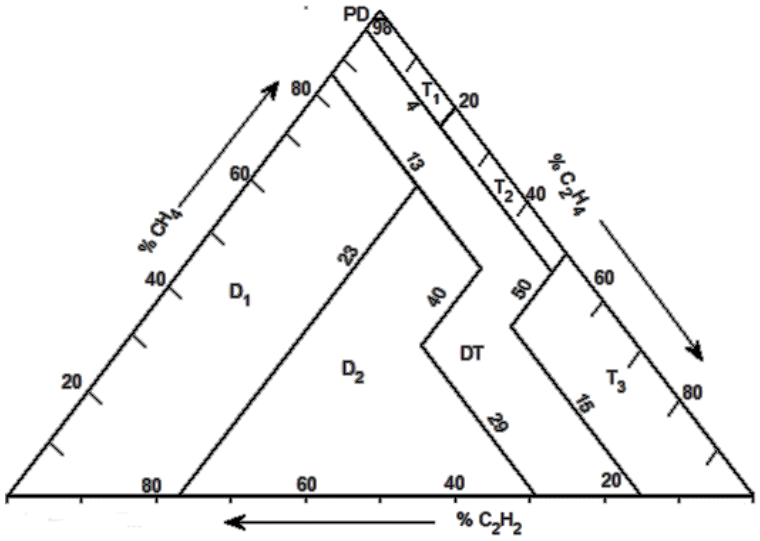


**Figure 2.5:** Duval Triangle [14].

The PD region indicates partial discharge, D1 indicates discharges of low energy, D2 indicates discharges of high energy, T1 indicates thermal faults of less than 300 ˚C, T2 indicates thermal faults between 300 ˚C and 700 ˚C, T3 indicates thermal faults greater than 700 ˚C, and DT indicates a mixture of thermal and electrical faults. Although, this method always gives a diagnosis, there is a chance of misclassification close to the boundaries between adjacent sections [14]. The classical Duval Triangle cannot accurately detect the PD and thermal fault. In order to overcome the limitation, Duval introduced Triangle 4 and 5 for mineral oil filled transformers. In Triangle 4, axes are presented by $H_2$, $CH_4$ and $C_2H_6$ gases. If the fault classification is a thermal fault (T1,T2) or a PD by the classical triangular method, then Triangles 4 must be used for further clarification [15]. Triangle 5 uses gas concentrations of CH4, $C_2H_4$ and $C_2H_6$ respectively that are formed specifically for faults of high temperature (T2, T3). In order to get more information about the thermal faults, triangle 5 should be used only if Triangle 1 identified the fault as T2 or T3. None of the Triangles 4 and 5 should be used for electrical fault D1 or D2. In practice, there are cases where contradictory classifications are produced by Triangles 4 and 5. Moreover, all triangles have an unclassified region. Consequently, the accuracy of

fault classification is dependent on the expert's experience supported by other ratio methods. Furthermore, it can only predict the amount of discharge from the changes of gases, not quantify the discharge, especially for small discharges like pico-coulombs (pC) range, nor can it locate the origin of a fault.

Over the last decade, a several artificial intelligence (AI) methods such as artificial neural networks (ANN), support vector machines (SVM) and fuzzy logic have been used by the researchers to analyse the DGA data to detect insulation degradation, identify faults, track performance and calculate health index of transformers [16-20]. The AI approaches have made it possible to analyse the DGA data sets into the multi-dimensional spaces to extract the pattern of the gases for faults detection and classification. Moreover, AI can integrate multiple factors and can deal with the non-linearity of gases production which is common in field measurements to reduce the error in decision making.

### 2.3.2 Oil Quality Test

Insulating oil quality testing is a common method for assessing the condition of in-service transformers. As the oil condition has a direct influence on the transformer's performance and the service life, condition monitoring of transformer oil has proven very effective. Over the service period, due to the oxidation, chemical reactions and variable stresses (thermal, electrical and chemical stresses) oil characteristics and condition changes. To quantify these changes and diagnose the severity, a number of physical, chemical and electrical tests like dielectric breakdown voltage (DBV), power factor, interfacial tension (IFT), acidity, viscosity, color and flash point are performed. DBV measures the strength of oil to withstand electrical stress without failure [21]. The power factor or dissipation factor test is used to measure the dielectric losses in the oil [22]. As the test is very sensitive to ageing products and soluble polar contaminants, it can assess the concentration of contaminants in the insulating oil. During service time, different types of acids are produced in the

transformer oil resulting from atmospheric contamination and oxidation products [23]. The acids, along with oxidation products, moisture and solid contaminants degrade different properties of the oil. Consequently, the acidity test plays an important role to assess the condition of oil. IFT measures the attraction force between oil and water molecules that can be used to assess the amount of moisture in oil [4]. The value of IFT can help to estimate the soluble polar contaminants and products of degradation that affect the physical and electrical properties of the insulating oil. Usually, new insulating oil in transformers shows high levels of IFT in the range of 40 to 50 mN/m, while an oil sample with IFT less than 25 mN/m indicates a critical condition [24]. A detailed procedure for IFT measurement is available in [25]. Viscosity of oil is a factor that plays an important role in heat transfer in transformers. With the increase of temperature, viscosity of pure oil decreases. Therefore, the strength of the insulation decreases. Different types of nanoparticles such as $SiO_2$, $Al_2O_3$ and ZnO can be added to insulating oil to control its viscosity, which can be measured by applying a COMPASS force field [26]. Additionally, tests such as color, flash point etc. are used to detect contaminants in service-aged oil [27]. Multiple results are correlated to assess the condition of each transformer and schedule its maintenance (reclamation or replacement) to avoid costly shutdown and premature failure. IEEE C57.106-2006 presents a classification of insulating oil based on variable test parameters and transformer rated voltage that has been shown in Table 2.3.

**Table 2.3:** Classification based on oil test parameters.

| Oil test parameters | U≤69 kV | 69 kV <U <230kV | 230kV≤U | Classification |
|---|---|---|---|---|
| Dielectric Strength (kV/mm) | ≥45 | ≥52 | ≥60 | Good |
| | 35-45 | 47-52 | 50-60 | Fair |
| | 30-35 | 35-47 | 40-50 | Poor |
| | ≤30 | ≤30 | ≤40 | Very Poor |
| Interfacial Tension (dyne/cm) | ≥25 | ≥30 | ≥60 | Good |
| | 20-25 | 23-30 | 50-60 | Fair |
| | 15-20 | 18-23 | 40-50 | Poor |
| | ≤15 | ≤18 | ≤40 | Very Poor |
| Neutralization Number (Acidity) | ≤0.05 | ≤0.04 | ≤0.03 | Good |
| | 0.05-0.1 | 0.04-0.1 | 0.03-0.07 | Fair |
| | 0.1-0.2 | 0.1-0.15 | 0.07-0.1 | Poor |
| | ≥0.2 | ≥0.15 | ≥0.10 | Very Poor |
| Water content (ppm) | ≤30 | ≤20 | ≤15 | Good |
| | 30-35 | 20-25 | 15-20 | Fair |
| | 35-40 | 25-30 | 20-25 | Poor |
| | ≥40 | ≥30 | ≥25 | Very Poor |
| Dissipation factor at 50 Hz (25°C) | | ≤0.1 | | Good |
| | | 0.1-0.5 | | Fair |
| | | 0.5-1.0 | | Poor |
| | | ≥1.0 | | Very Poor |

### 2.3.3 Infrared Thermograph Test

Infrared thermography is a non-destructive and quick imaging process that can visualize the external surface temperature of transformers without interrupting their operation [28]. The normal operating temperature of transformers lies between 65 to 100 °C [29]. The operating temperature of a transformer can rise based on variable reasons like short circuit current, high winding resistance, poor contact in cable/clump joint, oil leaks and faulty cooling system. With the increase of temperature, the ageing rate of insulation increases. The ageing rate of insulation becomes double at 6-8 K (Kelvin) from the reference value and reduces the residual working life quickly [4]. A temperature rise of 8 to 10 °C from nominal value is considered as a critical condition and reduces the design life by half [4]. According to [30], a transformer will fail immediately with an increase of 75 °C from normal temperature. The increased temperature could be an indication of problematic cooling system, or a problem in core, winding, bushing and joints. To identify faults, infrared

thermography converts the infrared radiation from targeted surface into colour coded pattern images. The test can localize the hot sport and visualize the temperature gradient at joints and surfaces. The test result can be verified by comparing with historical record or conducting a DGA on the same transformer. Consequently, this method can be used as an initial fault detector and supplement of DGA. However, thermograph cannot detect the internal temperature of a transformer tank [31]. A classification of heating severity based on infrared thermography has been summarized in Table 2.4.

**Table 2.4:** Heating severity classification [31].

| Increased Temperature | Classification |
|---|---|
| 0-9 ˚C | Attention |
| 10-20 ˚C | Intermediate |
| 21-49 ˚C | Serious |
| > 50 ˚C | Critical |

### 2.3.4 Excitation Current Test

This test is used to detect short circuited turns, ground faults, core de-laminations, core lamination shorts, poor electrical connections and load tap changer (LTC) problems. Since the magnitude of magnetizing current in high voltage (HV) winding is less, this test is performed by exciting the HV side, keeping the LV neutral grounded and all other terminals floating. Due to the grounded neutral, if there is any ground fault, a huge amount of current will flow into the HV side with low excitation voltage. During this test, the magnitude of single phase voltage and magnetizing current including their phase angle is measured [32]. The measured value is compared with historical test or other phases to detect faults. For 50 mA rated excitation current, a difference of >5% between phases is an indication of short circuited turns, ground faults, core de-laminations, core lamination shorts, poor electrical connection and LTC problems; whereas >10% deviation is an indication of

internal fault [4]. As the test result is influenced by the residual magnetism, this test must be conducted before any direct current test.

### 2.3.5 Power Factor/Dielectric Dissipation Factor Test

The dielectric dissipation factor $(tan\ \delta)$ test may be used to check the insulation integrity in windings, bushings and oil tank of transformers. When an alternating voltage is applied across the insulation, a leakage current having reactive (capacitive) and resistive components starts to flow. The magnitude of the resistive component is dependent on the moisture, ageing and conductive contaminants in the oil, while the capacitive current is dependent on the frequency. The ratio of resistive and capacitive current is known as the dissipation factor. At low frequencies, the magnitude of capacitive current is almost equal to the total leakage current. Consequently, another name of this test is the power factor test. According to IS-1866, at 90 $^0$C, the value of $tan\ \delta$ for fresh oil could vary from 0.010 to 0.015 depending on the transformer's rating. A mathematical correlation between power factor and $tan\ \delta$ can be established using the following equation [33].

$$cos\theta = \frac{tan\ \delta}{\sqrt{1+(tan\ \delta)^2}} \quad \text{Or} \quad \tan\delta = \frac{\cos\theta}{\sqrt{1-(\cos\theta)^2}} \tag{2.1}$$

Modern testing tools, like Doble M4100 measure the dielectric losses of insulation (including bushing) in Watts. A value of more than 0.5% $tan\ \delta$ deviation indicates problematic insulation, while >2% means the high chance of imminent failure [4]. However, a higher value of $\tan\delta$ could also be an indication of potential PD.

### 2.3.6 Polarization Index Measurement

The polarization index (PI) measurement is one of the common methods to assess the dryness and cleanness of windings solid insulation that depends on the insulation classes (A, B or C) and winding components [34]. A PI measurement determines the

ratio of 10 minutes resistance to 1 minute resistance after applying the test voltage to assess the insulation condition [35]. The winding temperature has a strong influence on the measurement of insulation resistance (IR). However, PI is determined by the ratio of two resistances, so the impact of winding temperature during the 10 minutes test is almost insignificant. With the increase of moisture and impurity in insulation, the PI value gradually decreases. According to [34], insulation having PI in the range 1.5-2 indicates dry insulation, the range 1-1.5 indicates dirty/wet insulation and less than 1 indicates severe pollution and humidity. Moreover, if the PI value rapidly decreases 25% from a previous measurement, it is advisable to clean the insulation [34]. Although, it is a comparatively quick and convenient testing method, it cannot detect the degradation of insulation due to the ageing and stresses over time.

### 2.3.7 Capacitance Measurement

The capacitance measurement is used to assess the condition of bushings and detect the gross winding movement. The bushings of a transformer are electrically equivalent to a number of series capacitors. If a bushing has a dielectric dissipation factor (DDF) tap, the capacitance between the bushing conductor and DDF tap is commonly known as $C_1$and the capacitance between DDF and ground is known as $C_2$. The average life time of bushing is about 30 years. Any problems in bushing like cracking of its resin-bonded paper or moisture ingress would increase the value of capacitance and reduce its service life. Consequently, the measured capacitance can diagnose the condition of bushings. In [4], it has been stated that about 90% of bushing failure is due to moisture ingress. The test can also be used to measure capacitance between windings and between individual windings and the main tank. Any deviation of the capacitance value can be used to detect the mechanical deformation of windings and core. As this test is less sensitive and only detects gross deformation of windings, a more sensitive approach such as transfer function measurement and SFRA may be used as a supplement to the capacitance testing.

### 2.3.8 Transfer Function Measurement

Transfer function (TF) measurement is one of the acknowledged methods that can predict moisture content in solid insulation [36] and detect mechanical faults like winding deformation and displacement due to the short circuit current, switching impulse and transportation [37-39]. The transfer function is a frequency-dependent parameter that is measured from the ratio of current and voltage of an input terminal, or from the ratio of output and input voltage on the same phase. During TF measurement, a known voltage is generally applied to the HV terminals and the resulting input current is measured from the same side while voltage is measured on the corresponding LV winding. A detailed test procedure for TF measurement is available in [37]. The TF measurement is sensitive enough to detect both axial and the radial buckling of windings, which cannot be detected by the conventional leakage reactance measurement. Moreover, TF measurement can specify faults without opening the unit and both on-line and off-line modes are available [38, 39].

### 2.3.9 Tap Changer Condition

The load tap changer (LTC) of a transformer is used to regulate the voltage despite variations in the load. A range of insulating materials like oil, fiberglass, cardboard and proxy resin are used in a tap changer as its insulation. Failure to a tap changer can result into a catastrophic failure of nearby transformers. The authors of [4] and [1], respectively state that 30% and 40% of transformer failure results from the tap changer malfunction and this could varies depending on the tap changer types, manufacturer, operation and maintenance frequency. Unlike in the main tank, a certain amount of combustible gas in the tap changers is considered normal, which is produced from the operation of LTC. The trapping of gases is depending on the breathing system. A sealed LTC can trap most of the gases while gas is rapidly vents from a free breathing system [40]. However, insufficient adoption of standards and the lack of guidelines make it hard to assess the condition of LTC directly from

DGA [1]. Consequently, a series of tests such as DGA, oil quality, contact resistances and acoustic signal are performed, at the same time the number of operations, temperature and motor current is monitored to assess the condition of tap changer and its insulation.

### 2.3.10 Cellulose Paper Insulation Tests

The solid insulation (paper) within transformers is composed of about 90% cellulose, 6-7% of hemicelluloses and 3-4% of lignin that have long chains of glucose rings [33]. The purpose of this paper is both to provide insulation and mechanical support against forces that arise from short circuit and inrush current, and holding the windings in position. The dielectric properties and tensile strength of the paper are dependent on the number and length of glucose rings [3]. Over time, due to the ageing, stresses and loading pattern, the electrical and mechanical properties of the paper degrades and a number of chemical compound and byproducts like water, acid and gases (CO and $CO_2$) are produced. These byproducts are used in several diagnostic techniques like furan analysis and the degree of polymerization (DP) and $CO_2$/CO ratio for assessing the condition of paper insulation. All three methods have been reviewed below.

#### 2.3.10.1 Ratio of $CO_2$ and CO

The ratio of $CO_2$/CO can help to assess the condition of paper insulation. Generally, without any fault occurring, during the service time, including $CO_2$ and CO different proportion of combustible gases are always produces in transformer and dissolved in the oil. The carbon oxide gases ($CO_2$ and CO) can be produced from the paper due to cellulose overheating, bad connection and problematic cooling system of transformers. However, oil decomposition can also produces these gases due to different faults [4]. A $CO_2$/CO>10 could mean atmospheric exposure of insulation and instant breakdown while a $CO_2$ to CO ratio less than 5 indicates faster

degradation of cellulose. For proper maintenance, the identification of gas sources is important. The $CO_2$/CO ratio method cannot distinguish the sources. Consequently, there is a chance of wrong diagnosis providing a major limitation of $CO_2$/CO ratio method. In order to overcome this limitation, additional tests such as furan analysis and the DP are recommended along with analysis of other key gases.

### 2.3.10.2Furan Analysis

Furan analysis is an integral, non-periodic and post-diagnostic technique that can assess the condition of cellulose paper inside transformers without interrupting the service. Due to the ageing, loading pattern and chemical reaction, the glucose rings of cellulose may break down and the following types of furanoid compounds, namely, 2-furfural (2-FAL), 5-Hydroxy methyl-2-furfural (5-HMF), 5-Methyl-2-furfural (5-MEF), 2-Furfurol (2-FOL) and 2-Acetylfuran (2-ACF) are produced which are partially soluble in oil [33]. The produced furanoid compounds develop a partition between the oil and the solid insulation interphase [41]. The production rate of furanoid compounds is influenced by the temperature, catalytic ageing byproducts such as moisture, acids, oxygen and CO, that produced by various faults and increase the degradation rate of paper [4]. Over time, these furanoid compounds dissolve in the insulating oil and changes its color. It is recommended to perform furan analysis, if the colour of oil changes remarkably and other catalytic ageing byproducts are present [31]. Cellulose paper gradually loses its mechanical strength with the increase of furan which can be measured by the gas chromatography (GC), mass chromatography (MC) or high performance liquid chromatography (HPLC) on collected oil sample following the American Society for Testing and Material (ASTM D5837) or IEC method 61198 [42-43]. A detailed method of HPLC for furan measurement is available in [44]. Moreover, the quantified furan can be used to estimate the remaining life time of transformers. If the strength of paper is reduced to such an extent that it cannot ensure the mechanical support to windings, the electrical integrity of transformer becomes threaten. The furan is very sensitive to the ageing of

paper and comparatively stable than other furanoid compounds. As furan increases consistently with paper ageing, researchers mostly analyze it. The main limitation of this method is that if the insulating oil of a transformer is replaced or reclaimed, it cannot accurately assess the condition of solid insulation prior to the change. The thresholds for analyzing ageing of paper insulation based on furan are shown in Table 2.5.

**Table 2.5:** Age profile of cellulose paper based on furan [1].

| Furaldehyde (ppm) | Service Life (Years) |
|---|---|
| 0.0-0.10 | <20 |
| 0.1-0.25 | 20-40 |
| 0.25-0.5 | 40-60 |
| 0.50-1.0 | >60 |
| >1.0 | - |

### 2.3.10.3 Degree of Polymerization

The degree of polymerization (DP) is another dependable method for assessing the health of paper insulation. The paper of transformers is a complex compound of carbon, hydrogen and oxygen ($C_5H_{10}O_5$) where glucose monomer molecules are linked in a special way to form cellulose. As the insulation ages, the glucose rings become fragile and start to break. In DP, the length of glucose molecules rings is measured as a way of estimating the integrity of the paper insulation [45]. To measure DP, paper samples are collected from multiple positions around the windings including the hotspot area, which is generally located at the centre of windings. The collection of paper samples from a live and free breath transformer are impractical and could be destructive or may cause complete failure of a transformer [46]. Consequently, paper samples are collected from the de-energised transformer and analysed by molecular weight estimation methods like viscometry or gel permeation chromatography (GPC). In the viscometry method, the DP value is

measured by averaging the length of cellulose chains based on their viscosity [47-48]. The accuracy of this method is influenced by the oxidative degradation of the samples and variation in ambient temperature [49-50]. In [51], Ali has shown that viscometry can only approximate the length of a cellulose chain, but GPC has greater potential than viscometry method to give more useful and detailed information about cellulose ageing. In GPC, a DP value is calculated by measuring the change in molecular weight distribution of the cellulose paper. As GPC is very sensitive to molecular weight, it can detect a small degradation of cellulose through the chromatogram [50]. A detail sampling and testing process for GPC is available in [50]. Due to the intrusive sampling process, furan analysis is more widely used than DP. The furan test can easily make estimates of furan from oil sampling of an in-service transformer. As furan splits glucose rings into small segments, with the increase of furan, the DP value decreases. Consequently, cellulose paper loses its insulation quality and tensile strength. The value of DP and the level of furan can be correlated to estimate the health of paper/solid insulation. A correlation between DP and furan to estimate insulation state are shown in Table 2.6.

**Table 2.6:** Correlation of 2-FAL and DP value with insulation health [31].

| 2-FAL (ppm) | DP Value | Significance |
|---|---|---|
| 0-0.1 | 700 - 1200 | Healthy Insulation |
| 0.1-1.0 | 450 - 700 | Moderate Deterioration |
| 1-10 | 250 - 450 | Extensive Deterioration |
| > 10 | < 250 | End of Life Criteria |

Although, the measurement of DP from the furan is non-destructive and relatively straightforward, the contamination of the oil and non-uniform ageing of the paper constrain the method in practice [47].

### 2.3.11 Dielectric Response Analysis

Dielectric response analysis (DRA) is a widely adopted method for evaluating the moisture content in the oil-paper insulation of transformers. In power transformers, both the oil and cellulose paper provides the insulation. Moisture occurs inside a transformer is produced from chemical reactions and is absorbed in the solid insulation (up to 99%) and oil. The production rate of moisture is influenced by the organic acids, gases, humidity, ambient temperature and oxygen content. A complex dynamic migration of moisture between oil and paper insulation always continues and the rate is influenced by the temperature. At high temperature, moisture from the solid insulation moves in to the oil but returns to the insulation with a decrease of temperature. The amount of moisture in solid insulation can be measured directly by the traditional Karl Fischer Titration (KFT) or Piper-Fessler isothermal model [52-53]. The oil moisture content with the help of an equilibrium chart can also indirectly estimate the moisture in solid insulation [52]. The collection of paper samples from different places for KFT is mostly impractical and unsuitable for onsite testing. Additionally, the accuracy of the Piper-Fessler method is affected by the insufficient and incorrect positioning of moisture sensors in the transformer tank [53]. Moreover, the influence of temperature also makes it hard to achieve the equilibrium state of moisture between oil and paper, which can lead to a significant error in the measurement accuracy [54]. Consequently, over the last decade, to overcome the above limitations, different indirect, sensitive and nondestructive methods like recovery voltage measurement, polarization and depolarization current analysis and frequency dielectric response have gained significant attention for accurately measuring the moisture content and its impact on the dielectric response to assess the insulation ageing [2, 29]. A review on different dielectric responses analysis techniques with their limitations has been provided below.

### 2.3.11.1 Recovery Voltage Measurement

Recovery voltage measurement (RVM) is a time domain dielectric response technique that is used to detect the moisture level in the insulation of transformers. The quantity of moisture in insulation gradually increases over time due to the ageing. The level of moisture is one of the key decisive factors used to measure insulation breakdown. Consequently, the individual knowledge of moisture level in the oil and paper insulation is crucial for evaluating the insulation health. RVM uses the polarization spectrum of the insulation recovery voltages for evaluating the actual state and ageing trend [2, 55]. The RVM method can be represented by the circuit diagram shown in Figure 2.6.

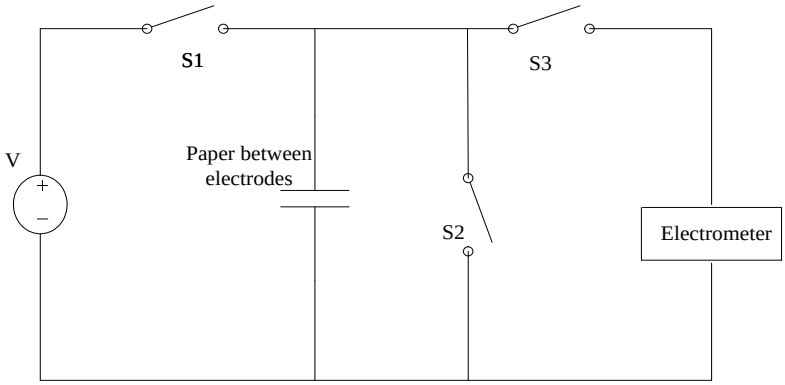


**Figure 2.6:** Circuit diagram for RVM [56].

To perform the test, a DC voltage *V* by a standard recovery voltage meter is applied across the dielectric by closing the switch $S_1$for a period of time $T_c$ and then the capacitor is discharged through a short circuit for a period of time $T_d$ by closing the switch $S_2$(having previously opened the switch $S_1$). After discharge in each cycle, the geometric capacitance $(C_0)$ loses its full charge but some charges are bounded in the dielectric insulation which amount is dependent on the insulation quality. The entire cycle of the measurement is repeated and increased from a fraction of second to the thousands of second by maintaining the charging and discharging time ratio ($T_c/T_d$) = 2. After charging and discharging on each cycle, when the circuit is open, a part of

the bounded charge will be transferred to the geometric capacitance. Eventually, a voltage is developed which is known as a recovery voltage (RV). The values of RV are recorded by a programmable electrometer having very high input impedance, as a function of time $T_c$ and plotted to get the RV spectra. The peak magnitude of the voltage and the corresponding time constant are the significant features of the polarization spectra. The value of central time constant decreases with the increase of moisture in the oil paper insulation and reflect the moisture content in the insulation [2]. According to [57], time constant of the insulation is inversely proportional to the moisture content and ageing. They also presented, the time constant is also inversely related to the temperature and the maximum return voltage decrease with the increase of moisture. Eventually, the moisture content and ageing trend can be estimated from the measured time constant and the RVM peak. However, the authors of [58] state that, that the influence of insulation geometry and separate conductivity of oil and paper insulation is ignored in the RVM. Consequently, the RVM spectra are not accurate. According to [59], it is hard to separate the impact of oil and paper from RVM spectra. However, the introduction of sophisticated software and proper modeling tools for dielectric phenomena which can combine the individual influencing factors like permittivity and conductivity of oil and paper insulation can overcome the limitation and improve the accuracy.

#### 2.3.11.2Polarization and Depolarization Current Analysis

The polarization and depolarization current (PDC) measurement is one of the latest and non-destructive technologies used to measure the oil conductivity and moisture content of homogenous and composite insulations of transformers. Due to the simplicity and capability to assess HV insulation, PDC technique gained immense popularity and are widely using as a supplement of other techniques. Moreover, PDC can quantify the moisture and appraise its impact on the ageing of the oil and paper insulation [60]. For assessing the state of transformer insulation (oil-paper), in PDC measurement, a DC voltage $U_0$ is applied across the oil-paper insulation for a period

of time (e.g., 10000 s) to measure the polarization current. As soon as the voltage is applied, a high magnitude current with different time constants corresponding to the insulating materials and conductivity starts to flow. Over time, the magnitude gradually reduces. The time constant of the charging current is dependent on the conductivity and polarization process of the individual insulating material [59]. The equation of the polarization current can be expressed as

$$i_p\ (t) = C_0 U_0 \left[\frac{\sigma}{\epsilon_0} + f(t)\right] \tag{2.2}$$

where $\sigma$, $\epsilon_0$, $C_0$ and $f(t)$ represent respectively, the composite conductivity, vacuum permittivity, geometric capacitance and dielectric response function of the oil-paper insulation.

The influence of the conductivity on the polarization current could be investigated by simulating the equation (2.2) using different values of oil and paper conductivity. The geometric capacitance $C_0$ between oil-paper insulation can be calculated using the following equation.

$$C_0 = \frac{C_m}{\epsilon_r} \tag{2.3}$$

where $C_m$ represents capacitance between transformer and ground, and $\epsilon_r$ is the effective relative permittivity of heterogeneous oil-paper insulation.

Now, for measuring the depolarization current, the voltage source is replaced by a short circuit. Consequently, an opposite directional depolarization current will start to flow without the contribution of insulation conductivity [59]. The depolarization current can be expressed by the following equation.

$$i_d\ (t) = C_0 U_0 \left[f(t) - f(t + t_c)\right] \tag{2.4}$$

where $t_c$ is the duration of the applied voltage.

The dielectric response function $f(t)$ can be measured experimentally by charging the insulation through a step voltage or measuring the depolarization current after replacing the step voltage with a short circuit. If the time $t + t_c$ is significantly long, the dielectric responses function for the polarization current $f(t + t_c) \cong 0$. Consequently, equation (2.4) can be rearranged as follows

$$f(t) \approx \frac{-i_d(t)}{C_0 U_0} \tag{2.5}$$

If the polarization and depolarization current of a composite insulation is known, the average conductivity of the combine insulation can be found by rearranging equation (2.2) and (2.4)

$$\sigma \approx \frac{\epsilon_0}{C_0 U_0}(i_p(t) - i_d(t)) \tag{2.6}$$

The combined conductivity can also be calculated from the nonlinearity factor, which is the ratio of average conductivity at different voltages [61]. According to [62], conductivity, ageing and moisture content of insulation can be estimated from the PDC curve shown in Figure 2.7.

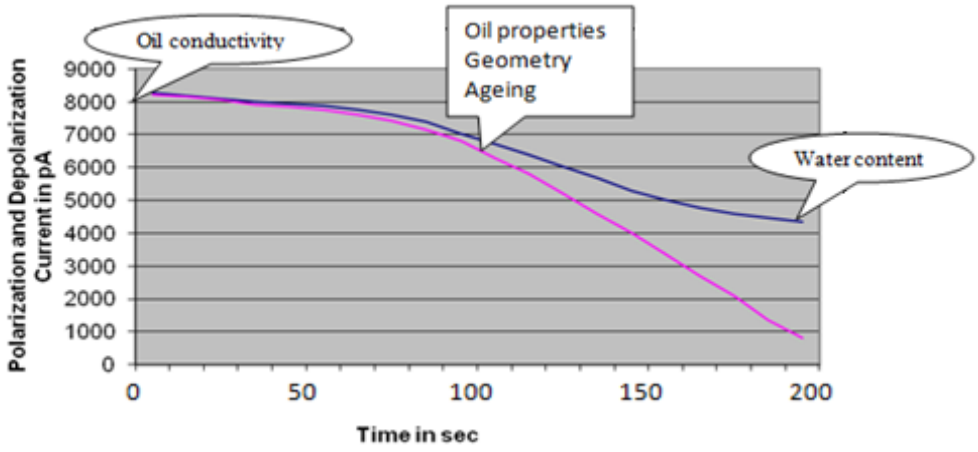


**Figure 2.7:** Oil conductivity, oil properties, geometry, ageing and water content influence on the PDC-Curves [62].

As can be seen from this curve, the PDC value is mainly influenced by the conductivity in a time range t< 100 s. The current increases in proportion to the conductivity. The oil property, ageing and geometry are apparent after 100s and the variation of moisture content is visible after 1000 s. In [63], the authors state that if the inherent nonlinearity of a homogeneous insulation is neglected, the difference between polarization and depolarization current (conduction current) is constant and time independent. Moreover, reference [59] states that, the initial conduction is very sensitive to the oil condition whereas long term current is mostly influenced by the condition of solid insulation. In the case of composite insulation, the difference is time dependent and is influenced by the separate conditions of oil and paper insulation, thus reflecting the true combined conductivity of the transformer's oil paper insulation [64]. Thus, PDC testing can be used to accurately assess the condition of oil-paper insulation. On the contrary, the accuracy of the PDC is dependent on the precise knowledge about the design and the composition of the oil-paper insulation and the measurement process is very time consuming. In practice, the exact design and insulation composition information is not easily available which is considered a major limitation of this method. In [59], a modeling process has been discussed to partially overcome the limitation.

#### 2.3.11.3 Frequency Dielectric Response

Frequency dielectric response (FDR) is a widely accepted technique to diagnose the ageing state and moisture content in the oil-paper insulation of power transformers [65]. As FDR is very reluctant to external frequency (noise) and capable of giving detail analysis, it has received more attention than the RVM and PDC methods [66]. In FDR, the dielectric response of composite oil paper insulation is measured at frequencies between 100 µHz and 1 kHz [65]. The range can vary depending on the moisture quantity in the insulation. However, the prominent resonance effect and impure dielectric response restricts the maximum frequency of FDR to 1 kHz. The ageing of insulation is mainly influenced by ingress of moisture, insulation geometry

and temperature. The amount of moisture and ageing state can be estimated from the correlation of temperature, moisture and insulation geometry with dielectric response spectrum. However, it is hard to separate the impact of moisture, ageing and geometric impact from the dielectric response that is used to quantify the moisture content and ageing state [67]. A detailed process to overcome these limitations based on the dependent variables is presented in [66]. According to [66], in the frequency range of $10^{-3}$-$10^{2}$ Hz, the relative permittivity ($\epsilon_r$) and dissipation factor (*tanδ*) of oil-paper insulation increases in proportion to the moisture. However, ($\epsilon_r$) and *tanδ* are only sensitive to the ageing between 10-3-10-1 Hz. Consequently, the frequency range $10^{-3}$-$10^{2}$ can be used to discriminate and quantify the effect of moisture and ageing on the insulation. However, a recent similar study in [65], states that the dielectric response of some pressboard sample may be used to determine moisture concentration (1%, 2 % and 3%). It was found that the slope of the dielectric response decreases with an increase in frequency. Above 100 Hz, all the sample slopes coincide and become flat. Eventually, the slope of the dielectric response below 100 Hz can be used to assess the condition of transformer paper insulation. According to [68], a typical dielectric response of oil paper insulation is as shown in Figure 2.8.

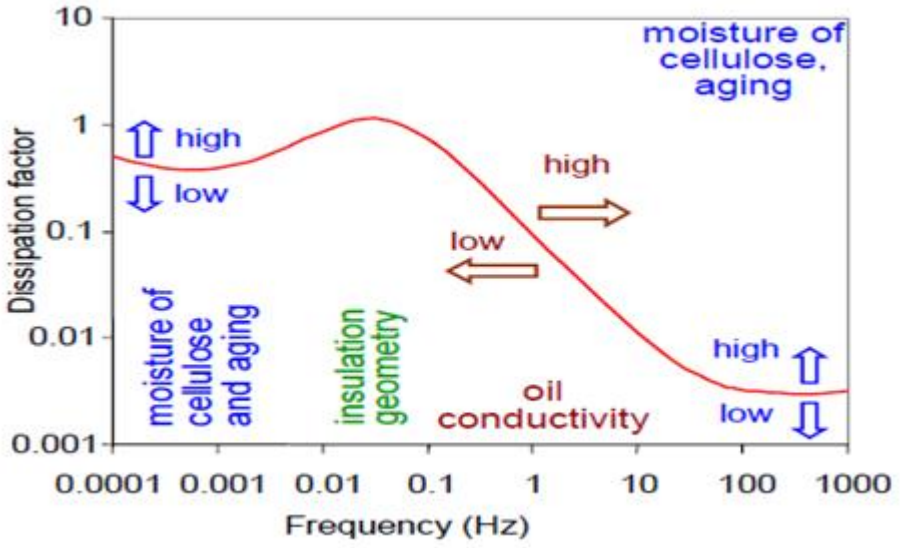


**Figure 2.8:** Dielectric response of oil paper insulation [68].

#### 2.3.11.4 Frequency Dielectric Response

Time-frequency domain dielectric response is the latest technology where the advantages of PDC and FDR have been combined to assess the condition of transformers insulation [69]. At low frequency, the PDC method is faster and represents the ageing of oil and paper insulation. At high frequency, the FDR method is faster than the PDC and can also assess the oil and paper insulation ageing. In this method, the advantages of both FDR and PDC have been combined to develop a faster, intelligent and powerful assessing method. The combined technology makes it possible to measure the dielectric response over a wider range of frequency (0.05 mHz to 5 kHz). The measured response could be compared with factory test data or historical measurement to accurately assess the state of oil and paper/pressboard insulation.

### 2.3.12Partial Discharge Analysis

Partial discharge (PD) is a dielectric discharge in a partial area of electrical insulation system experiencing high electrical field intensity. In many cases, PD phenomena are considered as a preliminary stage of a complete breakdown of the insulation. Consequently, for monitoring the condition of power transformers and to avoid unexpected hazards, PD measurement is used over a long period of time. In transformers, PD can happen in cellulose paper, oil or in the interface of oil-paper insulation when the electric field stress exceeds the breakdown strength of insulation. Any defect such as cavities and voids in solid insulation, gas bubbles or small floating metal particles in oil can damage the uniformity of electrical stress across the insulation and may initiate PD that can lead to a flashover. Additionally, over time insulating material lose its dielectric strength due to continuous electrical, thermal and dielectric stress that directly influences the possibility of PD. According to [70, 71], the inception voltage of PD decreases with an increase of temperature. The PD magnitude and repetition rate increase significantly with the size of gas bubbles in the

oil [72]. The surface discharges on transformer insulation increase and the inception voltage also decreases with an increase in total harmonic distortion [73]. Once PD starts, it propagates throughout the insulation until complete breakdown occurs. Consequently, it is very important to detect, quantify and localize PD during operation [74]. During PD, a range of phenomena like electromagnetic emission (in the form of radio wave, light and heat), acoustic emission (in audible and ultra-sonic ranges), ozone formation and the release of nitrous oxide gases may be observed [75]. By using different types of measurement techniques such as electrical, chemical, acoustic or optical, the PD phenomena can be detected and localized. A short review on different PD assessment methods have been included below.

#### 2.3.12.1Chemical Detection

This is one of the simplest methods that can detect PD chemically by observing the chemical change in the composition of insulating materials. It is based on the collection and measurements of gas and oil samples released from PD activity. To measure PD, two chemical techniques such as DGA and HPLC are currently available. In the DGA test, oil from a transformer is sampled to measure the level of key gases in it. The measured gases are finally analysed by the Duval Triangle Method to detect PD. Although online monitoring of this method is available, the reading, level of gases and classified faults are not calibrated and scientifically correlated [76]. The HPLC method measures the PD by evaluating chemically stable by-products such as glucose during insulation breakdown. As the sample collection and analysis process is time consuming, this method is not suitable for real time monitoring of PD. Moreover, the insufficient standard for assessing the severity of PD from glucose measurement increases the measurement uncertainty. Furthermore, both DGA and HPLC are unable to locate the origin of PD.

### 2.3.12.2Electrical Detection

This method is based on the detection of high frequency electrical pulses produce from a void due to a strong electric stress across it. The test can be performed in either on-line or off-line mode. In the case of off-line mode, a known value of a coupling capacitor is connected in series with the detection impedance that need to connect across the test object. After completing wiring, the circuit is energized from a high voltage AC source. The detection impedance can also be connected in series with test object (see Figure 2.9) for a better signal- to-noise ratio. Although, connecting the impedance in series with test object gives more sensitivity, it is commonly used in series with a capacitor to save the measuring device from potential damage due to the breakdown insulation of test objects. Moreover, the test object needs to be disconnected from ground to allow a detector to be connected in series with it. This is an unusual practice for power transformers. For the on-line mode, the inner grading foil layer of the bushing is used as a capacitor and an inductor is connected to the ground through the outer layer subject to the bushing tab being grounded. The circuit diagram of typical PD measurement methods is shown in Figure 2.9.

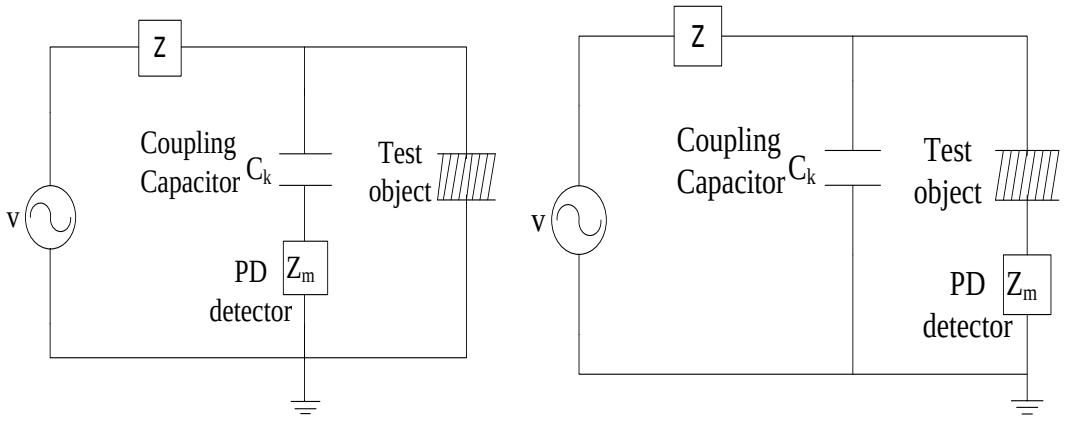


**Figure 2.9:**Measurement of apparent PD by connecting detector at different position.

If PD is present, the void behaves like a capacitor and the voltage across it will continue to increase until breakdown happen. Consequently, the capacitor will be

discharged and the voltage across it returns to zero. The charging and discharging process will continue throughout the cycle as long as the AC supply is connected. According to [77], the repetition rate of charging and discharging is over 1 MHz. The discharged energy will mostly be compensated by the coupling capacitor which is converted to a voltage signal through the detection impedance. Comparing with the AC cycle, the converted signal can give valuable information about PD like pulse shape, intensity, relative phase location, severity of insulation damage. Although this method is very sensitive to noise, time consuming and cannot localize PD sources, it can provide the most accurate result compared with other methods [78-79].

#### 2.3.12.3 Acoustic Detection

The acoustic emission method (AE) measures the amplitude, attenuation or phase delay of acoustic signals that are produced from PD, to detect and locate the position of PD. The AE is a PD phenomenon-based method that senses acoustic waves in a frequency spectrum up to 350 kHz to detect PD [78, 80]. During PD, mechanical stress of materials next to the point of origin, cause an audible or non-audible AE signal to be produced. In order to detect the signal a number of different sensors like piezoelectric transducers, microphones, accelerometers, sound-resistance sensors and fibre optic acoustic sensors are commonly used [81]. The sensors are mounted on the outside wall of a transformer tank at multiple positions. The relative travel times that the signal reaches multiple sensors are triangulated to detect the source of PD and assess the severity of insulation defect [78]. Although, AE signals are interfered with by the low frequency mechanical vibration of a transformer, compare to electrical detection, it shows strong immunity against electromagnetic interference. Due to this special characteristic and high signal to noise ratio (SNR), this is an ideal method for online PD detection [81]. On the contrary, measurement complexity, extensive data processing and low sensitivity to the damping of oil, core, conductors and main tank are considered the main limitation of this method [80].

#### 2.3.12.4Ultra-High Frequency Detection

The ultra-high frequency (UHF) detection is a routine and continuous PD monitoring procedure for power transformers. This method measures the electrical resonance in the frequency range between 100 MHz and 2 GHz to detect and locate PD [82]. As the sensor is installed inside the transformer, the shielding effect of the tank helps to suppress any external noise [83]. Moreover, the low signal attenuation in oil insulation and the high sensitivity for an on-site measurement has increased the use of this method to test transformers. To measure PD, several sensors equipped with high sensitivity wideband antennas are installed inside the transformer tank. A calibration technique is applied before commencing the test to measure the sensitivity of the sensors and understand their exact phase and amplitude relationship. The position of the sensors is chosen in such a way that at least three sensors in parallel can detect signal from relevant parts of a transformer like the windings or tap changer. High frequency cables with known attenuation and phase shift must be used for connecting the sensor to the control module. Finally, using the measured amplitude and travel time of the signals and applying established triangulation methods, a PD phenomenon may be detected and its source localized [84]. A detailed calibration and sensitivity checking procedure is available in [82].

#### 2.3.12.5Optical Detection

Optical detection is one of the latest technologies using to detect and locate PD of transformers. During PD, beside electromagnetic emission, light spectra such as ultraviolet, visible and infrared always radiate from the various ionization, excitation and recombination process. The radiated spectra transport information about the energy level of discharge that can be measured by an optical sensor to detect and locate PD [85]. The amplitude of the energy depends on the surrounding insulating material. The optical spectrum in oil due to PD starts at approximately 400 nm and can extend into the infrared region [85]. The wavelength can vary depending on the

insulation type and surrounding medium. Consequently, a sensor that can show the correct optical spectrum is crucial for PD detection. For transformers, a single or multimode fiber-optic sensor is immersed in the oil tank. According to [86], the equipment setup for optical detection is shown in Figure 2.10.

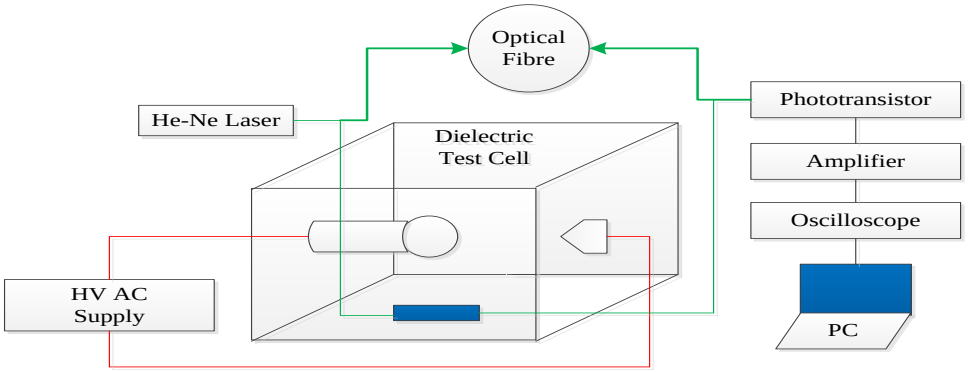


**Figure 2.10:** Schematic diagram for optical PD detection [86].

In the diagram, the setup consists of a He-Ne laser, phototransistor, amplifier, oscilloscope and multimode sensor to detect PD. He-Ne laser is operated in continuous wave mode to emit coherent power of 10 mW [86]. The PD source is simulated by using a HV source across the electrodes. The sensor collects the signals from the origin and guides it to the receiver (phototransistor). Output of the phototransistor automatically changes with the change of light intensity. After necessary conversion (optical to electrical) and amplification, the received signal is displayed by an oscilloscope to predict PD. Further analysis is required in computerized software to locate the PD source. As the method only receives optical signals, it is completely free from electromagnetic interference. Moreover, the high sensitivity and measurement capability in a wide bandwidth have made the method most popular in the high voltage industry. A detail procedure and analysis of this method is available in [85, 86].

#### 2.3.12.6 High Frequency Current Transformer Installation

An inductive coupling sensor such as a high frequency current transformer (HFCT) can be used to detect online PD in a power transformer [87]. In the HFCT method, an externally accessible loop (PD loop) is made on the LV side by connecting the cable shield next to the bushing, directly to the main ground. In order to monitor PD, a HFCT is permanently clipped around the loop cable. If active PD is present, it will generate a high frequency electromagnetic pulse that will transmit through the earth conductor. The HFCT will pick up this radiation due to induction. Although, this method allows online PD monitoring, it is less sensitive, susceptive to noise and the magnitude of the detected signal is very low. Consequently, for analysing the data, an amplifier must be installed before analysing devices such as oscilloscope, PD detectors or pulse counters [87-88].

#### 2.3.12.7 Transfer Function Measurement

A transformer winding's high frequency transfer function (TF) can be used to evaluate and localize the origin of PD that initiates within the windings [80, 89-90]. Each transformer windings may be divided into numerous winding sections. If the transfer function of individual sections of each winding is known, the transfer function of all windings can be calculated [91]. If PD is initiated at unknown allocation along the transformer winding, a signal will travel to both the bushing and neutral terminals, and will be distorted as it propagates. The distortion rate depends on multiple factors including the distance from origin to the detection impedance. The distorted PD signal can be measured either using narrow band or wide band techniques [80]. Although, the offline narrow band method cannot localize PD, it can quantify the apparent charge and measure the repetition rate, individual pulse energy and phase shift with the power frequency [80]. In accordance with IEC 60270, a frequency range of 9 to 30 kHz is suitable for this method. The wide band method uses the same technique as narrow band to detect PD. In addition, it can localize the

PD signal by analyzing the shape of it. In accordance with [92], about 10 MHz bandwidth is optimal for this method. In order to localize PD, this method uses the concept of a transfer function. Following the known sectional transformer function of a winding, it calculates the shape of a PD signal at multiple points within the windings from both bushing and neutral terminal. The point at which the calculated signals are comparable with the practical observations pinpoints the origin of PD [91]. On factory test, the accuracy of this method is satisfactory where background noise is controlled by some external means. During on-site test, background noise and the transformers own noise, which is similar in nature to PD, directly affect the sensitivity and accuracy of this method [80]. The noise from multiple sources has to travel through the complete winding, but the PD signal will travel through only some sections of the winding. Consequently, noise will face more attenuation than the PD signal [91]. Additionally, the calculated transfer function of the noise signal will be the same as the transformer's transfer function. This principle can be used to isolate noise in a laboratory environment. During on-site measurement, optical transducers, digital filters, amplifiers, windowing (software) and common mode rejection technique can be used to suppress the spurious sinusoidal and pulse shaped noise [91]. The accuracy of this method is dependent on the uncertainty of the windings' sectional transfer function. For old transformers, where transfer function is measured from step response, it can only localize the origin of PD within a quarter of the complete winding length. If the sectional transfer function of windings is known, the error of this method is only few percent [91]. A comparison of different available PD measurement methods has been summarized in Table 2.7.

**Table 2.7:** Comparison of different PD measurement techniques.

| Method | Advantage | Disadvantage |
|---|---|---|
| Electrical | High sensitivity<br>High measurement precision<br>Good in laboratory environment<br>Calibration of the apparent charge | Difficult to apply onsite measurement<br>Influenced by electromagnetic interference<br>Unsuitable for long-term monitoring |
| UHF | Better sensitivity then AE [84]<br>Higher immunity against noise<br>Lower signal attenuation | No direct correlation with conventional measurement following the IEC60270<br>Sensitivity need to check for individual transformer due to identical internal impedance<br>Insufficient scope to install sensors in old transformer |
| Chemical | Good in laboratory environment<br>High sensitivity | High uncertainty due to unknown relationship between glucose and severity |
| AE | Good in real time monitoring<br>Noise immunity<br>Detect the position of PD | Low sensitivity<br>Influenced by external noise |
| Optical | Immune to electromagnetic interference<br>Visualization of PD is possible<br>High sensitivity<br>High frequency response<br>Easy portability | No significant disadvantage |
| HFCT | Capable to do real time monitoring<br>Easy to install | Cannot detect source even the nearby phase<br>Influenced by external interference |
| TF | Good in laboratory environment<br>Capable to detect and locate PD | On-site test, vulnerable to background noise |

### 2.3.13 Leakage Reactance or Short Circuit Impedance Measurement

Short circuit impedance (SCI) is a frequency dependent parameter has been used over many years to detect winding deformation and core displacement of a transformer. Short circuit current is considered one of the main symptoms of mechanical deformation of core and windings. Any change in mechanical geometry of a transformer would change its SCI. A high value of SCI has a direct impact on the voltage regulation due to the significant amount of voltage drop across it. On the

contrary, low values indicate short circuit current. A deviation of ±3% is an indication of winding deformation and core displacement [93]. However, transformers over 100 MVA should not exceed ±1% from their nameplate value [94]. Ampere's force law states that, an attractive force will be observed between conductors if they carry current in same direction and vice versa. According to this formula, it can be summarized that the forces from one HV (or LV) winding loops to the next will be attractive but the force between HV and LV windings is repulsive. Eventually, the axial flux produced from short circuit currents create compressive force on inner windings but tensional force on outer windings that try to rupture the winding conductors [95-96]. The SCI can be measured either using 3 phase equivalent test or per-phase test methods. In order to measure SCI, an input voltage must be applied in HV windings one after another keeping the corresponding LV winding shorted. The measurement setup for SCI has been shown in Figure 2.11 (a) and (b).

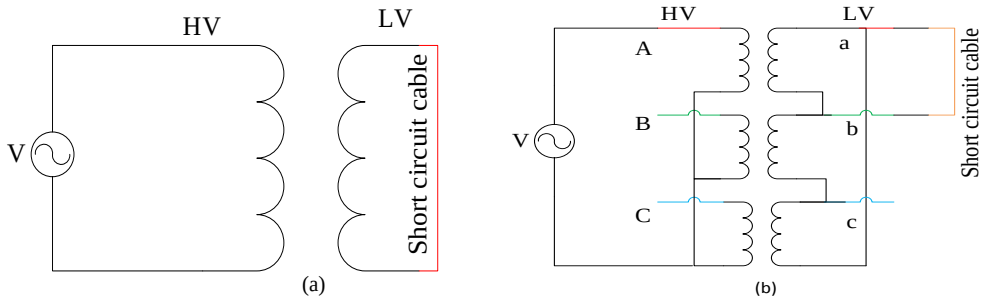


**Figure 2.11:** Circuit connection for single phase (a) and three phase (b) measurement.

To reduce the resistance of the shorting cable, it should be minimal in length and the cross-sectional area must be more than 30% greater than the winding conductors to handle a large amount of current [97]. The 3-phase equivalent test allows comparing the result with nameplate value and between phases to assess the mechanical integrity of a transformer. This result could be used as a finger print for future tests. Per-phase test can be performed as a follow up test. This method has a number of limitations [97] such as

i. It does not provide detailed information of windings state due to single frequency (50 or 60 Hz) test.
ii. It is less sensitive as significant deformation is required to cause a discrepancy.
iii. It cannot detect axial deformation like tilting or bending of conductors.

### 2.3.14 Ratio Test

The turn ratio test of a transformer (TTR) is used to detect open or short circuits between turns of the same winding. A deviation of more than 0.5% is an indication of insulation failure, short circuit or open turns [4]. In the TTR test, the ratio needs to check at all taps position. The TTR can provide evidence of gross winding resistance deviation. It is recommended to start the test at low voltage (100 volts) and verify the result against the nameplate value. If no significant deviation is found then it is safe to increase the voltage up to the rated voltage. This approach helps to avoid unwanted insulation breakdown.

### 2.3.15 Winding Resistance Test

Winding resistance test can be used to detect loose connection, broken stands or poor contacts in LTC. The resistance must be measured at all taps to verify the LTC contact resistances. The result can be analyzed by comparison with name plate information, historical data or between phases. When comparing with nameplate values, the test data must be converted to the reference temperature used during the factory test. This test could be used as a supplement of DGA and TTR, if DGA indicates generation of hot metal gases such as methane ($CH_4$), ethane ($C_2H_6$) and acetylene ($C_2H_2$) [4]. Depending on the percentage of deviation, a manual internal inspection may be organized.

### 2.3.16 Core to Ground Resistance Test

In most modern transformers, the core is intentionally connected to a single ground point through a small bushing, preventing circulating currents and detecting multiple grounds. During transportation, the grounding system could become loose or damaged. The core to ground resistance test is used to detect unintentional core grounding and check the integrity of intentional ground points. The test can be used as a supplement of DGA when it indicates hot metal gases. For checking multiple grounds, the insulation resistance between the core and tank is measured, while the intentional ground cable is kept open. The measured resistance may be used to detect and classify the severity of multiple grounds as indicated in Table 2.8.

**Table 2.8:** Insulation condition based on core-to-ground resistance [4].

| Resistance Value | Condition |
|---|---|
| Resistance >1000MΩ | New transformer |
| Resistance >100MΩ | Aged insulation |
| Resistance 10-100MΩ | Degraded insulation |
| Resistance <10MΩ | Destructive circulating current |

### 2.3.17 Sweep Frequency Response Analysis

The sweep frequency response analysis (SFRA) is a non-destructive, highly accurate, cost-effective and sensitive method that is used to detect mechanical deformation and displacement of a transformer core and windings [97]. Over time, the importance of SFRA is increasing due to its high sensitivity for detecting mechanical failures of a transformer. It can detects faults such as winding deformation (axial or radial), winding movement, tilting, hoop buckling, inter-turn faults, partial collapse of a winding, multiple core grounding, poor tank grounding and loose contact at HV and LV winding terminals without opening the main tank [97-98]. Generally, short circuit current, careless transportation, natural disasters like earthquakes and

combustible gas explosions inside a transformer are considered the main reasons for core and windings deformation [97]. Frequency response is a unique fingerprint of each transformer that changes with the onset of a mechanical defect. The impedance of a transformer, which is a frequency dependent parameter, change with mechanical deformation, leading to modified frequency response [99]. After commissioning, short circuit incidents or transportation, it is recommended to perform FRA to ensure the windings and core integrity of transformers. In a two-winding three-phase transformer, SFRA measurement can be performed for either transfer function or impedance measurement. Transfer function can be measured from non-transferred measurement and impedance can be measured from transferred measurement [98]. The measured transfer function can be used to detect short circuited turns of the windings [100]. The circuit diagrams of a transferred measurement and non-transferred measurement are shown in Figure 2.12 and 2.13 respectively.

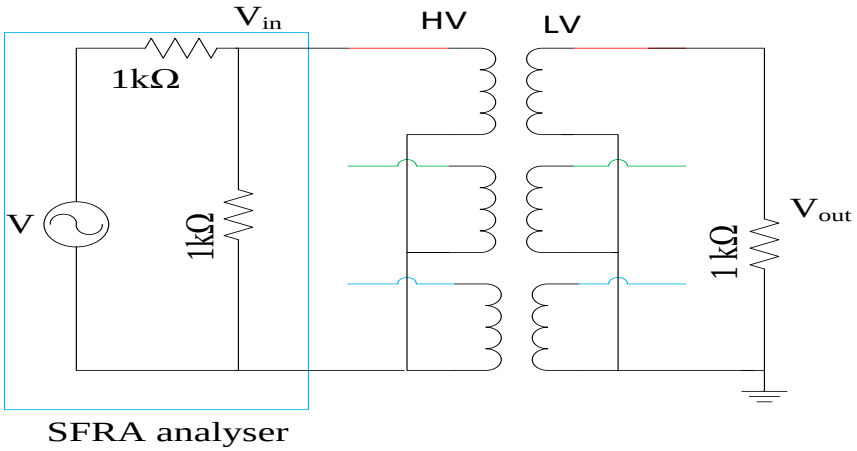


**Figure 2.12:** Transferred measurement.

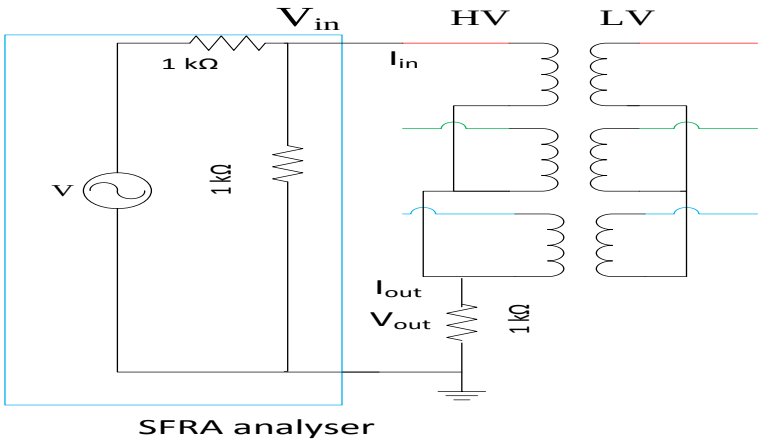


**Figure 2.13:** Non-transferred measurement.

In transferred measurement, an input voltage $V_{in}$ is injected at each HV terminal and the output voltage $V_{out}$ is measured from the corresponding LV winding, keeping the neutral terminals grounded and the other non-tested terminals floating or shorted to the main tank through 1 kΩ resistance [98, 101]. This measurement is acceptable only at frequencies lower than 8 kHz [102]. At higher frequency, it is influenced by inter-winding capacitance. Consequently, this test highlights the influence of coupling capacitance between HV and LV windings [98]. For the non-transferred measurement, input voltage is measured from HV windings and output voltage is measured from the respective neutral terminal of the same winding, keeping non-tested HV terminals open and LV terminals open or short circuited. In order to avoid the damping oscillation and reduce the impact of stray capacitance, it is recommended to add some resistance (1 kΩ) with both non-excited and excited terminals [98, 101]. After conducting SFRA and recording the response, the next important task is to analyse the result to verify the mechanical integrity. To analyse the data, it is important to know the upper limit of the frequency range for SFRA that is useful for fault detection. According to [98], the maximum reproducible range is at least 1 MHz. At higher frequencies (over 1.5 MHz), the distributed capacitance tended to work as a shunt capacitor with winding inductance, winding lead effects is

apparent and recurrence of resonance is less pronounced [101]. It is commonly accepted that the low frequency range (1 to 100 kHz) is useful for detecting core deformation, the medium frequency range (100 to 600 kHz) is dominated by winding structure and the high frequency range (600 kHz to 1 MHz) can identify problems in connection leads [97]. According to [103], the frequency response in different sections of the spectrum is shown in Figure 2.14. The frequency range can be extended up to 2 MHz for detecting minor faults like conductor bulging, small displacement and inter-turn fault [104]. Faults close to either high voltage terminal or low voltage terminal can be detected using the impedance value of low-voltage or high-voltage windings respectively, setting the opposite side open-circuited [104]. Although, SFRA can detect wide ranges of mechanical distortion sensitively, the interpretation and analyzation of data is not easy. As there is no standard procedure, it is still dependent on experts' judgement, visual inspection, statistical indices like standard deviation, correlation coefficient and relative factor, and comparison with historical data. If historical data is not available, data can be analysed by comparing between different phases of the same transformer or twin/symmetrical transformers. For comparing data between phases, the nominal difference must be allowed for due to any inherent constructional asymmetries.

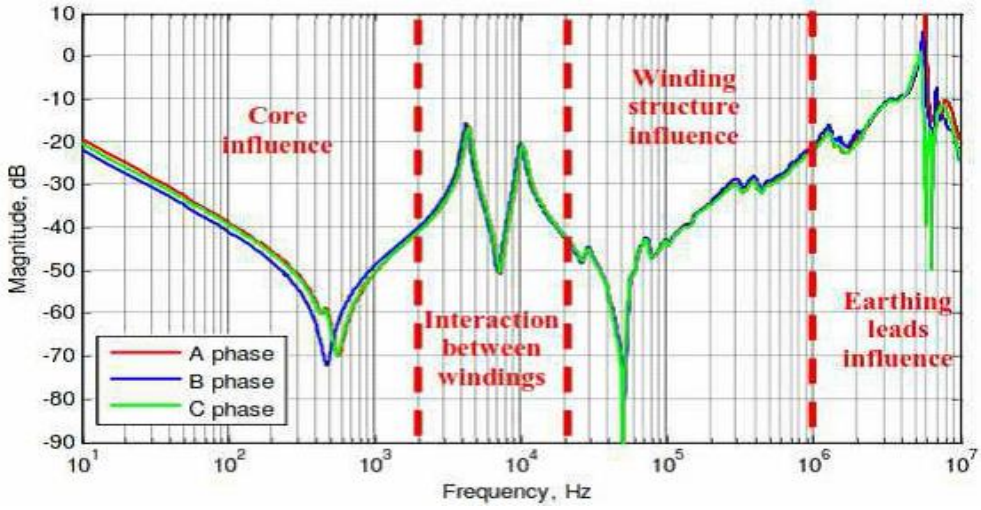


**Figure 2.14:** Transformer sweep frequency response [103]

## 2.4 Calculation of Residual Life

Due to economic and technical reasons, beside condition monitoring, the life time estimation of transformers has gained more attention from utilities. The estimated life time can help them to setup a strategy for refurbishment and develop a forecasting system for future investment. Over the decade, different techniques like health index calculation, probability of failure estimation, statistical depreciation analysis, correlation of operating temperature and DP with insulation life are using to calculate the remaining service life of transformer. A review of different life time estimation methods can be summarized as follows.

### 2.4.1 Hot Spot Temperature Calculation

The hot spot temperature (HST) of a transformer has a direct impact on its insulation life. The ageing rate of insulation is accelerated with the increase of HST. According to industry loading guides (IEE, IEC, CIGRE and ANSI), temperature is the principle factor for reducing the service life of transformers. The nominal HST of a transformer oil-paper insulation is considered as 110 $^{o}$C and could be acceptable up to 140 $^{o}$C [31, 49]. The effect of ambient temperature, windings faults, faulty cooling systems, over loading and unwanted harmonics (non-sinusoidal load) increase the HST and reduce the life of transformers. Consequently, the remaining service life of a transformer can be calculated from the correlation of HST and ageing rate of insulation. According to [105], the equation of HST in $^{o}$C can be expressed as follows

$$\theta_{HS} = \theta_A + \delta\theta_{TO} + \delta\theta_H \tag{2.7}$$

where $\theta_{HS}$ is the hot spot temperature, $\theta_A$ is the ambient temperature, $\delta\theta_{TO}$ is the top oil temperature raise and $\delta\theta_H$ is the winding HST raise over top oil temperature. The

value of $\delta\theta_{TO}$ is directly influenced by the transformer's load. According to [106], the impact of load variation on $\delta\theta_{TO}$ can be expressed by the following equation

$$\delta\theta_{TO} = (\delta\theta_{TO.U} - \delta\theta_{TO.i})(1 - e^{-t/\tau_{TO}}) + \delta\theta_{TO.i} \quad (2.8)$$

where $\delta\theta_{TO.U}$ is the top oil temperature gradient at ultimate state, $\delta\theta_{TO.i}$ is the initial top oil temperature gradient, $t$ is the duration of loading (in hours) and $\tau_{TO}$ is the oil time constant (in hours). However, winding HST is also influenced both by the operating load and its duration. A correlation between winding HST and loading time for various loads can be modeled by the following equation [106].

$$\delta\theta_{H} = (\delta\theta_{H.U} - \delta\theta_{H.i})(1 - e^{-t/\tau_{W}}) \quad (2.9)$$

where $\delta\theta_{H.U}$is the hot–spot temperature gradient at ultimate steady state, $\delta\theta_{H.i}$ is the initial temperature gradient, $t$ is the loading duration in hour and $\tau_W$ is the winding time constant (in hours). If the $\theta_{HS}$ is known, the Arrhenius Dakin formula can be used to calculate the life consumption. According to the formula

$$Per\ unit\ life\ consumption = Ae^{\left(\frac{B}{273+\theta_{HS}}\right)} \quad (2.10)$$

where $A$ and $B$ are the constants. The value of $A$ and $B$ represent the characteristics of insulation. The typical value of $A$ and $B$ are $9.8\times10^{-18}$ and 15000 respectively [105]. The ratio of per unit life at design temperature (110 $^{o}$C) relative to the per unit life at any other operating temperature ($\theta_{HS}$) is known as the ageing acceleration factor. According to [107], the ageing acceleration factor can be expressed by the following equation

$$F_{AA} = e^{\left(\frac{15000}{383} - \frac{15000}{\theta_{HS}+273}\right)} \quad (2.11)$$

According to [108], the loss of unit life and its percentage in a given period of time for a transformer can be approximated as:

$$`F_{EQA} = \frac{\sum_{n=1}^{N} F_{AAn}\,\delta t_n}{\sum_{n=1}^{N} \delta t_n} \quad (2.12)$$

where $F_{EQA}$ is the equivalent ageing factor, $F_{AAn}$ is the aging acceleration factor during the time interval $\delta t_n$ and N is the total number of time intervals.

$$\%\ Loss\ of\ life = \frac{F_{EQA} * t * 100}{Insulation\ design\ life} \quad (2.13)$$

In order to avoid the complexity of this calculation process, annual estimation of cyclic ambient temperature and load have been considered. Consequently, a transformer's unit life can easily be estimated from the hourly basis annual temperature and load curve. However, to improve the reliability of a transformer's estimated residual life, a more sophisticated modelling approach is necessary that can incorporate other ageing factors along with the environmental effect of ambient temperature and HST more accurately.

### 2.4.2 Concentration of Furan and DP Value Measurement

The DP value calculation and the furan concentration measurement is another method that is using to calculate the residual life of a transformer by assessing the degradation of the cellulosic paper insulation. Generally, for unaged paper, the value of DP is expected to be 1000-1200 [109-110], whereas paper having a DP value of 200-300 is considered to have reached its end of life [111]. Over time, due to chemical reactions, the DP value of a transformer paper decreases due to the influence of temperature, water content and oxygen. Consequently, it can provide valuable information about the mechanical strength and the degradation state of cellulose. According to the Arrhenius relation, the DP value can be linked with

temperature in terms of a time dependent reaction rate (k) by using the following equation [111]

$$DP(t) = \frac{DP(t_0)}{1+DP(t_0) * \int_{t_0}^{t} k(t)dt} \quad (2.14)$$

where $k = A * e^{-E_a/RT}$,$A$ is a constant that depends on the water content, oxygen or acidity, $E_a$ is the minimum activation energy in J/mol, required to start the chemical reaction, T is the temperature (in degrees Kelvin) and $R$=8.314 $mol^{-1}K^{-1}$ is the ideal gas constant. The DP value after any aging period $t_n$can also be calculated by the following Emsley's equation [112].

$$DP_n = \frac{1}{A*e^{-Ea/RT}*t_n + \frac{1}{DP_{n-1}}} \quad (2.15)$$

where the value of *A* is dependent on both the water content and the dissolved oxygen gas but not on the temperature [112-113]. Finally, the loss of life after any time period $t_n$ can be calculated by dividing the aging during the time interval by the expected life at a particular temperature [112]. Consequently, the life lost at a particular time interval can be expressed as follows

$$LL_n = \frac{t_n}{\frac{\frac{1}{200}-\frac{1}{1000}}{A} * e^{Ea/RT}} \quad (1.16)$$

The percentage of residual life

$$\%RL = (1 - \sum_{n=1}^{N} LL_n) * 100 \quad (1.17)$$

where *N* is the total number of time interval and $\%RL$ for a new transformer has been considered 100%.

As direct testing of DP value for a live transformer is critical and requires that the transformer be disconnected from the live network [42], the furan concentration is widely used to estimate the remaining residual life of a transformer. The furan (2-FAL) is released from the degradation of materials produced by the breakdown of cellulose and maintains an inverse relationship with DP. Consequently, different

correlation techniques have been developed to relate the furan concentration with DP to avoid the complexity of direct DP measurement. In [114], the value of DP has been correlated with the furan concentration using the following equation.

$$DP = \frac{\log(2FAL) - 1.51}{-0.0035} \tag{2.18}$$

where the concentration of furan (2FAL) is used in mg/l.

A summary of different correlation methods between DP and furan are also available in [115]. The calculated DP value, based on furan concentration, is ultimately used to calculate the residual life of a transformer. The benefit of this method is that, the error can be reduced by updating the measured quality parameters and DP value can be verified from the measured value of furan.

### 2.4.3 Probability of Failure Calculation

Failure of a transformer occurred after certain level of insulation and performance degradation. The probability of failure can be calculated by characterizing the degradation as a function of time. According to [116], the degradation model of transformers can be expressed by the following differential equation

$$\frac{d\chi}{dt} = -A_F R_0 \chi^k \tag{2.19}$$

where $A_F$ is an ageing factor, $k$ is a shape parameter, $R_0$ is a constant and $\chi$ is a performance parameter representing the ratio of initial and later performance. The ageing factor can be calculated from the assessment and observation of selected properties. As temperature increases the ageing rate of insulation, the effect of temperature on paper insulation degradation has been approximated by the following equation.

$$A_F = \delta^{\frac{1}{T_0}[\theta - 25]} \tag{2.20}$$

where $\theta$ and $T_0$ are the temperature in Celsius and Kelvin respectively and $\delta$ is the model coefficient. Suppose, a transformer fails at time *t*, for a degradation level$\chi_f$, the probability of failure for the transformer can be expressed as follows [116]

$$P(\chi) = 1 - exp\left[-(\frac{\chi}{\chi_f})^{\eta}\right] \tag{2.21}$$

where $P(\chi)$ is the probability of failure, $\chi$ is the initial degradation, $\chi_f$ is degradation after time *t* and $\eta$ is the shape parameter. Finally, the calculated probability of failure (99%) can be used to estimate the remaining service life of a transformer. According to [1], the remaining service life of a transformer in terms of probability of failure can be expressed by the following equation

$$\tau_R = \frac{\tau_{P(\chi)\approx 80-99\%} - \tau_e}{A_F} \tag{2.22}$$

where $\tau_R$ is the remaining life, $\tau_{P(\chi)}$ is the age at which probability of failure is in the range 80-99% and $\tau_e$ is the effective age. To get a safety margin for avoiding failure, it is recommended to calculate the remaining life based on slightly earlier failure probability (80%) than the 99%. This margin is dependent on a particular utility's strategy and maintenance practice. Additionally, the financial risk of replacing a faulty transformer and the consequences of an outage need to be considered. The probability of a transformer's failure at any time is dependent on the remaining insulation strength and active stress on that particular time. Over time, insulation loses its mechanical and dielectric strength and the probability of failure increases. The failure probability of transformers follows the typical bathtub curve, where the initial failure rate is high but greatly reduces and flattens after few years of faultless operation until it starts to steadily climb again as the transformer starts to age [31].

### 2.4.4 Health Index Calculation

The percentage health index (HI) calculation is one of the reliable methods for life time estimation of a transformer. In HI calculation, a large number of routine and diagnostic tests are combined for explicitly assessing the overall condition of a transformer. The following equation is typical of HI calculations [1]

$$(\%)HI = 60\% * \frac{\sum_{i=1}^{n-3} C_i DI_i}{\sum_{i=1}^{n-3} CD_{i\max} * C_i} + 40\% * \frac{\sum_{i=n-2}^{n} C_i DI_i}{\sum_{i=n-2}^{n} CD_{i\max} * C_i}. \quad (2.23)$$

Here $DI_i$ are the index scores; $C_i$ are the weight factors of each individual test, n is the number of tests (weight criteria) for a transformer and its LTC respectively. The formula allocates 40% of the total weight to the LTC and remaining 60% models the causes of direct transformer failure, based on a survey conducted by the CIGRE group. This could vary depending on the failure statistic of utilities [117]. A detail of this method is available in [1]. One of the drawbacks of this linear approach is that it is less sensitive to the individual test. For instance, if the condition of a bushing is very poor which could potentially lead transformers into a catastrophic failure, the overall HI score will not be changed significantly. To overcome the limitation, the test results can be combined in a multiplicative way so that if one test result is very poor, the overall HI score will be very low. The calculated HI can be correlated with approximate expected lifetime as follows in Table 2.9.

**Table 2.9:**Health index and remaining lifetime [1].

| Health Index | Description | Approximate Expected Lifetime |
|---|---|---|
| 85–100 | Minor deterioration of a limited number of components. | More than 15 years |
| 70–85 | Significant deterioration of some components. | More than 10 years |
| 50–70 | Widespread significant deterioration. | Up to 10 years |
| 30–50 | Widespread serious deterioration. | Less than 3 years |
| 0–30 | Extensive serious deterioration. | At end-of-life |

## 2.5 Conclusions

Transformers are unusual among industrial plant, since many of their operating components are not amenable to direct visual inspection as they are obscured within a bath of oil. This has necessitated a wealth of ingenious techniques that judge a transformer's operating condition from a diverse set of indirect measurements. This paper has investigated a wide range of established diagnostic tests to identify the most influential parameters on transformer performance and service life. To improve the measurement accuracy and detect fault types, testing methods have been organized following their sensitivity and detection capability against faults and insulation degradation. Based on the fault detection capability, routine and diagnostic tests have been summarized in Table 2.10. As previously stated, 70% of common faults can be diagnosed by DGA alone, but additional tests are needed to indicate when mechanical faults have occurred.

Few power transformers are privately owned and most are operated by utility companies that subject their assets to regular online monitoring and less frequent offline maintenance. The issue these companies face is targeting a limited pool of resources to get the greatest benefit to their assets whilst simultaneously minimizing the risk of unexpected and catastrophic failures. It is expected that condition monitoring and lifetime estimation approaches will help to correlate various tests to measure the actual level of insulation and performance degradation. For improving reliability, relevant industrial standards and survey results, such as CIGRE, IEEE and IEC, have been used on selected methods for understanding and interpreting the test results. These analytical and diagnostic techniques will help the maintenance engineers to interpret the test results and suggest the important parameters of transformers that need to be monitored. These techniques also help utilities to prevent unexpected failures and provide justification to asset manager for replacing unreliable aged transformers through proper prediction. This review provides a snap shot of current tests and power transformer condition monitoring techniques. This is

an area where there is significant ongoing research to better understand the characteristics of the various tests and to devise better methods for combining test results to monitor the condition of these expensive and critical devices. As the installed base of assets age, it seems likely that the importance of these techniques will only continue to increase.

**Table 2.10:** Comparison between online, routine and diagnostic tests for fault detection.

| Name of the tests | Online monitoring | Routine test | Diagnostic test | Type of faults detection | | |
|---|---|---|---|---|---|---|
| | | | | Electrical | Mechanical | Thermal |
| DGA | X | X | X | X | | X |
| Oil testing | | X | X | X | | X |
| Furan analysis | | | X | X | | X |
| DP measurement | | | X | X | | |
| SFRA | | X | X | | X | |
| Power factor measurement | X | X | X | X | X | |
| Leakage reactance | | | X | | X | |
| Insulation resistance | | X | X | X | | |
| PD measurement | X | | X | X | | X |
| Turns ratio measurement | | X | | | | X |
| Dielectric response analysis | | | X | | | X |
| Winding resistance | | X | | | | X |
| Core-to-ground resistance | | | X | | | X |
| Excitation Current | | | X | | | X |

## References

[1] A. Jahromi, R. Piercy, S. Cress and W. Fan, An approach to power transformer asset management using health index, IEEE Electr Insul Mag, Vol. 2, pp. 20-34, 2009.

[2] T.K. Saha and P. Purkait, Investigation of an expert system for the condition assessment of transformer insulation based on dielectric response measurements, IEEE Transactions onPower Delivery, Vol. 19, pp. 1127-1134, 2004.

[3] E. Gockenbach and H. Borsi, Condition monitoring and diagnosis of power transformers, In: International conference on condition monitoring and diagnosis, 2008. CMD 2008. IEEE, pp. 894-897.

[4] X. Zhang and E. Gockenbach, Asset-management of transformers based on condition monitoring and standard diagnosis [feature article], IEEE Electrical Insulation Magazine, Vol. 24, pp. 26-40, 2008.

[5] M.R. Florian Predl, Case studies on Tap Changer Diagonostics Using Dynamic Winding Resistance Measurement. Omicron Seminar, Perth WA, 24 April 2015.

[6] A.D. Ashkezari, T.K. Saha, C. Ekanayake and M. Hui, Evaluating the accuracy of different DGA techniques for improving the transformer oil quality interpretation, In:21st Australasian Universities Power Engineering Conference (AUPEC), 2011, pp. 1-6.

[7] V. Arakelian, Effective diagnostics for oil-filled equipment, IEEE Electr Insul Mag, Vol. 6 , pp. 26-38, 2002.

[8] Guidelines for life management techniques for power transformers,CIGRE, Technical Brochure 227, 2003.

[9] IEEE guide for the interpretation of gases generated in oil-immersed transformers, IEEE Std. C57.104, 2008.

[10] S. Tenbohlen and F. Figel, On-line condition monitoring of power transformers, In: IEEE Power Engineering Society Winter Meeting, pp. 2211-2216, 2000.

[11] IEEE Guide for the Interpretation of Gases Generated in Oil-Immersed Transformer, IEEE Std C57.104, 1991.

[12] A. Akbari, A. Setayeshmehr, H. Borsi and E. Gockenbach, A Software Implementation of the Duval Triangle Method, in: IEEE international symposium on electrical insulation, 2008, pp. 124-127.

[13] IEC International Standard for Mineral oil-impregnated electrical equipment in service – guide to the interpretation of dissolved and free gas analysis, International Electrotechnical Commission, IEC60599:2.1, 2007.

[14] S.N. Hettiwatte and H.A. Fonseka, Analysis and interpretation of dissolved gases in transformer oil: A case study, In: International Conference on Condition Monitoring and Diagnosis, 2012, pp. 35-38.

[15] M.M. Islam, G. Lee and S.N. Hettiwatte, A nearest neighbour clustering approach for incipient fault diagnosis of power transformers, Electrical Engineering,doi:10.1007/s00202-016-0481-3, pp. 1-11, 2016.

[16] A.E.B. Abu-Elanien, M.M.A. Salama and M. Ibrahim, Determination of transformer health condition using artificial neural networks, In: 2011 International symposium on innovations in intelligent systems and applications (INISTA), 2011, pp. 1-5.

[17] M. Pal and G.M. Foody, Feature Selection for Classification of Hyperspectral Data by SVM, IEEE Transactions on Geoscience and Remote Sensing, Vol. 48, pp. 2297-2307, 2010.

[18] A.E.B. Abu-Elanien, M.M.A. Salama and M. Ibrahim, Calculation of a Health Index for Oil-Immersed Transformers Rated Under 69 kV Using Fuzzy Logic, IEEE Transactions on Power Delivery, Vol. 27, pp. 2029-2036, 2012.

[19] N.A. Bakar and A. Abu-Siada, Fuzzy logic approach for transformer remnant life prediction and asset management decision, IEEE Trans Dielectr Electr Insul, Vol. 23 pp. 3199-3208, 2016.

[20] M.M. Islam, G. Lee and S.N. Hettiwatte, Incipient fault diagnosis in power transformers by clustering and adapted KNN, In: Australasian Universities Power Engineering Conference (AUPEC), 2016, pp. 1-5.

[21] IEC, Measurement of relative permittivity, dielectric dissipation factor and d.c. resistivity of insulating liquids, IEC 60247 Ed. 2.0, 2004.

[22] A.D. Ashkezari, H. Ma, T.K. Saha and C. Ekanayake, Application of fuzzy support vector machine for determining the health index of the insulation system of in-service power transformers, IEEE Trans Dielectr Electr Insul, Vol. 20, pp. 965-973, 2013.

[23] IEC, Insulating liquids - Determination of acidity - Part 1: Automatic potentiometric titration, IEC 62021-1, 2003.

[24] T.O. Rouse, Mineral insulating oil in transformers, IEEE Electr Insul Mag, Vol.14, pp. 6-16, 1998.

[25] N.A. Baka, A. Abu-Siada, S. Islam and M.F. El-Naggar, A new technique to measure interfacial tension of transformer oil using UV-Vis spectroscopy, IEEE Trans Dielectr Electr Insul, Vol. 22, pp. 1275-1282, 2015.

[26] Y. Li, J. Dai, M. Dong and L. Wang, Molecular dynamics simulation of temperature impact on the viscosity of transformer oil-based nanofluids, In: International Conference on Condition Monitoring and Diagnosis (CMD), 2016, pp. 376-379.

[27] IEEE Guide for the Reclamation of Insulating Oil and Criteria for Its Use, IEEE Std. 637, 2007.

[28] N. Utami, Y. Tamsir and A. Pharmatrisanti, Evaluation condition of transformer based on infrared thermography results, In: 9th International Conference on the Properties and Applications of Dielectric Materials, (ICPADM), 2009, pp.1055-1058.

[29] T. Saha and P. Purkait, Understanding the impacts of moisture and thermal ageing on transformer's insulation by dielectric response and molecular weight measurements, , IEEE Transactions on,Dielectrics and Electrical Insulation. Vol. 15, pp. 568-582, 2008.

[30] IEEE Guide for Loading Mineral-Oil-Immersed Transformers, IEEE Std. C57.91, 2002.

[31] M. Wang, A. Vandermaar and K.D. Srivastava, Review of condition assessment of power transformers in service, IEEE Electrical Insulation Magazine, Vol. 18, pp. 12-25, 2002.

[32] IEEE Standard Test Code for Liquid-Immersed Distribution, Power, and Regulating Transformers,IEEE Std. C57.12.90, 2006.

[33] H. Malik, A. Azeem and R. Jarial, Application research based on modern-technology for transformer health index estimation, In: 9th International Multi-Conference on Systems, Signals and Devices (SSD), 2012, pp. 1-7.

[34] F.K.H. Torkaman, Measurement variations of insulation resistance/polarization index during utilizing time in HV electrical machines – A survey, Elsevier Ltd. Measurement, Vol. 59, pp. 21–29, 2015.

[35] L. Xiao, L. Ruijin and L. Maochang, Influence of aging degree on polarization and depolarization currents of oil-paper insulation, In: Annual Report Conference on Electrical Insulation and Dielectric Phenomena, 2013, pp. 612-616.

[36] A. Baral and S. Chakravorti, Prediction of moisture present in cellulosic part of power transformer insulation using transfer function of modified debye model, IEEE Transactions on Dielectrics and Electrical Insulation, Vol. 21, pp. 1368-1375,2014.

[37] M. Florkowski and J. Furgał, Detection of transformer winding deformations based on the transfer function—measurements and simulations, Measurement science and technology, Vol. 14, 2003.

[38] T. Leibfried and K. Feser, Monitoring of power transformers using the transfer function method, IEEE Transactions on Power Delivery, Vol. 14, pp.1333-1341, 1999.

[39] M. Bigdeli, M. Vakilian and E. Rahimpour, A new method for detection and evaluation of winding mechanical faults in transformer through transfer function measurements, Advances in Electrical and Computer Engineering, Vol. 11, pp. 23-30, 2011.

[40] F. Jakob, K. Jakob, S. Jones and R. Youngblood, Use of gas concentration ratios to interpret LTC & OCB dissolved gas data, In: Proceedings of the Electrical insulation conference and electrical manufacturing and coil winding technology conference, 2003, pp. 301-304.

[41] J.R. Sans, K.M. Bilgin and J.J. Kelly, Large-scale survey of furanic compounds in operating transformers and implications for estimating service life, In: Conference

record of the IEEE international symposium on electrical insulation, 1998, pp. 543-553.

[42] R.D. Stebbins, D.S. Myers and A.B. Shkolnik, Furanic compounds in dielectric liquid samples: review and update of diagnostic interpretation and estimation of insulation ageing, In: Proceedings of the 7th International Conference on Properties and Applications of Dielectric Materials, 2003 pp. 921-926.

[43] C.T. Dervos, C.D. Paraskevas, P.D. Skafidas and N. Stefanou, Dielectric spectroscopy and gas chromatography methods applied on high-voltage transformer oils, IEEE Trans Dielectr Electr Insul, Vol. 13, pp. 586-592, 2006.

[44] Z. Poniran and Z.A. Malek, Life Assessment of Power Transformers via Paper Ageing Analysis, In: International Conference on Power Engineering, Energy and Electrical Drives, pp. 2007, 460-465.

[45] W. McDermid and D. Grant, Use of furan-in-oil analysis to determine the condition of oil filled power transformers, In: International Conference on Condition Monitoring and Diagnosis, 2008.

[46] A.B. Norazhar and A. Abu-Siada, S. Islam, A review on chemical diagnosis techniques for transformer paper insulation degradation, In: Australasian Universities Power Engineering Conference (AUPEC), 2013, pp. 1-6.

[47] P.J. Baird, H. Herman, G.C. Stevens and P.N. Jarman, Non-destructive measurement of the degradation of transformer insulating paper, IEEE Trans Dielectr Electr Insul, Vol. 13 pp. 309-318, 2006.

[48] N. Das, A. Abu-Siada and S. Islam, Impact of conducting materials on furan-spectral correlation of transformer oil, in: Australasian Universities Power Engineering Conference (AUPEC), 2013 pp. 1-4.

[49] A.E. Abu-Elanien and M. Salama, Asset management techniques for transformers, Electric power systems research, Vol. 80, pp. 456-464, 2010.

[50] T.K. Saha, Review of modern diagnostic techniques for assessing insulation condition in aged transformers, IEEE Trans Dielectr Electr Insul, Vol. 10, pp. 903-917, 2003.

[51] M. Ali, C. Eley and A.M. Emsley, Measuring and understanding the ageing of kraft insulating paper in power transformers, IEEE Electr Insul Mag, Vol. 12, pp. 28-34, 1996.

[52] C. Yi, M. Hui, T. Saha and C. Ekanayake, Understanding Moisture Dynamics and Its Effect on the Dielectric Response of Transformer Insulation, IEEE Transactions on Power Delivery, Vol. 30, pp. 2195-2204, 2015.

[53] D. Martin, C. Perkasa and N. Lelekakis, Measuring Paper Water Content of Transformers: A New Approach Using Cellulose Isotherms in Nonequilibrium Conditions, IEEE Transactions on Power Delivery, Vol. 28, pp. 1433-1439, 2013.

[54] C. Ekanayake, S.M. Gubanski, A. Graczkowski and K. Walczak, Frequency response of oil impregnated pressboard and paper samples for estimating moisture in transformer insulation, IEEE Transactions on Power Delivery, Vol. 21, pp. 1309-1317, 2006.

[55] M.A. Talib, N.M. Ghazali, M. Christie and W. Zakaria, Diagnosis of transformer insulation condition using recovery voltage measurements, In: Power engineering conference, PECon Proceedings. National. IEEE, 2003, pp. 329-332.

[56] M. Megherbi, M.Mekious and F. Bitam-Megherbi, A Recovery Voltage as non-Destructive Tool for Moisture Appreciation of Oil Impregnated Pressboard: An Approach for Power Transformers Testing International Journal on Electrical Engineering and Informatics, Vol. 5, pp. 422-432, 2013.

[57] A. Bognar, L. Kalocsai, G. Csepes and E. Nemeth, Diagnostic tests of high voltage oil-paper insulating systems (in particular transformer insulation) using DC dielectrometrics, Proc. CIGRE, 33-08, 1990.

[58] P.B. S.M. Gubanski, G. Csépes and V. D. Houhanessian, Dielectric response methods for diagnostics of power transformers, IEEE Electrical Insulation Magazine,Vol. 19, pp. 12-18, 2003.

[59] T.K. Saha and P. Purkait, Investigation of polarization and depolarization current measurements for the assessment of oil-paper insulation of aged transformers, IEEE Transactions onDielectrics and Electrical Insulation, Vol. 11, pp. (2004) 144-154, 2004.

[60] U. Gafvert, L. Adeen, M. Tapper, P. Ghasemi, B. Jonsson, Dielectric spectroscopy in time and frequency domain applied to diagnostics of power transformers, In: Proceedings of the 6th International Conference on Properties and Applications of Dielectric Materials, pp. 825-830, 2000.

[61] N.A.M. Jamail, M.A.M. Piah, N.A. Muhamad, Comparative study on conductivity using Polarization and Depolarization Current (PDC) test for HV insulation, In: 2011 International Conference on Electrical Engineering and Informatics (ICEEI), 2011, pp. 1-6.

[62] H.A.P. Silva, W. Bassi and A.C.T. Diogo, Noninvasive ageing assessment by means of polarization and depolarization currents analysis and its correlation with moisture content for power transformer life management, In: Transmission and Distribution Conference and Exposition: Latin America, 2004 IEEE/PES, 2004, pp. 611-616.

[63] Z.T. Yao and T.K. Saha, Analysis and modeling of dielectric responses of power transformer insulation, In: Power Engineering Society Summer Meeting, 2002 IEEE, I, pp. 417-421.

[64] A.K. Jonscher, Dielectric relaxation in solids, Journal of Physics D: Applied Physics, Vol. 32, R57, 1999.

[65] M. Jaya and T. Leibfried, M. Koch, Information within the dielectric response of power transformers for wide frequency ranges, In:Conference Record of the 2010 IEEE International Symposium on Electrical Insulation (ISEI), 2010, pp. 1-5.

[66] R. Liao, J. Liu, L. Yang and Y. Zhang, Extraction of Frequency Domain Dielectric Characteristic Parameter of Oil-paper Insulation for Transformer Condition Assessment, Electric Power Components and Systems, Vol. 43, pp. 578-587, 2015.

[67] M. Koch and T. Prevost, Analysis of dielectric response measurements for condition assessment of oil-paper transformer insulation, IEEE Transactions on Dielectrics and Electrical Insulation, Vol. 19, pp. 1908-1915, 2012.

[68] E. Santos, M. Elms and Z. Jabiri, End management of power transformers– operational perspective, unpublished work, presented at the Omicron Seminar, Perth WA, 2013.

[69] J. Liu, R. Liao, Y. Zhang and C. Gong, Condition Evaluation for Aging State of Transformer Oil-paper Insulation Based on Time-frequency Domain Dielectric Characteristics, Electric Power Components and Systems, Vol. 43, pp. 759-769, 2005.

[70] W. Hui, L. Chengrong and H. Huimin, Influence of temperature to developing processes of surface discharges in oil-paper insulation, In: Conference Record of the 2010 IEEE International Symposium on Electrical Insulation (ISEI), 2010, pp. 1-4.

[71] H. Wang, C.-r. Li, K. Sheng and Y. Miao, Experimental study on the evolution of surface discharge for oil-paper insulation in transformers, In: IEEE Conference on Electrical Insulation and Dielectric Phenomena (CEIDP ) 2009, pp. 405-408.

[72] X. Chen, A. Cavallini and G.C. Montanari, Improving High Voltage Transformer Reliability through Recognition of PD in Paper/Oil Systems, In: International Conference on High Voltage Engineering and Application, (ICHVE) 2008, pp. 544-548.

[73] R. Sarathi, I.P. Merin Sheema, J.S. Rajan and M.G. Danikas, Influence of harmonic AC voltage on surface discharge formation in transformer insulation, IEEE Transactions on Dielectrics and Electrical Insulation, Vol. 21, pp. 2383-2393, 2014.

[74] T. Pinpart and M.D. Judd, Experimental comparison of UHF sensor types for PD location applications, In: 2009 IEEE Electrical Insulation Conference, 2009, pp. 26-30.

[75] S. Tenbohlen, D. Denissov, S.M. Hoek and S.M. Markalous, Partial discharge measurement in the ultra high frequency (UHF) range, IEEE Trans Dielectr Electr Insul, Vol. 15, pp. 1544-1552, 2008.

[76] M.M. Yaacob, M.A. Alsaedi, J.R. Rashed and A.M. Dakhil, Review on partial discharge detection techniques related to high voltage power equipment using different sensors, Photonic Sensors, Vol. 4, pp. 325-337, 2014.

[77] S. Boggs and Partial discharge: overview and signal generation, Electrical Insulation Magazine, Vol. 6, pp. 33-39, 1990.

[78] J. Patrick, Acoustic Emission Properties of Partial Discharges in the time-domain and their applications, School of Electrical Engineering,Kungliga Tekniska Hogskolan, Stockholm Sweden, 2012.

[79] E. Howells and E. Norton, Detection of partial discharges in transformers using acoustic emission techniques, IEEE Transactions on Power Apparatus and Systems, Vol. 5, pp. 1538-1549, 1978.

[80] A. Akbari, P. Werle, H. Borsi and E. Gockenbach, Transfer function-based partial discharge localization in power transformers: a feasibility study, Electrical Insulation Magazine, Vol. 18, pp. 22-32, 2002.

[81] M.G. Niasar, Partial discharge signatures of defects in insulation systems consisting of oil and oil-impregnated paper, Royal Institute of Technology (KTH), Stockholm, Sweden, pp. 33-35, 2012.

[82] T.W. D. Gautschi and G. Buchs, Ultra high frequency (UHF) partial discharge detection for power transformers: Sensitivity check on 800 MVA power transformers and first field experience Cigre paper, 2012.

[83] M.M. Yaacob, M.A. Alsaedi, J.R. Rashed, A.M. Dakhil, S.F. Atyah, Review on partial discharge detection techniques related to high voltage power equipment using different sensors, Photonic Sensors, Vol. 4, pp. 325-337, 2014.

[84] S.M. Markalous, S. Tenbohlen and K. Feser, Detection and location of partial discharges in power transformers using acoustic and electromagnetic signals, IEEE Trans Dielectr Electr Insul, Vol. 15, pp. 1576-1583, 2008.

[85] R. Schwarz, M. Muhr and S. Pack, Partial discharge detection in oil with optical methods, In: IEEE International Conference on Dielectric Liquids (ICDL) 2005, pp. 245-248.

[86] N.K.R. S. Karmakar and P. Kumbhakar, Monitoring of high voltage power transformer using direct optical partial discharge detection technique, Springer, Vol. 38 pp. 207-215, 2009.

[87] W.G. Ariastina, I.A.D. Giriantari, I.K. Solin and O. Yolanda, Condition monitoring of power transformer: A field experience, In: IEEE 9th International Conference on the Properties and Applications of Dielectric Materials (ICPADM) 2009, pp. 1051-1054.

[88] T.R. Blackburn, B.T. Phung, Z. Liu and R.E. James, On-line partial discharge measurement on instrument transformers, In: Proceedings of 1998 International Symposium on Electrical Insulating Materials, 1998, pp. 497-500.

[89] A. Akbari, P. Werle, H. Borsi and E. Gockenbach, High frequency transformer model for computation of sectional winding transfer functions used for partial discharge localization, In: Proceedings of the 12th International Symposium on High Voltage Engineering, Bangalore, India, 2001, pp. 46-51.

[90] P. Werle, A. Akbari, H. Borsi, and E. Gockenbach, Localisation and evaluation of partial discharges on power transformers using sectional winding transfer functions, in: 12th International Symposium on High Voltage Engineering (ISH), Bangalore, India, 2001, pp. 856-859.

[91] E. Gockenbach and H. Borsi, Transfer function as tool for noise suppression and localization of partial discharges in transformers during on-site measurements, In: International Conference on Condition Monitoring and Diagnosis, (CMD) 2008, pp. 1111-1114.

[92] S. Tenbohlen, D. Uhde, J. Poittevin and H. Borsi, Enhanced diagnosis of power transformers using on-and off-line methods: Results, examples and future trends, CIGRE paper, 12-204, 2000.

[93] IEEE Guide for Diagnostic Field Testing of Electric Power Apparatus - Part 1: Oil Filled Power Transformers, Regulators, and Reactors, IEEE Std 62-1995, 1-64, 1995.

[94] P. Transformers—Part, 5: Ability to Withstand Short Circuit, IEC Standard, 60076-60075, 2000.

[95] J.A.S.B. Jayasinghe, Z.D. Wang, P.N. Jarman and A.W. Darwin, Winding movement in power transformers: A comparison of FRA measurement connection methods, IEEE Trans Dielectr Electr Insul, Vol. 13, pp. 1342-1349, 2006.

[96] V. Behjat and V. Tamjidi, Leakage Inductance Behavior of Power Transformer Windings under Mechanical Faults, In: Proceedings of the international conference on information technology and computer engineering (ITCE), 2015.

[97] M. Bagheri, M. Naderi, T. Blackburn and T. Phung, Frequency response analysis and short-circuit impedance measurement in detection of winding deformation within power transformers, IEEE Electr Insul Mag, Vol. 29, pp. 33-40, 2013.

[98] J.R. Secue and E. Mombello, Sweep frequency response analysis (SFRA) for the assessment of winding displacements and deformation in power transformers, Electric Power Systems Research, Vol. 78, pp. 1119-1128, 2008.

[99] K. Patel, N. Das, A. Abu-siada and S. Islam, Power transformer winding fault analysis using transfer function, In: 2013 Australasian Universities Power Engineering Conference (AUPEC), 2013, pp. 1-3.

[100] E. Rahimpour, J. Christian, K. Feser and H. Mohseni, Modellierung der Transformatorwicklung zur Berechnung der Ubertragungsfunktion fur die Diagnose von Transformatoren, Elektrie, Vol. 54, pp. 18-30, 2000.

[101] E.P. Dick and C.C. Erven, Transformer diagnostic testing by frequency response analysis, IEEE Transactions on Power Apparatus and Systems, PAS-97, Vol. 6, pp. 2144-2153, 1978.

[102] D.A.K. Pham, T.M.T. Pham and M.H. Safari, FRA-based transformer parameters at low frequencies, In: 2012 International Conference on High Voltage Engineering and Application (ICHVE), 2012, pp. 476-479.

[103] T. Prevost, Power Transformer Insulation Diagonostics, Omicron Seminar, Perth WA, 24 April2015.

[104] S. Birlasekaran, F. Fetherston, Off/on-line FRA condition monitoring technique for power transformer, IEEE Power Engineering Review, Vol. 19, pp. 54-56, 1999.

[105] ANSI/IEEE C57.91, IEEE Guide for Loading Mineral-Oil-Immersed Transformers, 1995.

[106] J. John and J. Winders, Power Transformers Principles and Applications, Marcel Dekker, Inc, Allentown, Pennsylvania, USA, 2002.

[107] IEEE Guide for Loading Mineral-Oil-Immersed Transformers, IEEE Std C57.91, 1996.

[108] C.f. Bai, W.S. Gao and T. Liu, Analyzing the Impact of Ambient Temperature Indicators on Transformer Life in Different Regions of Chinese Mainland, The Scientific World Journal,125896, 2013.

[109] A. Schaut, S. Autru and S. Eeckhoudt, Applicability of methanol as new marker for paper degradation in power transformers, IEEE Trans Dielectr Electr Insul, Vol. 18 pp. 533-540, 2011.

[110] P.A.A.F. Wouters A.V. Schijndel and J.M. Wetzer, Remaining lifetime modeling of power transformers: individual assets and fleets, IEEE Electr Insul Mag, Vol. 27 pp. 45-51, 2011.

[111] B. Gorgan, P.V. Notingher and J.M. Wetzer, Calculation of the remaining lifetime of power transformers paper insulation, In: 13th International Conference on Optimization of Electrical and Electronic Equipment (OPTIM), 2012, pp. 293-300.

[112] D. Martin, Y. Cui, C. Ekanayake, H. Ma and T. Saha, An Updated Model to Determine the Life Remaining of Transformer Insulation, IEEE Transactions on Power Delivery, Vol. 30, pp. 395-402, 2015.

[113] A.M. Emsley, X. Xiao, R.J. Heywood and M. Ali, Degradation of cellulosic insulation in power transformers. Part 3: effects of oxygen and water on ageing in oil, IEE Proceedings - Science, Measurement and Technology, Vol. 147, pp. 115-119,

[114] M. E, llerov, J. Hr, za, J. Velek, I. Ullman and F. St, ska, Life cycle management of power transformers: results and discussion of case studies, IEEE Trans Dielectr Electr Insul, Vol. 22, pp. 2379-2389, 2015.

[115] T.V. Oommen, Cellulose insulation in oil-filled power transformers: part II maintaining insulation integrity and life, IEEE Electr Insul Mag, Vol. 22, pp. 5-14.

[116] E. Gockenbach, X. Zhang, Z. Liu, H. Chen and L. Yang, Life time prediction of power transformers with condition monitoring, In: 44th International Conference on Large High Voltage Electric Systems, 2012.

[117] An international survey of failures in large power transformers in service, CIGRE Working Group 05,Electra no.88, pp. 21–48, 1983.

# Chapter 3: A Nearest Neighbour Clustering Approach for Incipient Fault Diagnosis of Power Transformers


## Abstract

Dissolved gas analysis (DGA) is one of the popular and widely accepted methods for fault diagnosis in power transformers. This paper presents a novel DGA technique to improve the diagnosis accuracy of transformers by analysing the concentrations of five key gases produced in transformers. The proposed approach uses a clustering and cumulative voting technique to resolve the conflicts and deal with the cases that cannot be classified using Duval Triangles, Rogers' Ratios and IEC Ratios Methods. Clustering techniques group the highly similar faults into a cluster providing a virtual boundary between dissimilar data. A cluster of data points may contain single or multiple types of faulty transformers' data with different distinguishable percentages. The *k*-nearest neighbour (KNN) algorithm is used for indexing the three closest clusters from an unknown transformer data point and allows them to vote for single or multiple faults categories. The cumulative votes have been used to identify a transformer's fault category. Performance of the proposed method has been compared with different conventional methods currently used such as Duval Triangles, Rogers' Ratios and IEC Ratios Method along with published results using computational and machine learning techniques such as rough sets analysis, neural networks (NNs), support vector machines (SVMs), extreme learning machines (ELM) and fuzzy logic. The experimental comparison with both published and utility provided data show that the proposed method can significantly improve the incipient fault diagnosis accuracy in power transformers.

## 3.1 Introduction

A power transformer is one of the most important and expensive components in power transmission and distribution systems [1]. Its precise operation is essential for ensuring the reliable and stable operation of a power system. Any fault in the power transformer may lead to the unscheduled outages resulting in interruption of power supply. Failure of transformers hampers the stability of operation and causes a great loss to the utilities. As sudden failure of a transformer can result in an explosion, it has significant implications both for quality of service and it poses a risk to both maintenance crew and the general public. Therefore, incipient fault diagnosis and condition monitoring of power transformers are both gaining attention [2], by the utilities to ensuring continuous operation and minimising the operational risks.

Due to the continuous operation and variable loading, transformers are always subjected to electrical, thermal, mechanical and chemical stresses. As a result, different types of combustible and non-combustible gases, such as Hydrogen ($H_2$), Oxygen ($O_2$), Nitrogen ($N_2$), Carbon dioxide ($CO_2$), Carbon monoxide (CO), Methane ($CH_4$), Ethylene ($C_2H_4$), Ethane ($C_2H_6$), Acetylene ($C_2H_2$), Propane ($C_3H_8$) and Propylene ($C_3H_6$) are released and dissolved in transformer oil [3]. Moreover, the excessive thermal, electrical and chemical stresses change the dielectric properties and mechanical strength of cellulose paper and produce furanoid compounds, namely, 2-furfural (2-FAL), 5-Hydroxy methyl-2-furfural (5-HMF), 5-Methyl-2-furfural (5-MEF), 2-Furfurol (2-FOL) and 2-Acetylfuran (2-ACF) which are partially soluble in oil [4-5]. In order to monitor the insulation condition and detect faults in a transformer, different techniques such as Dissolved Gas Analysis (DGA), Furan Analysis, Degree of Polymerisation (DP) measurement, Gas Chromatography (GC), Mass Chromatography (MC), High Performance Liquid Chromatography (HPLC) and moisture analysis are available [6]. Among these, DGA is a non-invasive, proven and widely accepted method to detect incipient faults in transformers. The DGA

method can be used to continuously monitor the overall condition of transformers and generate advance warnings of newly developing faults. Therefore, operators can conveniently plan their remedial action following the total gas production or the production rate of individual gases that minimizes the risk of premature failure.

In order to analyse the measured gas concentrations, DGA techniques such as the family of Duval Triangles, Key Gas, Modified Rogers' Ratios, Doernenburg and IEC Ratios have been used over the last few decades [7-8]. The Duval Triangles are one of the preferred methods for many utility companies, as they do very well in classifying incipient faults, and can assess the state of insulation in transformers. However, there are cases where the Duval Triangles fail to produce any classification and there is a chance of misclassification near to the boundary between adjacent regions [9]. In order to investigate these unusual cases, a link has been established with a large utility company in Western Australia having more than 350 power transformers in operation. The company primarily uses Duval Triangles to assess the overall condition of their transformers. They also consider IEC, Modified Rogers' Ratios and Key Gas methods before classifying their transformers into a fault category, especially for the cases when Duval Triangles fail or ambiguously classify a transformer. Additionally, over time, gases are produced by normal operation of transformers without indicating any fault. Consequently, there is a chance of misclassification of healthy transformers. According to [10], the permissible limit of dissolved gases in transformer oil corresponding to the operating time of a healthy transformer is shown in Figure 3.1.

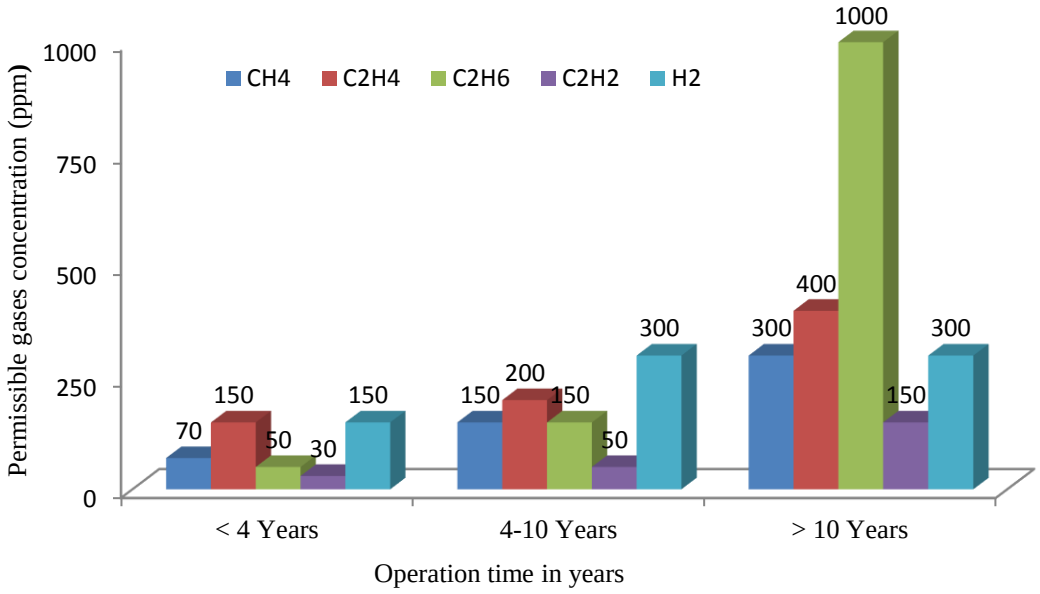


**Figure 3.1:** Permissible concentration of dissolved gases in a healthy transformer [10].

In this paper, a novel fault diagnosis technique has been proposed which can effectively classify the critical cases where there is a contradiction between various Duval Triangles and cannot be classified by the conventional ratio methods. The arrangement of the paper is as follows. Section 3.2 describes the motivation of the research. Section 3.3 presents the basic concept of k-means algorithm (KMA). Section 3.4 describes the proposed machine learning technique utilising k-means clustering and k-nearest neighbour pattern classification. Section 3.5 presents the results that were achieved with the method, section 3.6 presents a case study and section 3.7 presents a summary of the results and conclusions.

## 3.2 Motivation of Research

DGA is one of the proven methods that used widely by many utilities for condition monitoring and fault diagnosis in power transformers. Due to their continuous operation, the normal ageing of transformer insulation is inevitable. Frequent overloading and short circuit incidents can create electrical, mechanical and thermal

stresses in transformer insulation that degrade the dielectric properties of insulation and increase its ageing rate. The decomposition of insulating material increases the operational risk to transformers and produces several combustible and non-combustible gases that become partly dissolved in transformer oil. In DGA-based analysis, the concentration and production rate of gases are measured and continuously monitored to assess the insulation condition of a transformer and locate the sources of faults. In order to interpret the dissolved gases, a graphical technique like the Duval Triangles and different ratio methods such as Rogers' Ratios, Doernenburg Ratios, IEC Ratio, Single Gas Ratio and the Key Gas method are used over long periods of time. All of these conventional methods are very simple and easy to implement. However, different methods have different advantages and limitations. Therefore, comparison of the results from different methods on the same sample may lead to contradictions, and there is no clear way to prioritise one result over another, leading to ambiguity [11]. The accuracy of the IEC method is affected by the incomplete coding and absolute code boundary. It cannot identify the fault samples, if they fall outside the definite ratio limits. In addition, the interference problem between low energy discharge (D1) and high energy discharge (D2) of this method may lead to misleading classification [12]. The classification of Rogers' Ratios is not precise for detecting all faults [12]. It gives more accurate diagnosis for the low thermal (T1) fault. The Doernenburg method can only provide three types of diagnosis. It cannot distinguish the severity of thermal decomposition.

All these ratio methods do not involve any mathematical formulation and their accuracy is dependent on the concentration and ratio of the key gases. Moreover, in some cases, the calculated ratios do not fall within any of the fault classes and remain unclassified. The Duval Triangles always gives a fault diagnosis even when a transformer is known to be healthy. The classical Duval Triangle cannot accurately detect the partial discharge (PD) and thermal fault. For mineral oil filled transformers, if the fault classification is a thermal fault or a partial discharge by the

classical triangular method, then Triangles 4 and 5 must be used for further clarification. In practice, there are cases where contradictory classifications are produced by Triangles 4 and 5. Moreover, all triangles have an unclassified region. Consequently, the accuracy of fault classification is dependent on the expert's experience supported by other ratio methods. The classification of transformers' incipient faults following the Rogers' Ratios, and IEC ratios has been tabulated in Tables 3.1 and 3.2, respectively.

**Table 3.1:** Rogers' ratios [13].

| Case | R2= $C_2H_2/C_2H_4$ | R1= $CH_4/H_2$ | R5= $C_2H_4/C_2H_6$ | Suggested Fault Diagnosis |
|---|---|---|---|---|
| 0 | <0.1 | >0.1 to <1.0 | <1.0 | Unit normal |
| 1 | <0.1 | <0.1 | <1.0 | Low-energy density arcing (LEDA)/PD |
| 2 | 0.1 to 3.0 | 0.1 to 1.0 | >3.0 | Arcing-high-energy discharge (AHED) |
| 3 | <0.1 | >0.1 to <1.0 | 1.0 to 3.0 | Low temperature thermal (LTT) |
| 4 | <0.1 | >1.0 | 1.0 to 3.0 | Thermal <700 ˚C (T2) |
| 5 | <0.1 | >1.0 | >3.0 | Thermal >700 ˚C (T3) |

**Table 3.2:** Ratio limits for respective faults based on IEC60599 (2007).

| Case | Characteristic Fault | $C_2H_2/C_2H_4$ | $CH_4/H_2$ | $C_2H_4/C_2H_6$ |
|---|---|---|---|---|
| PD | Partial Discharge | - | <0.1 | <0.2 |
| D1 | Low Energy Discharges | >1 | 0.1-0.5 | >1.0 |
| D2 | High Energy Discharges | 0.6 to 2.5 | 0.1 to 1.0 | >2.0 |
| T1 | Thermal Fault <300 ˚C | - | >1.0 | <1.0 |
| T2 | Thermal Fault 300 to 700 ˚C | <0.1 | >1.0 | 1.0 to 4.0 |
| T3 | Thermal Fault >700 ˚C | <0.2 | >1.0 | >4.0 |

To overcome the limitations of these conventional approaches, various computational and machine learning techniques such as Support Vector Machines (SVMs) [2], Neural Networks (NNs) [14], Extreme Learning Machines (ELM) [15], Fuzzy Logic [16-17] and Rough Sets (RS) detection [18]have been combined with DGA interpretation techniques to analyse the incipient faults in transformers. These new techniques have improved the accuracy of fault diagnosis and solved the interference problem between fault classes. The combined approach is helping researchers and

utilities to explore the relationship between different fault patterns and their characteristic parameters. In this research, a modified clustering technique and k-Nearest Neighbour algorithm have been used, and a modified cumulative voting mechanism has been proposed to classify and predict the incipient faults in power transformers.

## 3.3 Basic Concepts of k-means Algorithm

Cluster analysis is prevalent in any discipline that aims to find the natural grouping, detect anomalies and identify salient features of data points in a given data set. The groups are called clusters and the region belonging to a cluster is a Voronoi cell [19], in which the density of similar data points is higher than in other regions. A good clustering technique generally uses the splitting, merging or randomized approaches for partitioning given data points into clusters so that the formal objective function is optimized [19]. The most common objective in clustering technique is to minimize the squared error between the empirical mean of a cluster and the points lying in its Voronoi cell. The k-means algorithm (KMA) is one of the simplest and widely used unsupervised learning algorithm that minimizes the clustering error and can be used to discover the natural grouping of data points [19-20]. For a set of *n* data points $X = \{x_1, x_2, \dots, x_n\}$, in a real *d*-dimensional space $\boldsymbol{R}^d$, KMA determines a set of *K* cluster $C = \{\mu_1, \mu_2, \dots, \mu_k\}$ in $\boldsymbol{R}^d$ such that the mean squared Euclidean distance from each data point to the nearest centre is minimized. Each of the clusters is associated with a subset of $X$ such that any $x_i$ is a member of only one cluster. The subset of $X$ that cluster around $\mu_k$ will be referred to as $C_k$. Each of the subsets is disjoint and therefore the union of all $C_k$ provides the entire set of points and can be expressed as,

$$\bigcup_{k=1}^{K} C_k = X. \tag{3.1}$$

According to [21], the sum of the squared-error for the set of clusters C can be defined as

$$\mathrm{J(C)} = \sum_{k=1}^{K} \sum_{x_i \in C_k} \left\| x_i - \mu_k \right\|^2 \qquad (3.2)$$

Although, the objective function $\mathrm{J(C)}$decreases with the increasing number of clusters *K*, and become zero when K= n, the number of cluster centres and data points are equal. It needs to be minimized when K< n using KMA. The steps of KMA are as follows [22-24]:

i. Place *K* centres into the *d*-dimensional space of the data points *X*. The locations are known as initial centres ($\mu_k$) of the $C_k$ clusters.
ii. Assign data points to the Voronoi cell (group) which centre has the closest distance to form subsets $C_k$.
iii. Compute new cluster centres $\mu_k$ from the mean of data points lying in their Voronoi cell.
iv. Repeat steps 2 and 3 until the square error is reduced to a pre-determined value or the centroids are immobilized.

Although KMA is a simple and popular method in clustering applications, it is very sensitive to the initial positions of the cluster centres [21]. It is an NP-hard algorithm and therefore a globally optimal solution cannot be found, except for unrealistically small values of *n* and *K*. However, there are well-established heuristic algorithms, such as those employed here, for providing adequate albeit suboptimal clustering when *n* and *K* are larger. In this work, a number of heuristics like *Lloyd's* algorithm and *Linde-Buzo-Gray* (LBG) have been combined with conventional KMA [19]. These approaches offer a more efficient clustering algorithm that can minimize the clustering error, employed by the conventional KMA as a local search procedure. To

solve the *K* clustering problem, the proposed hybrid approach proceeds in an incremental way. Initially, a single centre is calculated following the LBG algorithm and placed in the *d*-dimensional space. The centre is calculated from the geometric mean of the given data points. In each stage, the old centroids are split into two. Moreover, in each stage of the LBG algorithm, the nearest data points to each centre are computed and the centres are moved to the centroid of data points lying in their Voronoi cell. These steps are repeated until some convergence condition is met. The only difference between *Lloyd's* and LBG algorithm is that LBG specifies the initial placement of a centre which is absent in *Lloyd's* algorithm [19]. A detailed procedure of the LBG algorithm has been discussed in [25]. In the LBG algorithm, there is no guarantee that every cluster centre will have some data association. This limitation can be overcome by supervising the splitting and relocating any centres where cluster ($C_k$) becomes an empty set. The centres obtained from supervised LBG can be used as initial centres for KMA to take the advantage of global minima. This hybrid method reduces the clustering error that results from the local convergence. Finally, the feature of clusters with the collaboration of k-nearest neighbour (KNN) algorithm can be used in a diagnostic decision table to classify the fault category of transformers.

## 3.4 Methodology

The methodology involved a development of a clustering process combined with a cumulative voting technique to determine the fault category of a transformer. This section includes data collection, pre-processing, model development, neighbour selection and training stage which have been discussed below.

### 3.4.1 Data Collection and Processing

Data of combustible gases generated from the insulating oil in 376 power transformers have been collected by a large utility company in Western Australia. The gas concentrations are measured in parts per million (ppm) by analysing an oil sample drown from each transformer under laboratory conditions. The measured gas concentrations have been analysed using the Rogers' Ratios, Duval Triangles, Doernenburg and IEC ratio methods and verified by the utility's experts before labelling them into a fault category. It is presumed that the final classification from the combined approach of different conventional methods, sophisticated software analysis and expert's judgement is accurate and reliable. To verify the accuracy of suspected faulty transformers, these transformers have been removed from the services for investigation, and the findings have exactly matched with the expert's fault classification. The proposed method is based on a clustering technique that uses the percentage concentrations of the five combustible gases comprising Hydrogen ($H_2$), Methane ($CH_4$), Ethylene ($C_2H_4$), Ethane ($C_2H_6$) and Acetylene ($C_2H_2$). The sum of the five gas concentrations has been calculated as per (3.3). The summation is defined as the total combustible gases (TCG).

$$TCG = H_2 + CH_4 + C_2H_4 + C_2H_6 + C_2H_2 \quad (3.3)$$

Therefore, the percentage of those individual gases has been calculated and used as an input for the proposed method to classify the testing data sets into seven targeted fault categories. The individual percentage calculation procedure and the targeted fault category with their fault code have been shown in Table 3.3.

**Table 3.3:** Input and targeted output of the proposed method.

| Input | Targeted Fault Category | Fault Code |
|---|---|---|
| $\%H_2 = \frac{H_2}{TCG} * 100$ | Partial Discharge | PD |
| | Discharge of Low Energy | D1 |
| $\%CH_4 = \frac{CH_4}{TCG} * 100$ | Discharge of High Energy | D2 |
| $\%C_2H_4 = \frac{C_2H_4}{TCG} * 100$ | Thermal Fault, t<150˚C | S |
| | Thermal Fault, 150˚C < t <300 ˚C | O |
| $\%C_2H_6 = \frac{C_2H_6}{TCG} * 100$ | Thermal Fault, 300 °C < t <700 ˚C | C |
| $\%C_2H_2 = \frac{C_2H_2}{TCG} * 100$ | Thermal Fault, t >700 ˚C | T3 |

Moreover, the collected data sets are divided into two subsets. The first subset (318 measurements) is used as a training data set and the second subset (58 measurements) which could not be classified easily by the Duval Triangles or come with a conflicting classification due to the overlapping between different faults.

### 3.4.2 Proposed Model

In this work, a hybrid clustering technique has been used because it has advantages over the Duval Triangles method. In Duval Triangles, five dimensional key gases are mapped into a set of two dimensional spaces to make a classification of transformer faults based on a set of linear boundaries. This dimension reducing mapping throws away some valuable information. The proposed clustering technique preserves all of the five-dimensional gases information in the expectation that it can do better than the Duval Triangles and other ratio methods, in the cases when they fail or contradict each other. There are two stages in the proposed approach. Firstly, a set of clusters based around the global k-Means Algorithm (KMA) is generated. The clusters are representative of various fault categories. After clustering, the k-Nearest Neighbour algorithm (KNN) has been used to decide which clusters are closest to the data set of an unclassified transformer. In this research, three closest clusters have been identified based on their Euclidean distances from the testing data. The specific procedure for clustering the data points and neighbours selection has been discussed

in the following sections and a summary of the comparative performances can be seen in Tables 3.7-3.9. However, a workflow of the proposed model with the combination of Duval Triangles has been shown in Figure 3.2.

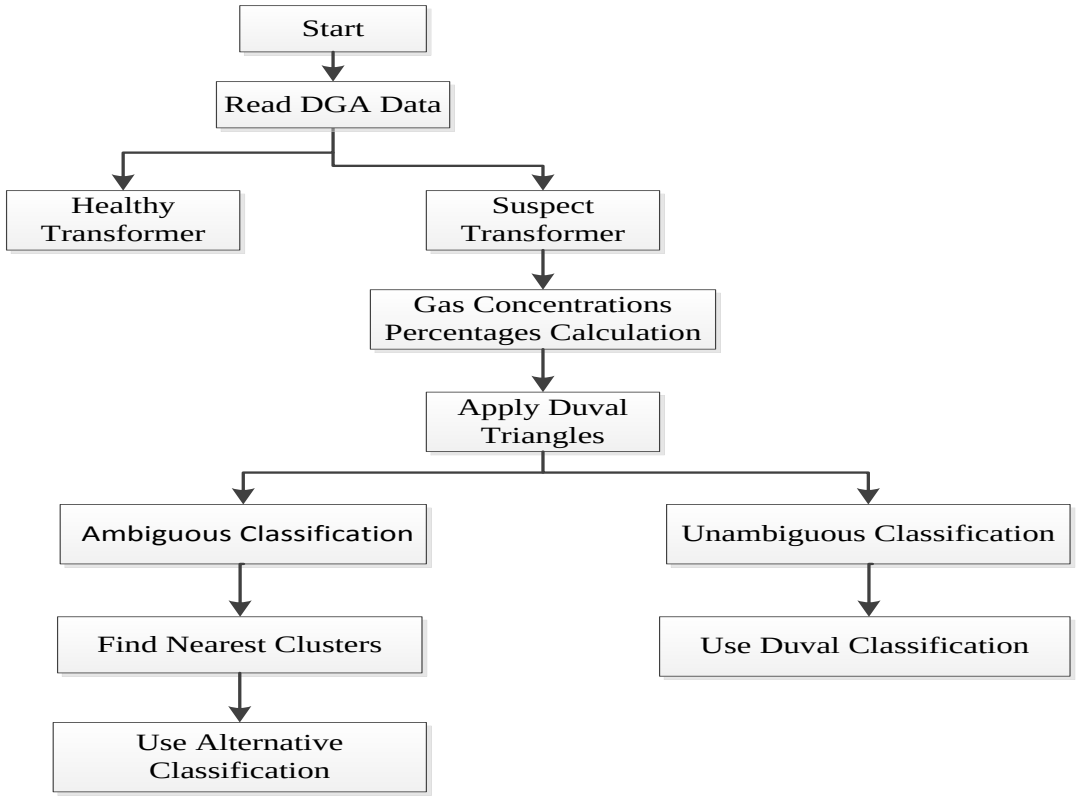


**Figure 3.2:** Workflow of the proposed model for practical application.

### 3.4.3 Clustering Procedure

The clustering of the training data points has been completed by using modified KMA. In order to perform the clustering of training data points $X = \{x_1, x_2, \dots, x_n\}$, an initial cluster centre $\mu_1 \in C$ for KMA is computed following the LBG algorithm (mean of all data points) and placed in the five-dimensional space ($R^5$) that formed by the percentages of five gas concentrations. The number of cluster centres

gradually increased to K (where $K = 2^n$ for $n = 1,2,\dots,6$ ) through successive iterations. In each stage of iteration, the old centre(s) are split into two and Euclidean distances from the centres to all data points are calculated. Let the $C_j$ represent the data points (neighbourhood) in a Voronoi cell for which $\mu_j$ is the nearest centre. The set of data points lying to the cluster $C_j$ can be expressed as follows:

$$C_j = \{x_i : ||x_i - \mu_j||^2 \leq ||x_i - \mu_k||^2 \quad \forall \quad k = 1,2,3,\dots,K\} \tag{3.4}$$

where $||x_i - \mu_j||^2$ is the Euclidean distance between a training data points $x_i$ $(i = 1,2,3,\dots,n)$ and the cluster centre $\mu_j$, and $K$ is the number cluster centres. After finishing the allocation of all data points to the Voronoi cells of cluster centres, for the next iteration, the position of cluster centres moves to the centroid of data in subset $C_j$. The new position of the cluster centres can be calculated by the following equation.

$$\mu_j = \frac{\sum_{x_i \in C_j} x_i}{\sum_{x_i \in C_j} 1} \tag{3.5}$$

In the next stage, the distances of all points from the new position of centres are again calculated and associated them to centres having smallest Euclidean distances. These steps are repeated until $\mu_j$ become immobilized or the square error $J(C)$ is reduced to a pre-determined value [22].

### 3.4.4 Neighbor Selection and Voting

In this section, the distances to three closest cluster centres $\mu_i$, $\mu_j$ and $\mu_k$ from any unknown transformer data point $x$ is measured and sorted into ascending order of distance. In a later stage, the clusters have been used in a voting mechanism to classify a faulty transformer. In the case of conventional voting, a decision is taken

based on the majority opinion. For instance, if one neighbouring cluster is associated with a T1 fault, the second one might be associated with T2 and third neighbour might be labelled as a T1 fault, then the majority votes for T1 will classify the transformer as having a T1 type fault. As the clusters are sometimes straddling the boundaries of the Duval Triangles method, a cumulative voting system has been introduced where each of the three clusters can vote for multiple fault categories. In most cases they vote for one fault category, sometimes they can also vote for two or three categories because they might be closer to a corner where three faulty regions join together. In the final step, a distance matrix has been used for cumulative voting. Hence the cluster that is closest has a stronger bearing on the overall result, the next farthest has a weaker bearing and the next most distant one has a still weaker bearing on the final result. Mathematically, the voting weight of any cluster can be expressed by the following equation.

$$W_p = \frac{S - ||x - \mu_p||^2}{2 * S} \tag{3.6}$$

where $S = \sum ||x - \mu_i||^2 + ||x - \mu_j||^2 + ||x - \mu_k||^2$ and $p \in \{i, j, k\}$ are the three nearest clusters centresfrom any data point $x$. Finally, the cumulative votes are added up in a weighted fashion to determine the classification of an unknown transformer most effectively.

### 3.4.5 Training Stage

During the training stage, 318 transformers gas concentrations out of 376 collected from the utility company have been used to develop the proposed clustering technique. These training data points were excluded from the test set. The fault categories of the training data points are labelled by the utility experts. The number of individual fault category of the training samples is shown in Figure 3.3.

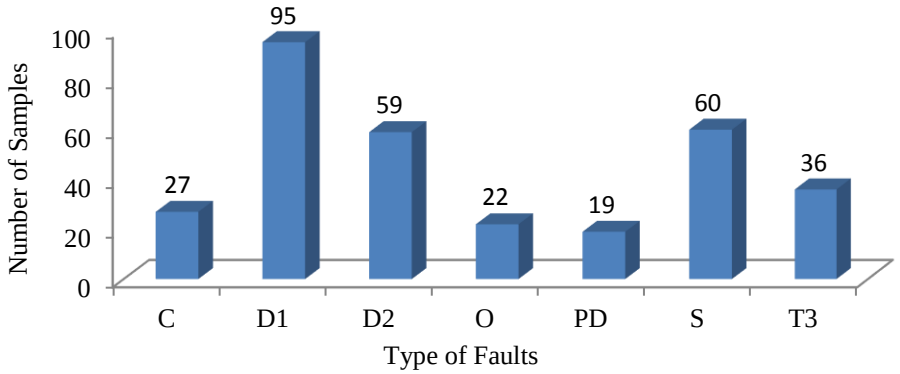


**Figure 3.3:** Training samples following the fault categories.

To create a cluster of points (rows) in a five-dimensional Euclidean space, the relative percentages of the five gases have been calculated and put into the individual columns of a matrix $X$. The matrix $X$ can be expressed as

$$\boldsymbol{X} = \begin{bmatrix} \%H_{2_{1,1}}, & \%CH_{4_{1,2}}, & \%C_2H_{4_{1,3}}, & \%C_2H_{6_{1,4}}, & \%C_2H_{2_{1,5}} \\ \%H_{2_{2,1}}, & \%CH_{4_{2,2}}, & \%C_2H_{4_{2,3}}, & \%C_2H_{6_{2,4}}, & \%C_2H_{2_{2,5}} \\ \dots & \dots & \dots & \dots & \dots \\ \dots & \dots & \dots & \dots & \dots \\ \dots & \dots & \dots & \dots & \dots \\ \dots & \dots & \dots & \dots & \dots \\ \%H_{2_{318,1}}, & \%CH_{4_{320,2}}, & \%C_2H_{4_{320,3}}, & \%C_2H_{6_{320,4}}, & \%C_2H_{2_{318,5}} \end{bmatrix}$$

After creating the Euclidean space, 64 five-dimensional cluster centres were created following the LBG algorithm so that the training data can be partitioned around the nearest cluster centres. After each LBG iteration, each cluster centroid (initial centre is the mean of $X$) was split into two until 64 clusters are formed. The centres having zero association with the training data points (where $C_j$ was an empty set) were removed, and the remaining were used as initial centres in KMA. To ensure optimum performance, the 34 best cluster centres have been chosen by using KMA. The selection process includes splitting the centres having large number of data

associations, and removing or combining the centres having lower numbers of data associations. The association is evaluated by indexing the data points to the centres based on their distances to them. The iterative process was continued until each of the clusters become representative of a particular fault class or multiple classes with different distinguishable percentages. Moreover, there was no cluster where $C_j$ was exceptionally large set. A summary of the probabilities of each fault category based on its association with each cluster centre are shown in Table 3.4.

**Table 3.4:** Probability of a transformer fault following its association to a cluster centre.

| Cluster Centres | C (%) | D1 (%) | D2 (%) | O (%) | PD (%) | S (%) | T3 (%) |
|---|---|---|---|---|---|---|---|
| $\mu_1$ | | 100 | | | | | |
| $\mu_2$ | | | | | 80 | 10 | 10 |
| $\mu_3$ | 10 | | | | | | 90 |
| … | …… | …… | ……. | ……. | …….. | …… | ….. |
| $\mu_{15}$ | 100 | | | | | | |
| $\mu_{16}$ | | 25 | | | | 75 | |
| $\mu_{17}$ | 67 | | | | | | 33 |
| … | …... | …… | ……. | ……. | …….. | …… | …. |
| $\mu_{25}$ | | 8 | 92 | | | | |
| $\mu_{26}$ | | 86 | 14 | | | | |
| $\mu_{27}$ | | | 100 | | | | |
| …. | …… | …… | ……. | ……. | …….. | …… | …. |
| $\mu_{32}$ | | | | 100 | | | |
| $\mu_{33}$ | | | | 100 | | | |
| $\mu_{34}$ | | | | | | 100 | |

The probability matrix of Table 3.4 shows that the single clustering technique could wrongly classify an unlabeled measurement, if it is close to a cluster on the boundary between multiple Voronoi regions (fault categories). The misclassification rate could increase greatly for a measurement closest to a cluster centre like $\mu_{17}$which Voronoi region comprises 67 percent *C* type faulty data points and 33 percent *T3* type faulty

data points. To deal with this interference problem, the k-Nearest Neighbour (KNN) algorithm has been used for the 1st, 2nd and 3rdnearest neighbouring cluster centres detection based on their distances. Moreover, the cumulative weighted voting, based on the distances from the centre has been proposed to identify a fault class of an unknown transformer. For instance, in case of three neighbours clustering approach, if the cluster centres $\mu_3$, $\mu_2$, and $\mu_{17}$ are the 1st, 2nd and 3rd nearest neighbours of a training data point, and their distance weight factors are 65%, 25% and 10% respectively, of total weight then the voting process can be expressed as the follows:

**Table 3.5:** Modified voting metrics.

| Neighbours | C | D1 | D2 | PD | S | T3 |
|---|---|---|---|---|---|---|
| $C_3$ | 10*0.65 | | | | | 90*0.65 |
| $C_2$ | | | | 80*0.25 | 10*0.25 | 10*0.25 |
| $C_{17}$ | 67*0.10 | | | | | 33*0.10 |
| Total Vote | 13.2 | | | 20 | 2.5 | 64.3 |

From Table 3.5, the maximum cumulative vote belongs to T3 since it has the largest column total. Consequently, the transformer will be classified as having a T3 type fault.

## 3.5 Results and Discussion

This research targeted the examples that cannot be classified easily by the Duval Triangles or come with a conflicting classification due to the overlapping between different faults. Therefore, a subset of 58 transformer measurement samples out of 376 have been selected as a test set and classified them according to the proposed method. All 58 were excluded from the training examples. A comparison of fault classification based on modified Roger's Ratios, the IEC ratios and proposed method on 58 targeted transformer measurements have been summarized in Table 3.6.

**Table 3.6:** Comparison of Rogers' ratios, IEC ratios and the proposed method.

| Test Methods | Unresolved Diagnosis | Wrong Diagnosis | Accuracy |
|---|---|---|---|
| Roger's Ratios | 21 | 9 | 75.67% |
| IEC Ratio | 27 | 8 | 74.19% |
| Proposed Method | - | 4 | 93.10% |

The accuracy of each method shown in Table 3.6 has been calculated by comparing them with expert classifications. The overall accuracy of the proposed method is 93%. The method makes occasional errors but it does provide a useful decision-support mechanism for engineers who are trying to deal with the critical cases. A similar type of experiment with slightly different method has been conducted by other researchers [12,15, 18]. They used their own training sets (Not disclosed in the literature) to train up their classifier to classify the test sets labelled by the experts in the power industry. To verify the performance of the proposed approach, it has been applied on their published test sets. In [18], researchers applied the rough sets (RS) analysis technique and artificial neural networks (ANNs) combined with RS and k-means clustering (KMC) algorithms to determine transformer fault categories. A comparison of their methods, different established methods and the proposed method are shown in Table 3.7.

**Table 3.7:** Fault diagnosis comparison between established and adapted methods.

| Case Number | $H_2$ | $CH_4$ | $C_2H_4$ | $C_2H_6$ | $C_2H_2$ | Diagnosis Result | | | | | | | |
|---|---|---|---|---|---|---|---|---|---|---|---|---|---|
| | | | | | | Expert Diagnosis | Duval Triangle | RS | RS-ANN | KMC-RS-ANN | Roger's Ratios | IEC Ratio | Proposed Method |
| 1 | 60 | 40 | 110 | 10 | 70 | D2 | D2 | D2 | D2 | D2 | D2 | D2 | D2 |
| 2 | 31 | 7 | 5 | 19 | 67 | D2 | D1 | - | D2 | D2 | - | - | D1 |
| 3 | 293 | 50 | 15 | 13 | 120 | D2 | D2 | D2 | D2 | D2 | D2 | D1 | D2 |
| 4 | 57 | 7 | 4.5 | 19 | 71 | D2 | D1 | - | D2 | D2 | - | - | D1 |
| 5 | 467 | 148 | 266 | 13 | 511 | D2 | D2 | D2 | DT | D2 | D2 | D1 | D2 |
| 6 | 160 | 90 | 17 | 27 | 58 | D1 | D1 | D1 | D1 | D1 | - | - | D1 |
| 7 | 402 | 81 | 27 | 39 | 25 | D1 | D2 | D1 | D1 | D1 | - | - | D1 |
| 8 | 4 | 79 | 312 | 112 | 0 | T2 | T1 | - | T2 | DT | T2 | T2 | T2 |
| 9 | 180 | 180 | 4 | 74 | 3 | DT | T3 | DT | DT | DT | - | - | T2 |
| 10 | 1300 | 740 | 2000 | 260 | 71 | T3 | T3 | T3 | T3 | T3 | - | - | T3 |
| 11 | 42 | 97 | 600 | 157 | 0 | T3 | T3 | Normal | Normal | Normal | T2 | T2 | T3 |
| 12 | 44 | 52 | 119 | 15 | 1 | T3 | T3 | T3 | T3 | T3 | T3 | T3 | T3 |
| 13 | 42 | 79 | 152 | 31 | 1 | T3 | T3 | T3 | T3 | T3 | T3 | T3 | T3 |
| 14 | 164 | 244 | 497 | 103 | 8 | T3 | T3 | T3 | T3 | T3 | T3 | T3 | T3 |
| 15 | 22 | 51 | 57 | 42 | 0 | T2 | T2 | T2 | T2 | T2 | T2 | T2 | T2 |
| 16 | 679 | 4992 | 3671 | 1823 | 0 | T2 | T1 | T2 | T2 | T2 | T2 | T2 | T2 |

The proposed method was also applied on the test samples available in [12] where each fault has been found by using a decision tree (formed from if-else conditions) based on the gas contrition limits for particular types of fault. They considered the decision tree method as a new approach to DGA. According to this method they found overlapping between different faults with the same gas limit used in the decision tree. To solve the overlapping problem, they included additional gas ratios in the decision tree and named it as Modified New Approach DGA. The proposed method has been compared with the decision tree method and different ratio methods to evaluate its performance. The comparison has been summarized in Table 3.8.

**Table 3.8:** Comparison between decision tree, ratio and proposed methods.

| Case Number | $H_2$ | $CH_4$ | $C_2H_4$ | $C_2H_6$ | $C_2H_2$ | Diagnosis Result | | | | | |
|---|---|---|---|---|---|---|---|---|---|---|---|
| | | | | | | Actual Diagnosis | New Approach DGA | Modified New Approach DGA | Roger's Ratios | IEC Ratio | Proposed Method |
| 1 | 117 | 17 | 3 | 1 | 1 | PD | PD, D1 | PD | - | - | PD |
| 2 | 32930 | 2397 | 0 | 157 | 0 | PD | PD, D1 | PD | PD | PD | PD |
| 3 | 78 | 20 | 13 | 11 | 28 | D1 | D1, D2 | D1 | - | D1 | D2 |
| 4 | 1230 | 163 | 233 | 27 | 962 | D1 | D1, D2 | D1 | D2 | D1 | D1 |
| 5 | 8200 | 3790 | 4620 | 250 | 277 | D2 | D2, T1 | D2 | - | - | D2 |
| 6 | 130 | 140 | 120 | 2 | 0 | T1 | D2, T1 | T1 | T3 | T3 | T2 |
| 7 | 78 | 66 | 2.6 | 283 | 0 | T1 | D2, T1 | T1 | Normal | PD | T1 |
| 8 | 30.4 | 117 | 138 | 44.2 | 0.1 | T2 | T2, T3 | T2 | T3 | T2 | T2 |
| 9 | 27 | 90 | 63 | 42 | 0.2 | T2 | T1, T2 | T1 | T2 | T2 | T2 |
| 10 | 1100 | 1600 | 2010 | 221 | 26 | T3 | T2, T3 | T3 | T3 | T3 | T2 |

In [15], the researchers have used different artificial intelligence and machine learning techniques such as ANN, SVM, ELM, and SaE-ELM to classify the fault category of a transformer. They compared the classification of all the four methods and the decision taken from the majority votes. A comparison of their methods and the proposed method is shown in Table 3.9.

**Table 3.9:** Comparison of different adapted fault diagnosis methods.

| Case Number | $H_2$ | $CH_4$ | $C_2H_4$ | $C_2H_6$ | $C_2H_2$ | Diagnosis Result | | | | | | | |
|---|---|---|---|---|---|---|---|---|---|---|---|---|---|
| | | | | | | ANN | SVM | ELM | SaE-ELM | Duval Triangle | Roger's Ratios | IEC Ratio | Proposed Method |
| 1 | 103 | 5.8 | 7.3 | 5 | 0.7 | T1 | T3 | T1 | T1 | S | - | - | T1 |
| 2 | 416 | 21 | 43.1 | 10.5 | 1 | T1 | T3 | T1 | T3 | T3 | - | - | T3 |
| 3 | 59 | 53 | 60.3 | 17.7 | 0.8 | T2 | T2 | T2 | T2 | C | - | - | T2 |
| 4 | 10.5 | 4.8 | 4.8 | 5 | 2.2 | D1 | D1 | D1 | D1 | DT | - | - | D1 |
| 5 | 137 | 97 | 29 | 12 | 1.5 | T2 | T2 | T2 | T2 | C | LEDA/PD | - | T2 |
| 6 | 89 | 73 | 6.8 | 6 | 5 | D2 | D2 | D2 | D2 | DT | - | - | T2 |
| 7 | 240 | 157 | 127 | 98 | 0.8 | T2 | T2 | T2 | T2 | C | LEDA/PD | - | T2 |
| 8 | 116 | 104 | 51 | 36 | 0 | T2 | T2 | T2 | T2 | C | LEDA/PD | - | T2 |

## 3.6 Case Study and Analysis

To provide a deeper understanding, all 34 literature cases have been used in a case study. The proposed method differs from the experts' diagnoses in three cases (Case number 2, 4 and 9), out of 16 shown in Table 3.8. According to the experts' judgements, cases 2, 4 and 9 are D2, D2 and DT faults but are classified as D1, D1 and T2 respectively, by the proposed method. Duval Triangle classified the faults as D1, D1 and DT correspondingly, but the other two conventional methods: Roger's ratio and IEC ratio failed to diagnose these cases. As the DT fault category has been omitted from the proposed method due to the insufficient training data points, it has been classified as a T2 fault. Moreover, gas concentrations collected from the utility company predominantly used Duval Triangles to classify their transformers' fault categories could be a reason for misclassification in cases 2 and 4, respectively. The proposed method effectively solved the over-lapping problem in 7 cases out of 10 shown in Table 3.9. The IEC method could not detect any faults in the 8 cases shown in Table 3.9. Even the performance of Roger's ratio is not satisfactory, but the proposed method accurately classified all cases except for case number 6. That case is classified by the ANN, SVM, ELM, and SaE-ELM methods as a D2 fault. According to the Duval Triangle, the fault category of the sample is DT fault, which is a combination of thermal and dielectric. The proposed method has classified the case as a T2 type fault. As the data point close to the three neighbouring cluster centres, which Voronoi regions comprise multiple types of faults with closed percentage of probabilities, it is clear the case 6 has been misclassified. This problem could be overcome by increasing the number of clusters with a much larger number of training data points.

In this research, the number of cluster centres and their positions are carefully chosen through a continuous iteration process and their performances have been tested before being applied to an unlabelled measurement. Deliberately preserved extra dimensional information has helped to accurately classify 93 percent of the cases,

which other conventional established methods could not cope with. Moreover, the proposed method performed well on the published data as shown in Table 3.7, 3.8 and 3.9 respectively.

## 3.7 Conclusions

A new DGA diagnosis technique has been developed that is based around a clustering approach combined with a modified KNN cumulative voting approach that considers inter-neighbour distances. The experimental results show that it correctly classifies 93% of the difficult cases where Duval's triangle is unable to make a classification. This result is compared with other methods like the Rogers' Ratios and IEC method, all of which fail in a significant fraction of cases (See Tables 3.7-3.9). The focus of this work has been to develop a method that compliments Duval's widely adopted triangles method rather than replacing it. The interaction can be seen from the workflow diagram shown in Figure 3.2. It can be seen that the proposed method is very suitable for incipient fault diagnosis in power transformers.

One of the weaknesses of the proposed technique is that it does not deal well with the mixture of dielectric and thermal (DT) faults. Most other systems considered also have difficulties differentiating DT from other fault categories. Further work needs to be done in this area, particularly building classifiers with large number of training examples that can deal with very uncommon faults more effectively.

## References

[1] N. Das, A. Abu-Siada and S. Islam, Impact of conducting materials on furan-spectral correlation of transformer oil, In: Australasian Universities Power Engineering Conference (AUPEC), 2013, pp. 1-4.

[2] Khmais Bacha, Seifeddine Souahlia and M. Gossa, Power transformer fault diagnosis based on dissolved gas analysis by support vector machine, Electric Power Systems Research, Vol. 83, pp. 73–79, 2012.

[3] A. Abu-Siada, S. Hmood and S. Islam, A new fuzzy logic approach for consistent interpretation of dissolved gas-in-oil analysis, IEEE Trans Dielectr Electr Insul, Vol. 20, pp. 2343-2349, 2013.

[4] H. Malik, A. Azeem and R.K. Jarial, Application research based on modern-technology for transformer Health Index estimation, In: 9th International Multi-Conference on Systems, Signals and Devices (SSD), 2012, pp. 1-7.

[5] A. Abu-Siada, S.P. Lai and S.M. Islam, A Novel Fuzzy-Logic Approach for Furan Estimation in Transformer Oil, IEEE Transactions on Power Delivery, Vol. 27, pp. 469-474, 2012.

[6] T.K. Saha, Review of modern diagnostic techniques for assessing insulation condition in aged transformers, IEEE Trans Dielectr Electr Insul, Vol. 10, pp. 903-917, 2003.

[7] A.D. Ashkezari, T.K. Saha, C. Ekanayake and H. Ma, Evaluating the accuracy of different DGA techniques for improving the transformer oil quality interpretation, In: 2011 21st Australasian Universities Power Engineering Conference (AUPEC), 2011, pp. 1-6.

[8] N.A. Bakar, A. Abu-Siada and S. Islam, A review of dissolved gas analysis measurement and interpretation techniques, IEEE Electr Insul Mag, Vol. 30, pp. 39-49, 2014.

[9] S.N. Hettiwatte and H.A. Fonseka, Analysis and interpretation of dissolved gases in transformer oil: A case study, In: International Conference on Condition Monitoring and Diagnosis (CMD), 2012, pp. 35-38.

[10] S. Singh and M.N. Bandyopadhyay, Dissolved gas analysis technique for incipient fault diagnosis in power transformers: A bibliographic survey, IEEE Electr Insul Mag, Vol. 26, pp. 41-46, 2010.

[11] IEC, 60599 Ed. 2.1 Mineral oil-impregnated electrical equipment in service - Guide to the interpretation of dissolved and free gases analysis, 1999.

[12] S.S.M. Ghoneim and I.B.M. Taha, A new approach of DGA interpretation technique for transformer fault diagnosis, International Journal of Electrical Power & Energy Systems, Vol. 81, pp. 265-274, 2016.

[13] IEEE guide for the interpretation of gases generated in oil-immersed transformers, IEEE Std. C57.104. 2008.

[14] F. Zakaria and D. Johari, I. Musirin, Artificial neural network (ANN) application in dissolved gas analysis (DGA) methods for the detection of incipient faults in oil-filled power transformer, In: IEEE International Conference on Control System, Computing and Engineering (ICCSCE), 2012, pp. 328-332.

[15] S. Li, G. Wu, B. Gao, C. Hao and D. Xin, Interpretation of DGA for transformer fault diagnosis with complementary SaE-ELM and arctangent transform, IEEE Trans Dielectr Electr Insul, Vol. 23, pp. 586-595, 2016.

[16] Y.C. Huang and H.C. Sun, Dissolved gas analysis of mineral oil for power transformer fault diagnosis using fuzzy logic, IEEE Transactions on Dielectrics and Electrical Insulation, Vol. 20, pp. 974-981, 2013.

[17] A. Abu-Siada, M. Arshad and S. Islam, Fuzzy logic approach to identify transformer criticality using dissolved gas analysis, In: IEEE PES General Meeting, 2010, pp. 1-5.

[18] Y.H. Sheng-wei Fei, A multi-layer KMC-RS-SVM classifier and DGA for fault diagnosis of power transformer, In: R.P.o.C. Science (Ed.), 2012, pp. 238-243.

[19] T. Kanungo, D.M. Mount and N.S. Netanyahu, An efficient k-means clustering algorithm: analysis and implementation, IEEE Transactions on Pattern Analysis and Machine Intelligence, Vol. 24, pp. 881-892, 2002.

[20] M. Yin, Y. Hu, F. Yang and X. Li, A novel hybrid K-harmonic means and gravitational search algorithm approach for clustering, Expert Systems with Applications, Vol. 38, pp. 9319-9324, 2011.

[21] A.K. Jain, Data clustering: 50 years beyond K-means, Pattern Recognition Letters, Vol. 31, pp. 651-666, 2010.

[22] T. Niknam, E. Taherian Fard and N. Pourjafarian, A. Rousta, An efficient hybrid algorithm based on modified imperialist competitive algorithm and K-means for data clustering, Engineering Applications of Artificial Intelligence, Vol. 24, pp. 306-317, 2011.

[23] W. Kwedlo, A clustering method combining differential evolution with the K-means algorithm, Pattern Recognition Letters, Vol. 32, pp. 1613-1621, 2011.

[24] Y. Li and H. Wu, A Clustering Method Based on K-Means Algorithm, Physics Procedia, Vol. 25, pp. 1104-1109, 2012.

[25] H.B. Kekre and M.T.K. Sarode,Vector Quantized Codebook Optimization using K-Means, International Journal on Computer Science and Engineering, Vol. 1, pp. 283-290, 2009.

# Chapter 4: Application of Parzen Window Estimation for Incipient Fault Diagnosis in Power Transformers


## Abstract

Accurate incipient faults diagnosis in oil-filled power transformers is important to utilities for schedule maintenance and minimizes the operation cost. Dissolved Gases Analysis is one of the proven tools for incipient fault diagnosis in power transformers. To improve the accuracy and solve the cases that cannot be classified using Rogers' Ratios, IEC Ratios and Duval Triangles Methods, a novel DGA technique based on Parzen Window estimation has been presented in this paper. The model uses the concentrations of five combustible gases such as Hydrogen ($H_2$), Methane ($CH_4$), Ethylene ($C_2H_4$), Ethane ($C_2H_6$) and Acetylene ($C_2H_2$) to compute the probability of transformers in different fault groups to identify their fault categories. Performance of the proposed method has been compared with different conventional methods and artificial intelligence-based techniques such as Rough Sets Analysis, Neural Networks, Support Vector Machines and Extreme Learning Machines for the same set of transformers. A comparison with other soft computing approaches shows that the proposed method is reliable and effective for incipient fault diagnosis in power transformers.

## 4.1 Introduction

Power transformers are the most expensive and critical components in power transmission and distribution networks. Failure of a transformer can be catastrophic, uneconomical and cause serious problems in power system stability. Therefore, its precise operation is essential to ensure continuous power supply and prevent a great financial loss for the utility companies. According to [1], about 80% of transformer faults occur from incipient deterioration that could be identified through predictive maintenance and online monitoring techniques. Therefore, incipient fault diagnosis and condition monitoring techniques are gaining more attention from the utilities to prevent unscheduled outages and minimize their operational risks.

Due to continuous operation, faults and overloading, power transformers are subjected to thermal, electrical, chemical and mechanical stresses throughout their operating life. These stresses may cause decay of insulating oil and release some gases which become dissolved in the dielectric fluid. These gases include Hydrogen ($H_2$), Oxygen ($O_2$), Nitrogen ($N_2$), Carbon dioxide ($CO_2$), Carbon monoxide (CO), Methane ($CH_4$), Ethylene ($C_2H_4$), Ethane ($C_2H_6$), Acetylene ($C_2H_2$), Propane ($C_3H_8$) and Propylene ($C_3H_6$). The gas concentrations may be measured by Gas Chromatography [2] and analysed by different Dissolved Gas Analysis (DGA) techniques to identify the fault afflicting a transformer. The gas concentrations observed in transformers under incipient fault condition increases as a function of temperature, and their individual concentration depend on the type of fault allowing them be used as a fault detector [3]. For instance, $H_2$ and $CH_4$ start to form under low thermal stress at about 150 $^{\circ}$C and is an indicator of partial discharge, while temperatures over 500 $^{\circ}$C lead to formation of $C_2H_2$ which is an indicator of arcing. Moreover, the concentration of $CO_2$,CO and their ratios can be used to assess the condition of paper insulation as they are produced from the degradation of solid insulation [4]. As DGA is a non-invasive, proven and widely accepted method to detect incipient faults in transformers, its popularity has increased over time.

To analyse the gas concentrations of a transformer, different DGA techniques such as Key Gas, Modified Rogers' Ratios, Doernenburg, IEC Ratios and Duval Triangles have been used over the last few decades [5-6]. Some of the methods use gas ratios, while others use specific gas concentrations to evaluate the condition of a transformer. Although these conventional methods are very simple and easy to implement, they have shortcomings, such as incorrect diagnosis or unresolved diagnosis. Additionally, over time, gases are produced by normal operation of transformers that do not indicate any fault. Consequently, there is a chance of misclassification of healthy transformers based on ratio approaches. According to [4], [7], the permissible limit of dissolved gases in transformer oil corresponding to the operating time of a healthy transformer is shown in Table 4.1.

**Table 4.1:** Permissible concentration of dissolved gases in a healthy transformer [7].

| Gas | < 4 years | 4-10 years | >10 years |
|---|---|---|---|
| $CH_4$ | 70 | 150 | 300 |
| $C_2H_4$ | 150 | 200 | 400 |
| $C_2H_6$ | 50 | 150 | 1000 |
| $C_2H_2$ | 30 | 50 | 150 |
| $H_2$ | 150 | 300 | 300 |

In order to overcome limitation in classical methods and develop a reliable incipient fault classifier, different artificial intelligence and machine learning techniques such as artificial neural networks (ANNs) [8], support vector machines (SVMs) [9], fuzzy logic [10-11], neuro fuzzy systems [12], and the nearest neighbour clustering approach (NNCA) [13] have been proposed by the researchers. To deal with the critical cases where the Duval Triangles and conventional ratio methods fail or ambiguously classify a transformer, DGA data set of 376 transformers from a large utility company in Western Australia has been collected. The combustible gas concentrations have been analysed by a novel probabilistic density function based on the Parzen Window method, which can effectively classify the critical cases that cannot be classified using the conventional ratio or Duval Triangles methods due to overlap between different faults. The arrangement of the rest of the paper is as

follows: Section 4.2 describes the motivation for the research. Section 4.3 presents the basic concept of Parzen Window estimation. Section 4.4 describes the methodology, while section 4.5 presents the results that were achieved with the method. Section 4.6 evaluate and compare the proposed method with other methods. Section 4.7 presents a case study and section 4.8 presents a summary of the results and conclusions.

## 4.2 Motivation of Research

Dissolved gases analysis (DGA) is a widespread diagnostic method that has gained worldwide acceptance for incipient fault diagnosis in transformers [14]. Due to continuous operation, faults and variable stresses (electrical, mechanical and thermal), the dielectric properties of oil and solid insulation such as paper, pressboard and transformer board, which are all made of cellulose, become degraded over time. The decomposition of insulating material produces different combustible and non-combustible fault gases and increases the operational risk to transformers. In DGA-based analysis, the concentration and production rate of gases are measured and regularly monitored to assess the insulation condition of a transformer and locate the sources of faults. In order to interpret the dissolved gases, a graphical technique such as the Duval Triangles or different ratio methods such as Rogers' Ratios, Doernenburg Ratios, IEC Ratio, Single Gas Ratio and the Key Gas method are used over long periods of time. All of these conventional methods are very simple and easy to implement. However, each method has different advantages and limitations. Therefore, comparison of the results from different methods on the same sample may lead to contradictions, and there is no clear way to prioritise one result over another [15]. The accuracy of the IEC method is affected by the incomplete coding (limited classifications) and absolute code boundary (strict to ratio limits). It cannot identify the faulty samples, if they fall outside the defined ratio limits. In addition, the low energy discharge (D1) and high energy discharge (D2) of this method may interfere leading to a misleading classification [16]. The classification of Rogers' Ratios is not

precise for detecting all faults [16]. Its diagnosis is most accurate for the low thermal (T1) fault [13]. The Doernenburg method can only provide three types of diagnosis by comparing the different limit values. It cannot distinguish the severity of thermal decomposition. The detailed procedure for this method is available in an IEEE standard [17]. All these ratio methods do not involve any mathematical formulation and their accuracy is dependent on the concentration limits and ratios of the key gases. Moreover, in some cases, the calculated ratios do not fall within any of the fault classes and remain unclassified.

The Duval Triangles always gives a fault diagnosis even when a transformer is known to be healthy. The classical Duval Triangle cannot accurately detect the partial discharge (PD) and thermal faults. For mineral oil filled transformers, if the fault classification is a thermal fault or a partial discharge by the classical triangular method, then Triangles 4 and 5 must be used for further clarification. In practice, there are cases where contradictory classifications are produced by Triangles 4 and 5. Moreover, all triangles have an unclassified region. Consequently, the accuracy of fault classification is heavily dependent on an expert's experience supported by other ratio methods. To improve the diagnostic capability of these standard methods, different artificial intelligences and machine learning techniques such as the ANN, SVM, fuzzy logic and NNCA have been introduced [8-11, 13]. Although, they are able to solve the problem of many unresolved and wrong diagnoses to a large extent, each of them has limitations. For instance, an ANN needs to train with a large training dataset to ensure a reliable output. Likewise, in fuzzy logic the derivation of rules may prove very difficult. Similarly, the wavelet network has high efficiency but low convergence [3]. Finally, in NNCA, detection of cluster centres and partitioning them into different fault categories is critical.

## 4.3 Basic Concepts of Parzen Window Estimation

Probability Density Function (PDF) estimation is prevalent in many statistical applications for analysing numerical data. Different PDF methods are currently available to estimate the density of unknown measurements. Parzen Windows is one of the popular nonparametric methods is used here to estimate the probability of an unknown transformer fault class based around the PDF of known transformer measurements [18-19]. It is a form of inductive learning that generalises the PDF from a finite set of examples drawn from the distribution. Being nonparametric, it does not need to estimate the values of a large set of synaptic weights as would be the case with ANNs.

Parzen Windows (PW) estimates the common probability density function $p(x)$ for an independent and identically distributed finite observation of any measurements $X$. The shape of the density function $p(x)$ is entirely dependent on the sample data and its accuracy moves towards the true value with an increased number of observations [19]. Therefore, no functional form of assumption is necessary to estimate the PDF of unknown measurements [20]. According to [21], the probability that a measurement $x$ belongs to a region $\mathcal{R}$ that is a subset of the domain can be expressed by (4.1).

$$P = \int_R p(x)dx \tag{4.1}$$

If the region $\mathcal{R}$ is assumed to be very small, the probability density $p(x)$ within $\mathcal{R}$ can be considered constant. Therefore, (4.1) can be approximated (4.2).

$$P = p(x)\mathrm{V} \tag{4.2}$$

where $V$ is the volume of $\mathcal{R}$.

If $N$ samples $X_{1,}, X_{2,}, X_{3,}, \ldots X_N$ are drawn from a distribution in $D$-dimensional space where each will be a vector $X_n = [x_{n,1,}, x_{n,2}, \ldots, x_{n,D}]$, then a probability density$p(x)$,

predicts the number of samples $K$ out of $n$ fall inside the $\mathcal{R}$ region can be estimated by:

$$K \simeq NP \tag{4.3}$$

Rearranging (3.2) and (3.3), the probability density can be approximated as:

$$p(x) \cong {}^{K}/_{nV} \tag{4.4}$$

If the region $\mathcal{R}$ is treated as a hypercube centred on $X_n$ with side length $\sigma$, then its volume will be $V = \sigma^D$. The number of samples ($K$) belonging to the region $\mathcal{R}$ can be calculated through a function $k(x)$ that meets the following conditions [19]:

$$k(\boldsymbol{x}) = \begin{cases} 1 & |x_i| \leq 0.5 \;\; i = 1,2,\dots,D \\ 0 & otherwise \end{cases} \tag{4.5}$$

where $\boldsymbol{x} = [x_1, x_2, \dots, x_D]$. Therefore, the value of $K$ can be defined as

$$K = \sum_{n=1}^{N} k\left(\frac{x - X_n}{\sigma}\right) \tag{4.6}$$

The new expression for probability density at any sample point $x$ can be calculated by substituting the value of $K$ from (4.6) into (4.4) which is shown in (4.7).

$$p(x) = \frac{1}{N\sigma^D} \sum_{n=1}^{N} k\left(\frac{x - X_n}{\sigma}\right) \tag{4.7}$$

Equation (4.7) is considered to be the basic formulation of PW estimation where $k(x)$ is a statistical kernel [22] or window function. Different kernels such as rectangular (4.5) or Gaussian kernels can be applied to define a window function. As the Gaussian function is smooth, in this research, a multivariate Gaussian kernel is commonly applied to obtain a smoother density model. Moreover, in a special form of radially symmetrical Gaussian, function can be completely specified by using a

variance parameter only [22]. Thus, the PW density function using a Gaussian kernel function with a common covariance $\Sigma$ can be written as:

$$p(x) = \frac{1}{N\sqrt{(2\pi)^D * |\Sigma|}} \sum_{n=1}^{N} exp\left(-\frac{(x-X_n)^T \Sigma^{-1} (x-X_n)}{2}\right) \quad (4.8)$$

where $\Sigma$ is a the kernel covariance matrix (multivariate standard deviation) that decides the shape of the estimated probability density function [20]. From (4.8), it can be seen that the final density function is obtained by summing the kernels of representative samples drawn from the total measurements. The smoothness of the function increases with the increased value of $\Sigma$ and gradually starts to loss information [21]. However, if the value is too small, the model becomes very sensitive to noise. The optimal value of $\Sigma$ can be estimated by analysing the training set discussed in a following section. After estimating the optimal value of $\Sigma$, the probability density of any test measurement can be calculated by using (4.8).

## 4.4 Methodology

This section involved a development of PDF based on a limited number of transformer's measurements to identify the fault category of a previously unseen transformer. In this sense, it is like training an ANN from a training set and then testing with a second disjoint set of measurements. In order to develop an efficient PDF, the nonparametric PW density method has been introduced. Different subsections of the methodology such as data collection, pre-processing, Density Function Estimation, Training and Feature Selection have been discussed below.

### 4.4.1 Data Processing and Normalization

To perform the research, concentration of five combustible gases such as Hydrogen ($H_2$), Methane ($CH_4$), Ethylene ($C_2H_4$), Ethane ($C_2H_6$) and Acetylene ($C_2H_2$) were collected from 376 power transformers of a utility company located in Western

Australia. The concentrations of gases were measured in parts per million (ppm). The concentrations have been measured by sampling the oil of each transformer's main tank and analysing them in a laboratory. In the case of an abrupt change in concentration between successive scheduled measurements, the sample was recollected then re-examined in multiple laboratories to verify the actual concentration. In order to differentiate the faulty transformers and classify their fault categories, the gas concentrations were analysed using conventional approaches such as Rogers' Ratios, Duval Triangles, Doernenburg and IEC ratio methods. Moreover, sophisticated software and expert judgements have also been used to determine the ultimate fault category of a transformer. In some cases, a faulty transformer has been removed from service to investigate the ultimate fault category. In most of the cases, the findings exactly match the expert classification. Therefore, in this work it is assumed that the final fault category of transformers decided from the combination of expert judgement and established methods is reliable and accurate. In the proposed PDF estimation technique, the amount of total combustible gases (TCG) for each transformer has been calculated by adding their five combustible gases such as Hydrogen ($H_2$), Methane ($CH_4$), Ethylene ($C_2H_4$), Ethane ($C_2H_6$) and Acetylene ($C_2H_2$) as in (4.9).

$$TCG = H_2 + CH_4 + C_2H_4 + C_2H_6 + C_2H_2 \tag{4.9}$$

After calculating the TCG, individual percentages of the combustible gases have been computed and used as an input to the proposed PW method. The percentage calculation procedure and the seven-targeted fault classification based on PW method are summarized in Table 4.2.

**Table 4.2:** Input and targeted output of the proposed method.

| Input | Targeted Fault Category |
|---|---|
| $\%H_2 = \frac{H_2}{TCG} * 100$ | Partial Discharge (PD) |
| $\%CH_4 = \frac{CH_4}{TCG} * 100$ | Discharge of Low Energy (D1) |
| $\%C_2H_4 = \frac{C_2H_4}{TCG} * 100$ | Discharge of High Energy (D2) |
| $\%C_2H_6 = \frac{C_2H_6}{TCG} * 100$ | Thermal Fault, t<150˚C (S) |
| $\%C_2H_2 = \frac{C_2H_2}{TCG} * 100$ | Thermal Fault, 150˚C < t <300 ˚C (O) |
| | Thermal Fault, 300 °C < t <700 ˚C (C) |
| | Thermal Fault, t >700 ˚C (T3) |

Finally, 376 collected measurements have been divided into disjoint training (85% of measurements) and testing (15% of measurements) subsets. The testing subset has been purposely selected to include the critical cases that could not be classified unambiguously by the conventional methods and comes with a conflicting classification by using Duval Triangles method due to the overlapping between different faults. Therefore, measurements from 318 transformers have been used as a training set to develop the proposed model and the remaining 58 transformer measurements are used to evaluate the performance of the model.

### 4.4.2 Density Function Estimation

In this research, a nonparametric based PW technique has been applied to estimate the density function. Each of the concentrations shown in Table 4.2 has been concatenated to form a point in a five-dimensional space. For PDF estimation, a Gaussian kernel function has been centred on each of the 318 training set drawn from 376 power transformers measurements collected from the utility company. The individual kernels are added together for determining a common width that is known as the smoothing parameter to estimate the probability density of each measurement. A mathematical expression of PDF is shown in (4.8). The challenging task when applying the proposed method is to precisely estimate the value of the covariance matrix ($\Sigma$) for five-dimensional data which is also known as a smoothing factor. The

smoothing parameter is very important as the shape of probability density function depends on it. Therefore, it has a great influence on the measured performance. Although, a larger value of $\Sigma$ will make the estimated PDF curve smoother, the estimated curve will also start to lose finer details. However, a smaller value of $\Sigma$ may lead to false spikes in PDF curve depending on the specific distribution of the training points and thus becomes prone to noise. The optimal value of $\Sigma$ depends on the size of the training set, their type and the amount of noise they are corrupted by [18]. Probability distributions of Hydrogen ($H_2$) are shown in Figure 4.1, where the $Y$ axis represents probability $p(x)$.

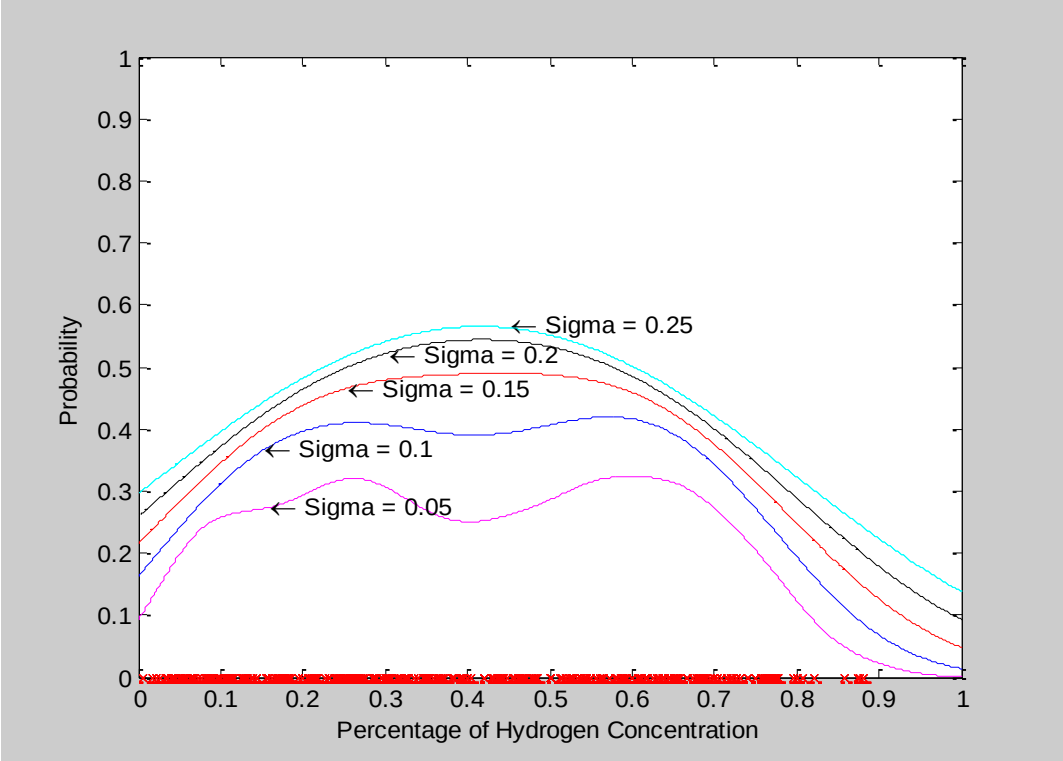


**Figure 4.1:** Probability Distribution of $H_2$.

From Figure 4.1, it is obvious that the probability distribution of $H_2$ becomes smoother with the increased value of sigma (covariance). To estimate the optimal value for Σ, different methods such as Silverman's rule of thumb [23], or a leave-one-

out estimator [18] can be used. Zewen Hu in [19], chose the optimal value of covariance $\Sigma$ from $a/\sqrt{n}$ where $a$ is a constant and $n$ is the sample size. These methods proved not to be effective on the proposed higher dimensional method. Therefore, the value of $\Sigma$ has been estimated by search increment of the multiplicative factor ($E$) between values 0.0001 to 1.0 with the covariance matrix computed from the training data points. From this experimental search, the optimal value of $E$ was found to be 0.25. However, to calculate the inverse of $\Sigma$ following (3.8), in some fault classes, the covariance matrix becomes singular due to their limited number of features (some gases are absent). This means it is impossible to calculate the matrix inverse as needed by (4.8). To overcome the singularity problem, a regularisation technique [24] has been applied. In this approach, a matrix with very small diagonal values (having same dimensions as $\Sigma$) has been added to the covariance matrix. The diagonal values have been controlled by a small multiplicative factor $\lambda$. The equation of covariance calculation for the proposed five-dimensional case can be expressed by (4.10).

$$\Sigma = E\Sigma_S + \lambda I \tag{4.10}$$

where $\Sigma_S$ is the covariance of the training samples, $\lambda$ is a constant and $I$ is an identity matrix having same dimensions of the samples.

### 4.4.3 Training and Feature Extraction

To train-up the proposed model, the percentages of combustible gas concentrations from 318 transformers have been used. The fault classifications of the transformers are labelled by the utility experts through a combination of different established methods, software analysis and their professional experience. The training sample based on fault categories is shown in Figure 4.2, where X-axis represents the fault categories.

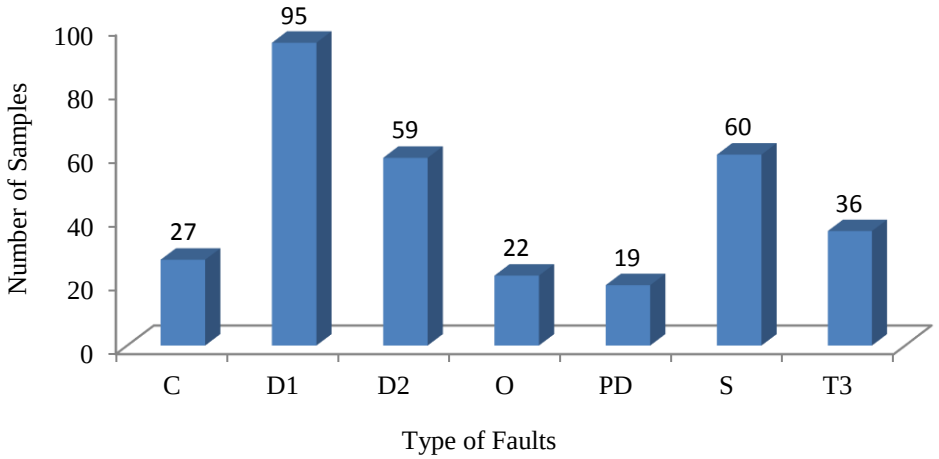


**Figure 4.2:** Training samples following the fault categories.

It can be seen from Figure 4.2 that the utility experts have classified their transformers into seven faulty categories. These categories have been used to form groups following their percentages of gas concentrations where each group contain certain number of faulty transformers. For instance, fault group *C* formed from 27 faulty transformers, fault group D1 contains 95 transformers, while 59 transformers belong to fault group D2 and so on. Now following the proposed method, the probability density of each transformer in each group of faulty transformers has been calculated for different values of $E$ and $\lambda$ to get an estimation of their optimal values. Transformers having the highest probability in a particular faulty group will be classified by the fault category of those transformers. From experiments, it has been seen that with a small value of $E$= 0.01, the classifications of the training data points exactly match with the expert's opinion but performance on the test set is unsatisfactory. With an increased value of $E$, although the performance of training data slightly decreases, the accuracy of testing data fault classification increases. Therefore, the value of $E$ was increased gradually through a continuous iterative process while keeping the value of $\lambda$ constant at 0.01 (a value also found experimentally). A satisfactory result (94.82% accuracy) was found for the test set when $E = 0.25$. If the value of $E$ is further increased, the accuracy again starts to

drop. As a result, this value is considered as a near-optimal point for this experiment. Bearing in mind that the proposed method specialises on cases where the existing methods fail. A workflow for combining the approach with the existing Duval Triangles method has been shown in Figure 4.3. This allows each of these methods to be used on the test measurements where they are most effective.

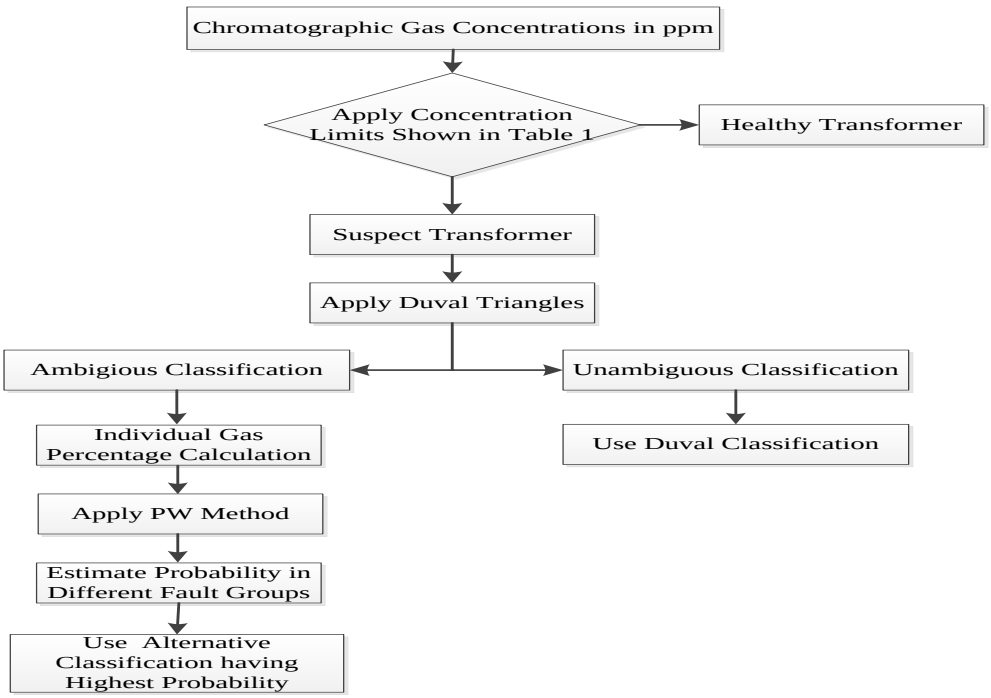


**Figure 4.3:** Workflow of the proposed model for practical application.

## 4.5 Results and Discussion

In order to test the efficacy of the proposed Parzen windows method, the percentage of combustible gas concentrations from transformers have been analysed to generate a classification into one of seven fault categories. Categories are labelled as partial discharge (PD), discharge of low energy (D1), discharge of high energy (D2), thermal fault <150˚C (S), thermal fault between 150˚C to 300 ˚C (O), thermal fault between 300 ˚C to 700 ˚C (C) and thermal fault >700 ˚C (T3). In each case a domain

expert has also classified the transformer using the same fault labels. In this work, critical cases have been chosen that cannot be classified unambiguously by using conventional ratio methods or the low-dimensional Duval Triangles graphical approach. Therefore, a subset of 58 transformer measurements out of 376 have been selected as a test set, omitted from the training phase, and classified using the Parzen windows method. Performance of the proposed method was compared to the modified Roger's Ratios, IEC ratios and previous work using the Nearest Neighbour Clustering Approach (NNCA) [13] and have been summarised in Table 4.3.

**Table 4.3:** Comparison of Rogers' ratios, IEC ratios, NNCA and the proposed method.

| Test Methods | Unresolved Diagnosis | Wrong Diagnosis | Accuracy |
|---|---|---|---|
| Roger's Ratios | 21 | 9 | 75.67% |
| IEC Ratio | 27 | 8 | 74.19% |
| NNCA | - | 4 | 93.10% |
| Proposed Method | - | 3 | 94.82% |

The accuracy of the proposed method shown in Table 4.3 is higher than NNCA when compared with expert decisions. (However, given the small test set, it is unclear whether this improvement is statistically significant). The overall performance of this method is 95% accurate, which is much higher than the conventional ratio methods. In 3 cases, the method wrongly diagnoses the fault category of transformers, but it provides a useful decision-support mechanism for engineers who are trying to deal with these critical cases. Moreover, this new approach shows probable advantages over earlier NNCA methods. In NNCA, which is a combination of the k-Means algorithm (KMA), k-Nearest Neighbour algorithm (KNN) and Linde-Buzo-Gray, determination of actual centre locations is critical. As KMA only converges to the local minima, different positions of initial cluster centres lead to different final clusterings [25]. To overcome this problem partially, a number of variants like Lloyd's algorithm and Linde-Buzo-Gray have been combined with conventional

KMA [26]. However, there is no guarantee that data will be optimally assigned to the various clusters. The advantages of the Parzen window method are as follows:

i. Information of the cluster centres is not necessary.
ii. It can be used to solve problems without the probability distribution knowledge of a training set.
iii. No assumptions are required to classify a faulty class of transformers.
iv. The complexity and correlation of input random variables do not affect the performance of the proposed algorithm.

## 4.6 Evaluation and Comparison with Other Methods

To better evaluate the performance of the proposed method, it has also been applied to the test sets generated by other researchers [16, 27-28]. The authors of these papers have done a similar type of experiment but have focused on different approaches to identify the fault category of transformers. They have also trained their classifiers using training data, labelled by the utility experts. In [16], researchers diagnosed the category of a faulty transformer using a decision tree based on the concentration of combustible key gas limits and named it as a New Approach DGA. They found that different faults having the same gas limit overlapped. To deal with the overlapping problem, an additional gas ratio was included into the decision mechanism and renamed it as the Modified New Approach DGA. The performance of the proposed Parzen windows (PW) method has been compared to the decision tree approach [16] and conventional ratio methods in Table 4.4.

**Table 4.4:** Comparison between decision tree, ratio, NNCA and the proposed method (shown in bold).

| Case Number | $H_2$ | $CH_4$ | $C_2H_4$ | $C_2H_6$ | $C_2H_2$ | Diagnosis Result | | | | | |
|---|---|---|---|---|---|---|---|---|---|---|---|
| | | | | | | Actual Diagnosis | New Approach DGA | Modified New Approach DGA | Roger's Ratios | IEC Ratio | **Proposed Method** |
| 1 | 117 | 17 | 3 | 1 | 1 | PD | PD, D1 | PD | - | - | **PD** |
| 2 | 32930 | 2397 | 0 | 157 | 0 | PD | PD, D1 | PD | PD | PD | **PD** |
| 3 | 78 | 20 | 13 | 11 | 28 | D1 | D1, D2 | D1 | - | D1 | **D1** |
| 4 | 1230 | 163 | 233 | 27 | 962 | D1 | D1, D2 | D1 | D2 | D1 | **D1** |
| 5 | 8200 | 3790 | 4620 | 250 | 277 | D2 | D2, T1 | D2 | - | - | **D2** |
| 6 | 130 | 140 | 120 | 2 | 0 | T1 | D2, T1 | T1 | T3 | T3 | **T3** |
| 7 | 78 | 66 | 2.6 | 283 | 0 | T1 | D2, T1 | T1 | Normal | PD | **T1** |
| 8 | 30.4 | 117 | 138 | 44.2 | 0.1 | T2 | T2, T3 | T2 | T3 | T2 | **T2** |
| 9 | 27 | 90 | 63 | 42 | 0.2 | T2 | T1, T2 | T1 | T2 | T2 | **T2** |
| 10 | 1100 | 1600 | 2010 | 221 | 26 | T3 | T2, T3 | T3 | T3 | T3 | **T3** |

From Table 4.4, it can be seen that the correct diagnosis rate of the proposed PW method is higher than those of the IEC and Roger's ratios methods. Moreover, the proposed method has accurately classified all the cases except case number 6.

The proposed method was also applied on the test sets disclosed in literature [27] where fault categories have been determined by applying a rough sets (RS) analysis technique and artificial neural networks (ANNs) combined with RS and k-means clustering (KMC) algorithms. A comparative performance of their methods, different established methods and proposed method has been summarised in Table 4.5.

**Table 4.5:** Fault diagnosis comparison between established and adapted methods.

| Case Number | $H_2$ | $CH_4$ | $C_2H_4$ | $C_2H_6$ | $C_2H_2$ | Diagnosis Result | | | | | | | |
|---|---|---|---|---|---|---|---|---|---|---|---|---|---|
| | | | | | | Expert Diagnosis | Duval Triangle | RS | RS-ANN | KMC-RS-ANN | Roger's Ratios | IEC Ratio | Proposed Method |
| 1 | 60 | 40 | 110 | 10 | 70 | D2 | D2 | D2 | D2 | D2 | D2 | D2 | **D2** |
| 2 | 31 | 7 | 5 | 19 | 67 | D2 | D1 | - | D2 | D2 | - | - | **D1** |
| 3 | 293 | 50 | 15 | 13 | 120 | D2 | D2 | D2 | D2 | D2 | D2 | D1 | **D2** |
| 4 | 57 | 7 | 4.5 | 19 | 71 | D2 | D1 | - | D2 | D2 | - | - | **D1** |
| 5 | 467 | 148 | 266 | 13 | 511 | D2 | D2 | D2 | DT | D2 | D2 | D1 | **D2** |
| 6 | 160 | 90 | 17 | 27 | 58 | D1 | D1 | D1 | D1 | D1 | - | - | **D1** |
| 7 | 402 | 81 | 27 | 39 | 25 | D1 | D2 | D1 | D1 | D1 | - | - | **S** |
| 8 | 4 | 79 | 312 | 112 | 0 | T2 | T1 | - | T2 | DT | T2 | T2 | **T2** |
| 9 | 180 | 180 | 4 | 74 | 3 | DT | T3 | DT | DT | DT | - | - | **T2** |
| 10 | 1300 | 740 | 2000 | 260 | 71 | T3 | T3 | T3 | T3 | T3 | - | - | **T3** |
| 11 | 42 | 97 | 600 | 157 | 0 | T3 | T3 | Normal | Normal | Normal | T2 | T2 | **T2** |
| 12 | 44 | 52 | 119 | 15 | 1 | T3 | T3 | T3 | T3 | T3 | T3 | T3 | **T3** |
| 13 | 42 | 79 | 152 | 31 | 1 | T3 | T3 | T3 | T3 | T3 | T3 | T3 | **T3** |
| 14 | 164 | 244 | 497 | 103 | 8 | T3 | T3 | T3 | T3 | T3 | T3 | T3 | **T3** |
| 15 | 22 | 51 | 57 | 42 | 0 | T2 | T2 | T2 | T2 | T2 | T2 | T2 | **T2** |
| 16 | 679 | 4992 | 3671 | 1823 | 0 | T2 | T1 | T2 | T2 | T2 | T2 | T2 | **T2** |

Application of this linear approach to classify a transformer's fault category may not be effective for critical cases. To deal with the nonlinear problem, different artificial intelligence and machine learning techniques such as ANN, SVM, extreme learning machine(ELM), and self-adaptive evolutionary extreme learning machine (SaE-ELM) were proposed in [28]. They classify each testing transformer following these four methods and the final decision taken following the majority of votes. A comparison of the artificial intelligence and machine learning techniques with the PW probability density estimation method is shown in Table 4.6.

**Table 4.6:** Comparison of different adapted technique and proposed methods.

| Case Number | $H_2$ | $CH_4$ | $C_2H_4$ | $C_2H_6$ | $C_2H_2$ | Diagnosis Result | | | | | | | |
|---|---|---|---|---|---|---|---|---|---|---|---|---|---|
| | | | | | | ANN | SVM | ELM | SaE-ELM | Duval Triangle | Roger's Ratios | IEC Ratio | **Proposed Method** |
| 1 | 103 | 5.8 | 7.3 | 5 | 0.7 | T1 | T3 | T1 | T1 | S | - | - | **T1** |
| 2 | 416 | 21 | 43.1 | 10.5 | 1 | T1 | T3 | T1 | T3 | T3 | - | - | **T2** |
| 3 | 59 | 53 | 60.3 | 17.7 | 0.8 | T2 | T2 | T2 | T2 | C | - | - | **T2** |
| 4 | 10.5 | 4.8 | 4.8 | 5 | 2.2 | D1 | D1 | D1 | D1 | DT | - | - | **D1** |
| 5 | 137 | 97 | 29 | 12 | 1.5 | T2 | T2 | T2 | T2 | C | LEDA/PD | - | **T2** |
| 6 | 89 | 73 | 6.8 | 6 | 5 | D2 | D2 | D2 | D2 | DT | - | - | **T2** |
| 7 | 240 | 157 | 127 | 98 | 0.8 | T2 | T2 | T2 | T2 | C | LEDA/PD | - | **T2** |
| 8 | 116 | 104 | 51 | 36 | 0 | T2 | T2 | T2 | T2 | C | LEDA/PD | - | **T2** |

## 4.7 Case Study

To provide a better insight, all the cases in literature have been used in the case study. Except for case number 6, the proposed method has solved all the over-lapping problems shown in Table 4.3. Case number 6 differs from the expert classification (T1), has been classified as T3. The method also has successfully classified 12 cases out of 16 shown in Table 4.4. The wrongly classified cases are 2, 4, 7 and 9. The expert has classified those problems as D2, D2, D1 and DT while the proposed method classifies them as D1, D1, S and T2 respectively. Duval Triangle classified the faults as D1, D1, S and DT correspondingly, but the other two conventional methods: Roger's ratio and IEC ratio failed to diagnose these cases as their ratios fall outside the defined limits. As the gas concentrations collected from the utility company predominantly used Duval Triangles to classify their transformers' fault categories, it could be a reason for misclassification in cases 2, 4 and 7 respectively. The DT fault which is a combination of thermal and dielectric fault was not included in the targeted categories. Therefore, it has been classified as a T2 type thermal fault. A similar problem also arises in case number 6 shown in Table 4.5. That case is classified by the ANN, SVM, ELM, and SaE-ELM methods as a D2 fault. Moreover, for the cases shown in Table 4.5, IEC method could not detect any faults and the performance of the Roger's ratio is not satisfactory. The problems of the proposed

method could be overcome by increasing the number of random samples drawn from the larger number of training measurements.

In this research, the optimal value of covariance for five-dimensional data sets is carefully chosen through a continuously supervised iterative process. All the five-dimensional gas concentrations' information has been deliberately preserved throughout the proses aiming to get a better result than with the Duval Triangles. In the Duval triangle, gas concentrations are mapped into low dimensional spaces prior to classifying a transformer fault category. Deliberately preserved extra dimensional information has helped to accurately classify 95 percent of the cases. Moreover, the performance of this method is satisfactory on the published data which has been shown in Tables 4.3, 4.4 and 4.5.

## 4.8 Conclusions

A new procedure for DGA analysis based on PDF estimation by using the PW method is introduced in this paper. The method is specialized to deal with the difficult cases where Duval's triangle fails to provide a definitive fault classification. To develop a reliable and effective fault classifier, five key gas concentrations from 376 power transformers were normalised into percentage form. The new approach is straight forward and easy to apply without the knowledge of cluster centres. The comparative results shown in Tables 4.4, 4.5 and 4.6 demonstrate that the performance of the PW method is much better than the conventional ratio-based diagnostic strategies and comparable with different artificial intelligences and machine learning techniques such as the ANN, SVM, ELM, SaE-ELM and NNCA. The experimental results in Table 4.3 show that it correctly classifies 94.8% of these difficult cases where Duval's triangle provides an ambiguous classification. As the accuracy of this method is dependent on the number of training samples, the accuracy could be improved and the repair cost for a transformer may be reduced by having a larger number of training samples.

## References

[1] N.K. Dhote and J.B. Helonde, Diagnosis of power transformer faults based on five fuzzy ratio method, WSEAS Transactions on Power Systems, Vol.7, pp. 114-125, 2012.

[2] M. Agah, G.R. Lambertus, R. Sacks and K. Wise, High-Speed MEMS-Based Gas Chromatography, Journal of Microelectromechanical Systems, Vol.15, pp.1371-1378, 2006.

[3] S.A. Khan, M.D. Equbal and T. Islam, A comprehensive comparative study of DGA based transformer fault diagnosis using fuzzy logic and ANFIS models, IEEE Transactions on Dielectrics and Electrical Insulation, Vol.22, pp. 590-596, 2015.

[4] S. Singh and M.N. Bandyopadhyay, Dissolved gas analysis technique for incipient fault diagnosis in power transformers: A bibliographic survey, IEEE Electr Insul Mag, Vol.26, pp. 41-46, 2010.

[5] A.D. Ashkezari, T.K. Saha, C. Ekanayake and H. Ma, Evaluating the accuracy of different DGA techniques for improving the transformer oil quality interpretation, In: The 21st AustralasianUniversities Power Engineering Conference (AUPEC 20111), September 25-28, 2011 Brisbane, Australia.

[6] N.A. Bakar, A. Abu-Siada and S. Islam, A review of dissolved gas analysis measurement and interpretation techniques, IEEE Electrical Insulation Magazine, Vol.30, pp.39-49, 2014.

[7] S. Singh and M.N. Bandyopadhyay, Dissolved gas analysis technique for incipient fault diagnosis in power transformers: A bibliographic survey, IEEE Electr Insul Mag, Vol.26, pp. 41-46, 2010.

[8] A. Akbari, A. Setayeshmehr, H. Borsi, E. Gockenbach and I. Fofana, Intelligent agent-based system using dissolved gas analysis to detect incipient faults in power transformers, IEEE Electrical Insulation Magazine, Vol.26, pp. 41-46, 2010.

[9] M. Pal and G.M. Foody, Feature Selection for Classification of Hyperspectral Data by SVM, IEEE Transactions on Geoscience and Remote Sensing, Vol. 48, pp. 2297-2307, 2010.

[10] Q. Su, C. Mi, L.L. Lai and P. Austin, A fuzzy dissolved gas analysis method for the diagnosis of multiple incipient faults in a transformer, IEEE Transactions on Power Systems, Vol.15, pp. 593-598, 2000.

[11] S.M. Islam, T. Wu and G. Ledwich, A novel fuzzy logic approach to transformer fault diagnosis, IEEE Trans Dielectr Electr Insul, Vol.7, pp. 177-186, 2000.

[12] R. Naresh, V. Sharma and M. Vashisth, An Integrated Neural Fuzzy Approach for Fault Diagnosis of Transformers, IEEE Transactions on Power Delivery, Vol. 23, pp. 2017-2024, 2008.

[13] M.M. Islam, G. Lee and S.N. Hettiwatte, A nearest neighbour clustering approach for incipient fault diagnosis of power transformers, Electrical Engineering, DOI:10.1007/s00202-016-0481-3, pp.1-11, 2016.

[14] T.K. Saha, Review of modern diagnostic techniques for assessing insulation condition in aged transformers, IEEE Trans Dielectr Electr Insul, Vol.10, pp. 903-917, 2003.

[15] IEC, 60599 Ed. 2.1 Mineral oil-impregnated electrical equipment in service - Guide to the interpretation of dissolved and free gases analysis, in 1999.

[16] S.S.M. Ghoneim and I.B.M. Taha, A new approach of DGA interpretation technique for transformer fault diagnosis, International Journal of Electrical Power & Energy Systems, Vol. 81, pp.265-274, 2016.

[17] IEEE Guide for the Interpretation of Gases Generated in Oil-Immersed Transformer, IEEE Std. C57.104, 1991.

[18] C. Archambeau, M. Valle, A. Assenza and M. Verleysen, Assessment of probability density estimation methods: Parzen window and finite Gaussian mixtures, In: IEEE International Symposium on Circuits and Systems, May 21-24 2006.

[19] Z. Hu, M. Xiao, L. Zhang, S. Liu and Y. Ge, Mahalanobis Distance Based Approach for Anomaly Detection of Analog Filters Using Frequency Features and Parzen Window Density Estimation, Journal of Electronic Testing, Vol.24, pp.901-907, 2008.

[20] E. Parzen, On Estimation of a Probability Density Function and Mode, Annals of Math Statistics, Vol.33, pp.1065-1076, 1962.

[21] I.M. Overton, G. Padovani, M.A. Girolami and G.J. Barton, ParCrys: a Parzen window density estimation approach to protein crystallization propensity prediction, Bioinformatics, Vol.24, pp. 901-907, 2008.

[22] V.S. Babu and P. Viswanath, An Efficient and Fast Parzen-Window Density Based Clustering Method for Large Data Sets, In: First International Conference on Emerging Trends in Engineering and Technology, July 16-18 2008, pp. 531-536.

[23] B.W. Silverman:, Density Estimation: Chapman & Hall/CRC, number of iterations as parameter, London, 1986.

[24] S. Noschese and L. Reichel, Inverse problems for regularization matrices, Numerical Algorithms, Vol. 60, pp. 531-544, 2012.

[25] A.K. Jain, Data clustering: 50 years beyond K-means, Pattern Recognition Letters, Vol. 31, pp.651-666, 2010.

[26] T. Kanungo, D.M. Mount, N.S. Netanyahu, C.D. Piatko and R. Silverman, An efficient k-means clustering algorithm: analysis and implementation, IEEE Transactions on Pattern Analysis and Machine Intelligence, Vol.24, pp.881-892, 2002.

[27] Y.H. Sheng-wei Fei, A multi-layer KMC-RS-SVM classifier and DGA for fault diagnosis of power transformer, In: R.P.o.C. Science (Ed.), Vol.10, pp. 238-243, 2012.

[28] S. Li, G. Wu, B. Gao, C. Hao, D. Xin and X. Yin, Interpretation of DGA for transformer fault diagnosis with complementary SaE-ELM and arctangent transform, IEEE Trans Dielectr Electr Insul, Vol. 23, pp.586-595, 2016.

# Chapter 5: Missing Measurement Estimation of Power Transformers Using a GRNN


## Abstract

Many industrial devices are monitored by measuring several attributes at a time. For electrical power transformers, their condition can be monitored by measuring electrical characteristics such as frequency response and dissolved gas concentrations in insulating oil. These vectors can be processed to indicate the health of a transformer and predict its probability of failure. One weakness of this approach is that missing measurements render the vector incomplete and unusable. A solution is to estimate missing measurements using a General Regression Neural Network on the assumption that they are correlated with other measurements. If these missing values are completed, the entire vector of measurements can be used as an input to a pattern classifier. To test this approach, known values were deliberately omitted allowing an estimate to be compared with actual values. Tests show the method is able to accurately estimate missing values based on a finite set of complete observations.

## 5.1 Introduction

Missing data is a common problem in the wide range of industrial asset management systems. It can create a problem in many applications and decision-making processes that are dependent on the complete set of vector measurements and how vectors change over time. To monitor the performance of a plant, often measurements are made in a group in the same period. In practice, due to unavoidable situations, such as problem with a sensor or a broken data transmission line, some measurements may be missed out. Therefore, experts have to take decision based on the available dimensions of the measured vectors.

To illustrate the missing data problem, in this work, measurements of electrical power transformers have been used as a basis of these experiments. Measurements such as dissolved gas analysis and dielectric insulation tests can be used to assess the condition of a transformer and indicate its likelihood of imminent failure. Due to financial constraints, environmental conditions and other technical issues, utility cannot always perform all the required measures resulting in the set $\{X_1, X_2, \cdots, X_n\}$ being incomplete or containing outdated measurements. To handle this situation, utility experts often take decisions based on their knowledge and past experiences. It is beneficial in automated decision making if a reasonable estimate of missing values can be made from a finite set of complete measurements. Therefore, the measurements can also be used in a data analysis system like an artificial neural network that requires complete vectors of measurements. To estimate the missing input vector elements different statistical and artificial intelligence techniques have been used [1]. All these approaches try to find the correlations between variables which are inherent in the input space. One of the well-known missing data estimation techniques is the expectation maximization (EM) algorithm [2]. EM can estimate the missing value of a multidimensional vectors if one or more values are missing at random (MAR) [3-4]. A value is considered MAR if it is dependent on the other specified dimensions such that the missing data is traceable [5]. The algorithm

creates a model that approximates a missing value based on its maximum likelihood from the available set of vectors. The accuracy of the EM model is limited as it uses finite number of estimators (kernels) to estimate the missing values [3]. Moreover, the performance of the algorithm is dependent on the initial accuracy of the estimated missing value in the E-step which tries to improve by following an expectation maximization step or M-step based on the finite set of complete vectors. Abas in [3] presents an alternative approach and shows that, if the missing value in a multi-dimensional vector can be estimated with high accuracy initially, the performance of the EM model can be improved. To estimate the missing value an Incremental General Regression Neural Network (IGRNN) [3] was applied as a replacement of the initial E-step of the EM algorithm. The estimated values were then used in the M-step to estimate the parameters of the model and provide better performance than the EM. This paper presents a General Regression Neural Network (GRNN)[1] which is quite similar to the Abas' method except the model's smoothing parameter was estimated from an experimental search based on the complete set of measurements using a holdout method [6]. The GRNN considers the missing data as a function interpolation problem consisting of a nonlinear mapping from a set of input variables (its domain) onto a single output variable (its codomain). To estimate the distribution of measurements, a multivariate Gaussian Kernel is adopted in this work because it has small number of parameters that need to be estimated and computing its derivative is simple. The arrangement of the paper is as follows: Section 5.2 describes methodology of the research. Section 5.3 presents the proposed machine learning technique. Section 5.4 presents the results that were achieved with the method and section 5.5 presents the conclusions.

## 5.2 Methodology

This section used a GRNN technique to find the correlation between different dimensions of a multidimensional vector (of measurements). The GRNN uses a

[1] More detail about GRNN introduction is available in the next chapter, page 140.

statistical Gaussian kernel for exploring a best-fitting model to predict the missing value of a measurement based on the complete set of training measurements. Various aspects of the methodology section are discussed in the subsections below.

### 5.2.1 Input Selection

To check the operating condition of insulation in power transformers various dielectric and chemical tests are regularly performed. These tests help to monitor the key performance parameters of the paper and oil insulation such as dielectric breakdown voltage (DBV), moisture content, acidity, furan, power factor (pf), total dissolved combustible gases (TDCG) and interfacial tension (IFT) of the insulating liquid [7-8]. As these measurements act as indicators of a small set of underlying fault conditions, the values are often inter-related resulting in a statistical correlation between the various values. To estimate the missing values of these multidimensional vectors only the correlated measurements need to be considered. In the collected data set, it was found that the *pf* of oil was the most commonly missing dimension. Therefore, only the measurements having some degree of correlation with *pf* were used in this experiment. During operation, some power is always dissipated through the oil of a transformer as a form of heat energy. This loss increases the overall temperature of a transformer and accelerates its aging rate. The ageing by-products contaminate oil and increase the conductivity and permittivity of this insulating liquid [9]. Therefore, oil resistance decreases, resulting in an increase in the dissipation factor. The amount of degradation due to the dissipated power and contamination is evaluated by the *pf* test [10-11]. The oxidative degradation of paper and oil produce hydrophilic carboxylic acids that affect the chemical (acidity) and physical (interfacial tension) properties of the fluid. In an IFT test, the surface tension between oil and water is measured and this decreases with the increase of hydrophilic materials in the insulating oil. The correlation between the IFT and pf based on the collected data is shown in Figure 5.1.

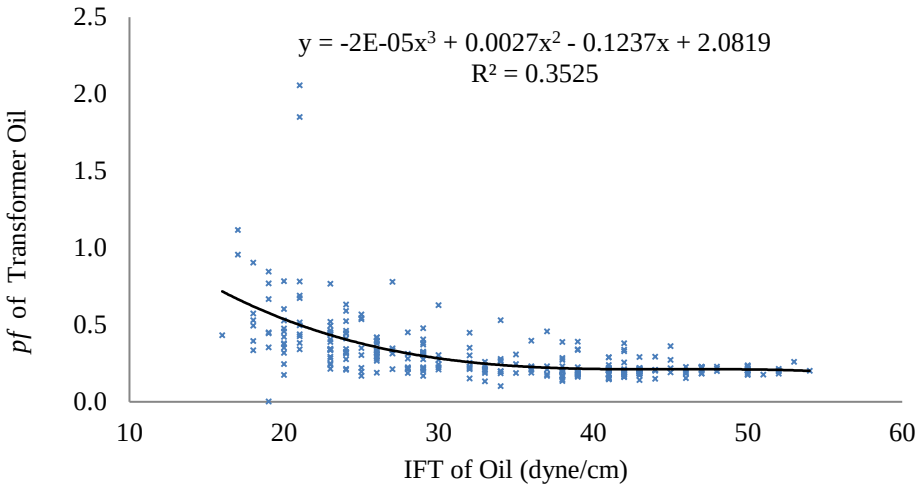


**Figure 5.1:** Correlation between IFT and *pf* of oil

It can be seen from Figure 5.1 that the *pf* of oil has an inverse correlation with IFT.

Moisture is one of the most unexpected by-products in a transformer since it is produced from the degradation of paper insulation. It reduces the dielectric strength of oil and paper insulation resulting in an increase in the ageing and dissipation factor. The moisture can also come from several sources such as the surrounding atmosphere and leaky seals of transformers [12]. A correlation between the percentage of moisture concentration and *pf* of the oil is shown in Figure 5.2.

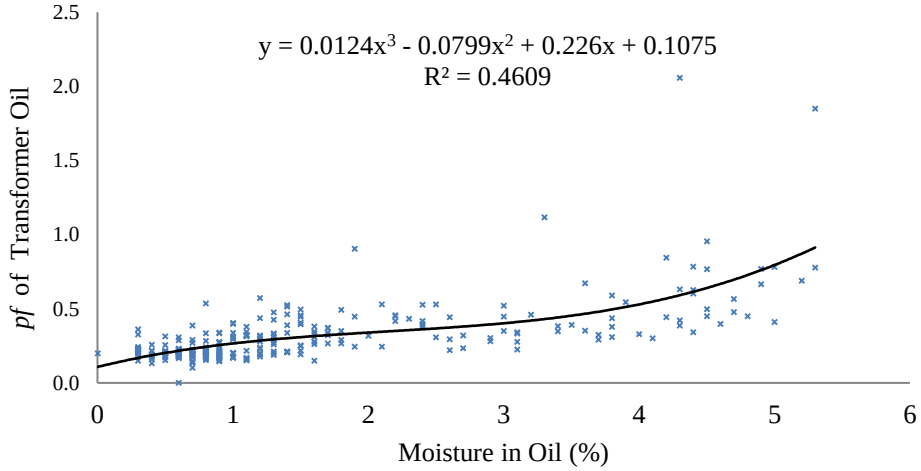


**Figure 5.2:** Correlation between Moisture and *pf* of Oil.

Figure 5.2 shows that the *pf* of oil increases with an increase of moisture concentration in it.

The ageing and variable operating stresses also produce gases in transformers that partially dissolve in the insulating oil. The collected data shows a degree of correlation between *pf* and TDCG. Therefore, TDCG can also be used as an input. However, the DBV, furan and acidity of oil did not show any correlation with its *pf*, hence they were excluded from the input. As the operating age of a transformer has a significant effect on its condition of insulation, it has been also considered here.

### 5.2.2 Data Processing and Normalization

In this work, a vector of measurements from 345 power transformers based on their oil tests data were provided by a large utility company in Australia. All the tests on the collected oil samples were conducted in 2014. In the data set, 35 vectors were incomplete due to missing values in single or multiple dimensions of the vectors. There was no way of testing these missing values as the actual missing values are unknowable. Therefore, another 20 incomplete vectors were created from the 310 complete measurements by deliberately obscuring some of the dimensions to mimic the actual missing values. The remaining 290 complete vectors were used to construct a training set for the proposed model. The performance of the model was verified using a test set comprised of these obscured values. The test set was sorted so that vectors with the fewest missing values were processed first. The dimensions of the vectors were normalized by dividing by their corresponding maxima to scale each in the range zero to unity. Therefore, the GRNN model was free from the dominant influence of any particular dimension.

### 5.2.3 Proposed Model

In this research, a nonparametric GRNN model technique has been applied to estimate the missing value of the multidimensional vector (s). To develop the proposed GRNN model, both the training and test sets were divided into dependent (missing dimension) and independent variables. The dependent variable $Y = \{Y_n\}$ of the test set is predicted from the number of *D*-dimensional independent measurements $\boldsymbol{X} = \{X_n\}$ of the training set where $X_n \in \mathcal{R}^D$, $here\ D = 4$ . The prediction is the most probable value of *Y* for each value of *X* based on a finite set of $n$ training measurements and their associated *Y* values. Thus, the GRNN learns a mapping from an input domain containing *X* to an output co-domain containing *Y*, where either space can be multidimensional, but here *Y* is a scalar. If a GRNN is trained with a finite number of available measurements, it can estimate a linear or nonlinear regression surface to predict the most probable value of *Y* for any new measurement of $x$.According to [13], the basic equation for the GRNN function $g(x)$ based on a multivariate Gaussian kernel can be written as:

$$g(x) = \frac{\sum_{n=1}^{N} Y_n exp\left(-\frac{{D_n}^2}{2}\right)}{\sum_{n=1}^{N} exp\left(-\frac{{D_n}^2}{2}\right)} \tag{5.1}$$

where $x$ is a multidimensional independent variable of the test set, $Y_n$ is the dependent variable for the training set and ${D_n}^2 = (x - X_n)^T \Sigma^{-1}(x - X_n)$ is the distance between the training set and the point of prediction. The exponential terms of (5.1) reflect the contribution of each training point to the dependent variable of$x$ that has been intentionally kept missing to validate the performance of the model.

The performance of the model is dependent on the smoothing parameter $\Sigma$ which is the multivariate covariance matrix of the independent variables of training set. Larger values within the matrix will result in a smoother interpolation but force the model to ignore some important features of the training samples [14]. Conversely, if the values are very small then the model will over fit the training examples and losses its

generalization capability [15]. Therefore, a trade-off between the maximum and minimum element values of the $\Sigma$ matrix is necessary such that all useful features of the training set can be taken into account.

## 5.3 Training and Testing

During the training stage, the dependent variables of the 290 training set were estimated using their four dimensional independent variables. The $\Sigma$ value for the model was directly calculated from the training set. To vary the values in the $\Sigma$ matrix, a scalar multiplicative factor $E$ was added in front of it. Therefore, large value of $E$ result in a smoother interpolation and small value mean potential for over fitting the dat. The new equation of $\Sigma$ can be written as,

$$\Sigma = E\Sigma_S \tag{5.2}$$

where$\Sigma_S$ is the covariance matrix of the training samples and $E$ is a multiplicative factor chosen to vary the amount of smoothing.

An optimal value of $E$ was estimated based on the holdout method [6]. In this approach, one sample from the training set was removed at a time and a network was constructed using all of the other samples. The network was used to estimate the dependent variable of the missing sample for a small value (0.001) of $\Sigma$ following equation (5.1). The process was repeated for all samples and the mean-squared error between actual and estimated values were computed and stored. Then the value of $E$ was increased linearly up to 1 with a very small step and the whole process is repeated. The mean-squared error at all values of $E$ was computed. Finally, the value of $E$ (0.2539 shown as square box in Figure5.3) given the smallest error was selected for the proposed model. A detailed procedure of the holdout method has been discussed in the previously published work [16]. The mean-squared error at different values of $E$ for oil tests is shown in Figure 5.3.

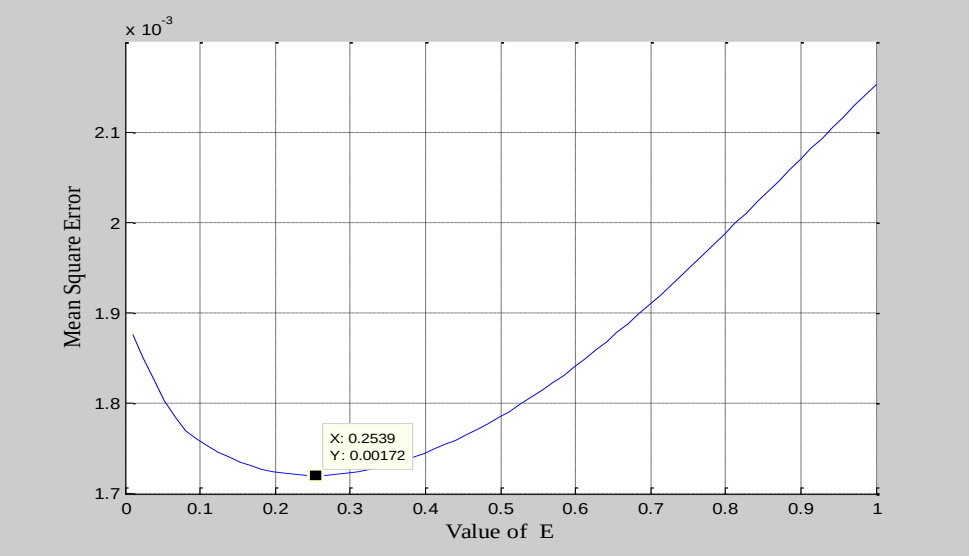


**Figure 5.3:** Mean-squared error at different values of $E$

After estimating an optimal value of $E$, the independent variables of the test set were computed and compared with their true values to validate the performance of the model. To estimate the actual missing values of the 35 measurements that were sorted orderly in the previous data processing section, all the complete measurements (training and test sets) were used. The steps of the GRNN algorithm are described as follows:

i. The estimation of the first missing value $g(x)$ is computed as a weighted average of all the 310 observed dependent values $Y_n$, where each observed value is weighted exponentially according to its distance from the point of prediction as shown in (5.1).
ii. After estimating one missing value, the vector is added to the complete ones and then used to estimate the next missing value.

Step1 and Step 2 are repeated until all missing values in the sorted measurements were completed.

As the GRNN is very versatile at learning mappings, it can also to estimate multiple missing value of a vector. For instance, if a vector is $Z = [A\ B\ C\ D\ ]$ and its two elements $C$ and $D$ are missing, the mapping is started as $\mathcal{R}^2 \rightarrow \mathcal{R}$ using $A\ and\ B$ to estimate $C$. After an initial estimation of $C$, the value of $A\ B\ and\ C$ are used to create a mapping of $\mathcal{R}^3 \rightarrow \mathcal{R}$ to estimate the most likely value of $D$. Now $C$ and $D$ can be used to estimate each other following the last step in an iterative way until they are convergence.

## 5.4 Results and Discussion

In order to analyse the performance of the proposed GRNN model, initially it was trained with a significant number of training examples to extract an optimal value of the smoothing parameter $\Sigma$. After estimating appropriate smoothing, the model was applied on the 20 test cases to estimate their missing values where the true values were known. The estimated result is shown in Table 5.1.

**Table 5.1:** Estimation of known missing data based on four dimensional vectors.

| Serial Number | Operating Age (Years) | IFT (dyne/cm) | Moisture (%) | TDCG (ppm) | Actual pf of Oil | Estimated pf of Oil | Error (%) |
|---|---|---|---|---|---|---|---|
| 1 | 50 | 24 | 2.7 | 176 | 0.3203 | 0.3348 | -4.53 |
| 2 | 50 | 28 | 2.2 | 198 | 0.4504 | 0.4472 | 0.71 |
| 3 | 50 | 25 | 4.7 | 195 | 0.5670 | 0.5619 | 0.90 |
| 4 | 51 | 19 | 4.9 | 78 | 0.7701 | 0.7628 | 0.95 |
| 5 | 51 | 23 | 3.1 | 300 | 0.3340 | 0.3351 | -0.33 |
| 6 | 51 | 26 | 4.6 | 188 | 0.3993 | 0.3876 | 2.93 |
| 7 | 50 | 29 | 3.7 | 296 | 0.3254 | 0.3196 | 1.78 |
| 8 | 50 | 34 | 2.5 | 205 | 0.5310 | 0.5325 | -0.28 |
| 9 | 52 | 24 | 5.0 | 423 | 0.4115 | 0.4120 | -0.12 |
| 10 | 52 | 30 | 2.9 | 282 | 0.3034 | 0.3151 | -3.86 |
| 11 | 52 | 21 | 5.0 | 318 | 0.7828 | 0.7644 | 2.35 |
| 12 | 52 | 17 | 4.5 | 432 | 0.9557 | 0.8233 | **13.85** |
| 13 | 52 | 19 | 4.9 | 119 | 0.6671 | 0.5778 | **13.39** |
| 14 | 52 | 24 | 3.8 | 184 | 0.5907 | 0.5046 | **14.58** |
| 15 | 52 | 21 | 5.2 | 179 | 0.6899 | 0.7216 | -4.59 |
| 16 | 53 | 21 | 4.5 | 228 | 0.4969 | 0.4715 | 5.11 |
| 17 | 54 | 26 | 1.0 | 122 | 0.3976 | 0.3745 | 5.81 |
| 18 | 54 | 19 | 3.6 | 116 | 0.3534 | 0.3421 | 3.20 |
| 19 | 54 | 29 | 3.4 | 259 | 0.3832 | 0.3570 | 6.85 |
| 20 | 54 | 21 | 3.1 | 656 | 0.3418 | 0.3442 | -0.70 |

From Table 5.1, it can be seen that in most cases, the proposed GRNN model estimated the *pf* of oil accurately with a reasonable amount of over and under estimation (less than 7% error). However, in the three cases (shown in bold), serial numbers 12, 13 and 14 significant amounts of errors were observed. It was because of the limited distribution of the training examples in the space where the three points are located. The errors could have been reduced with a large number of training examples such that the underlying GRNN function will be continuous [6]. After getting satisfactory performance on the estimation of the known missing values, the model was applied to estimate the 35 missing values in the data set collected from a large utility company. Therefore, it is expected that the estimated values are very

close to their true values and will help the utility experts to take correct decisions on schedule maintenance by looking at the complete set of measurements.

## 5.5 Conclusions

In this paper, a new application of the general regression neural network has been presented to estimate missing values of transformer measurements. Five correlated performance parameters of transformers such as operating age, IFT, percentage of moisture, TDCG and *pf* of oil were used as inputs to estimate any missing values. The performance parameter of the model $\Sigma$ which was controlled by a multiplicative scalar $E$ estimated using the well-known holdout method such that the mean square error between the actual value and the estimated value is reduced. Comparative results presented in Table 5.1 indicate that this method could be effective to estimate the missing data in the industrial and utility sectors.

## References

[1] V. Fulufhelo, Nelwamondo, S. Mohamed and T. Marwala, Missing Data: A Comparison of Neural Network and Expectation Maximisation Techniques, School of Electrical and Information Engineering, University of the Witwatersrand, South Africa, 2007.

[2] A.P. Dempster, N.M. Laird and D.B. Rubin, Maximum Likelihood from Incomplete Data via the EM Algorithm, Journal of the Royal Statistical Society, Vol.39, pp. 1-38, 197.

[3] A.R. Abas, Using incremental general regression neural network for learning mixture models from incomplete data, Egyptian Informatics Journal, Vol.12, pp.185-196, 2011.

[4] L. Hunt and M. Jorgensen, Mixture model clustering for mixed data with missing information, Computational Statistics & Data Analysis, vol. 41, pp. 429-440, 2003.

[5] R.J.A. Little and D.B. Rubin, Statistical Analysis with Missing Data, John Wiley & Sons, Incorporated, Somerset, United States, 2014.

[6] D.F. Specht, A general regression neural network, IEEE Transactions on Neural Networks, Vol. 2, pp. 568-576, 1991.

[7] M.M. Islam, G. Lee and S.N. Hettiwatte, A review of condition monitoring techniques and diagnostic tests for lifetime estimation of power transformers Electrical Engineering. doi:10.1007/s00202-017-0532-4, 2017.

[8] M.M. Islam, G. Lee, and S.N. Hettiwatte, A nearest neighbour clustering approach for incipient fault diagnosis of power transformers, Electrical Engineering. doi:10.1007/s00202-016-0481-3, 2016.

[9] I. Fofana and Y. Hadjadj, Electrical-Based Diagnostic Techniques for Assessing Insulation Condition in Aged Transformers, Energies, doi:10.3390/en9090679, 2016.

[10] A.E.B. Abu-Elanien, M.M.A. Salama and M. Ibrahim, Calculation of a Health Index for Oil-Immersed Transformers Rated Under 69 kV Using Fuzzy Logic, IEEE Transactions on Power Delivery, Vol. 27, pp. 2029-2036, 2012.

[11] J. Singh, Y. R. Sood and P. Verma, Experimental Investigation Using Accelerated Aging Factors on Dielectric Properties of Transformer Insulating Oil, Electric Power Components and Systems, Vol 39, 2011.

[12] T.V. Oommen and T.A. Prevost, Cellulose insulation in oil-filled power transformers: part II maintaining insulation integrity and life, IEEE Electr Insul Mag, Vol. 22, pp. 5-14, 2006.

[13] J. Song, C.E. Romero, Z. Yao and B. He, A globally enhanced general regression neural network for on-line multiple emissions prediction of utility boiler, Knowledge-Based Systems, Vol. 118, pp. 4-14, 2017.

[14] O. Polat and T. Yıldırım, Hand geometry identification without feature extraction by general regression neural network, Expert Systems with Applications, Vol.34, pp. 845-849, 2008.

[15] I.M. Overton, G. Padovani, M.A. Girolami and G.J. Barton, ParCrys: a Parzen window density estimation approach to protein crystallization propensity prediction, Bioinformatics, Vol. 24, pp. 901-907, 2008.

[16] M.M. Islam, G. Lee and S.N. Hettiwatte, Application of a General Regression Neural Network for Health Index Calculation of Power Transformers, International Journal of Electrical Power and Energy Systems, Vol. 93, pp. 308-315, 2017

# Chapter 6: Application of a General Regression Neural Network for Health Index Calculation of Power Transformers


## Abstract

A power transformer is one of the most important components in a transmission network. To assess the overall condition of this valuable asset, health index calculations are recently gaining more attention from the utility companies that operate networks. Only limited research has been conducted on health index calculations of transformers. Most of the past approaches are based on the linear combination of weighted scores of measurements following the industry standards such as IEEE, IEC and CIGRE. A few previous methods based on artificial intelligence and statistical approaches such as fuzzy logic, multivariate analysis and binary logistic regression have been published in recent years. In this paper, a General Regression Neural Network (GRNN) which has a nice nonlinear property and can work with measurements without quantization has been evaluated. The GRNN allows multi-dimensional measurements to be combined through an optimal weighting and scoring system to compute a quantitative health index of power transformers. The weighting of each test was assigned based on a smoothly interpolated continuous function. The efficacy of the model has been validated against expert classifications and data sets published in the literature. The comparative results demonstrate that, the proposed method is reliable and very effective for condition assessment of transformers through an automated health index calculation.

## 6.1 Introduction

Power transformers are the most valuable assets in a power grid and comprise a significant fraction of the total investment in a power delivery system. The failure of a transformer can have a profound impact on the end users or utilities along with the cost implications of replacement, lost revenue and customer impacts [1-2]. Moreover, a sudden failure can damage the environment through oil leakages and can pose a risk to utility personal by causing fire and explosions. Therefore, to maintain an optimal balance among maintenance costs, safety and capital investments, proper condition assessment of these valuable assets is essential.

Over recent decades, health index (HI) calculations have been used as a powerful tool to assess the condition of transformers. In these HI calculations, a transformer's current information such as various test results, expert observations and field inspection data are combined into a single quantitate index to reflect its overall condition. Although the HI cannot reflect the status of any particular part of a transformer, it measures the level of long-term degrading that cannot be easily determined by one-off inspections. The calculated HI score is a result of interaction between different routine and diagnostic tests that are not considered by the classical condition monitoring techniques [3]. Thus, the calculated HI can identify the transformers that are close to their end-of-life and differentiate the transformers that have a higher probability of failure [4-6]. This information helps utilities to manage their assets appropriately, through clearly identifying the transformers that need more attention or major capital expenditure.

The challenging task in any HI calculation is to identify the most significant measurements and incorporate them through justified weightings. One of the established practices of many utilities is to use the recommended conditional score and weighting factors supplied by industry standards organizations such as IEEE,

IEC and CIGRE and combine the test results in a linear way. Mathematically, the linear approach can be expressed by the following equation.

$$h(\boldsymbol{x}) = \frac{w_1 x_1 + w_2 x_2 + \cdots + w_n x_n}{w_1 + w_2 + \cdots + w_n} \tag{6.1}$$

where$h$ is a health index metric, $w$ and $x$ represent the weight and conditional score of each test respectively and $n$ represents the number of tests included in a HI calculation.

After computing the HI, the conditional categories of transformers are determined based on the standard deviation within a known set of calculated scores. A similar approach has been used by Jahromi [4] where the HI scores of each transformer have been calculated by summing the product of scores and weights based on 24 tests. One of the limitations of this method is that a large number of tests need to be conducted simultaneous to apply the method. As some of the tests are conducted irregularly, at most points in time the set $\{x_1, x_2, \cdots, x_n\}$ is incomplete or contains outdated measurements. Moreover, a wide range of test results are treated equally and the method is insensitive to a single but critical result that could potentially lead a transformer to a catastrophic failure. Ahmed in [5], has used a Fuzzy Logic approach where the membership of a measurement in the five health condition categories was calculated using a number of Fuzzy sets (membership functions). To calculate the degree of membership, a certain portion of each set was overlapped with neighbouring sets using linear boundaries. Therefore, a measurement could be a member of single or multiple sets. The percentage of the overlapping zone is completely subjective and dependent on the experts' knowledge. Moreover, the derivation of the expert rules is also critical, since the tests are applied as a decision tree; hence the order of tests is important. Ahmed gave most importance to the furan concentration over other tests. However, the actual estimation

of furan from oil sampling in some cases is difficult as furan can disappear due to evaporation through the open breathing system or become disassociated under oxidizing and increased temperature conditions [7-8]. Oil treatment in the form of reclamation, replacement or top-up also has an impact on the furan concentration. Therefore, the calculated HI based on Fuzzy rules may have a certain degree of inaccuracy. Weijie in [9] also proposed another nonlinear approach where the conditional HI scores of transformers were calculated by using a binary logistic regression (BLR). The regression model can be expressed by (6.2).

$$H(x;\beta) = \frac{1}{1+e^{-\left(\beta_0+\sum_{i=1}^{n}\beta_i x_i\right)}} \tag{6.2}$$

where $\beta_0$ is a constant and $\beta_i$ is a coefficient that reflects the contribution of each independent test $x_i$ .

It is apparent from (6.2) that the accuracy of the method is dependent on the estimation of a set of coefficients $\{\beta_i\}$. Although, the BLR model can learn a sigmoidal surface that is similar to a single layer perceptron, it has much more limited interpolation than can be achieved by a general regression neural network (GRNN) as used here.

In order to overcome the shortcomings of the currently available methods, a novel GRNN technique has been adopted for this work. The GRNN tackles the HI calculation as a function interpolation problem consisting of a nonlinear mapping from a set of six input variables (containing information about the operational condition of transformers) onto a single output variable representing the predicted overall health condition of transformers. The GRNN is a non-parametric method as opposed to Fuzzy Logic and Binary Logistic Regression that require a manual choice of model complexity and estimation of the resulting parameters (or coefficients). This means the GRNN will naturally form a model whose complexity is justified by the

availability of training examples, complying with Risannen's minimum description length principle [10]. The GRNN has the ability to control model complexity when the set of transformer data is constrained and this is a significant contribution arising from this work. This property also makes the GRNN well suited to multivariate interpolation of high-dimensional training examples. The GRNN is from the family of radial basis function networks and its sole parameter controls the smoothness of interpolation offered. It can learn quickly the underlying function of high dimensional measurements from limited number of training examples. The performance of the model is evaluated by making a comparison between predicted and measured values based on the mean square error. The arrangement of the paper is as follows. Section 6.2 describes the overview of general regression neural network. Section 6.3 presents the methodology followed in this research. Section 6.4 describes results that were achieved with the method. Section 6.5 presents the comparative analysis with other methods and section 6.6 presents a summary of the results and conclusions.

## 6.2 Overview of General Regression Neural Network

The general regression neural network (GRNN) is a single-pass learning algorithm that uses radial basis functions as a form of standard statistical kernel regression [11-12]. It is a kind of probabilistic neural network that has the capability to converge to the underlying function of measurements by induction from a limited number of training examples. The GRNN possesses a simple network structure that is fast when learning and quickly converges to the optimal regression surface. It exhibits excellent approximation to arbitrary functions having inputs and outputs from sparse and noisy sources, and can achieve optimal performance by adjusting a single smoothing parameter. Therefore, it has numerous applications in engineering and scientific data analysis.

In the GRNN, the value of a dependent variable $Y = \{Y_n\}$ is predicted from a number of given *D*-dimensional independent measurements $\boldsymbol{X} = \{X_n\}$ where $X_n \in \mathcal{R}^D$ .The prediction is the most probable value of *Y* for each value of *X* based on a finite set of $n$measurements and their associated *Y* values. Thus, the GRNN learns a mapping from an input domain containing *X* to an output codomain containing *Y*, where either space can be multidimensional, but here *Y* is assumed as a scalar. If a GRNN is trained with a finite number of available measurements, it can estimate a linear or nonlinear regression surface to predict the most probable value of *Y* for any new measurement of *X*. If the joint continuous probability distribution function (pdf) $f(\boldsymbol{X}, Y)$ of a random variable vector $\boldsymbol{X}$ and a scalar random variable *Y* is known, the conditional expectation [11] of *Y* for a given value of *X* can be expressed as:

$$E[Y|\boldsymbol{X}] = \frac{\int_{-\infty}^{+\infty} Y f(\boldsymbol{X}, Y) dy}{\int_{-\infty}^{+\infty} f(\boldsymbol{X}, Y) dy} \tag{6.3}$$

In practice, for most cases the joint probability distribution function of $\boldsymbol{X}$ and *Y* is unknown. However, the joint pdf can be empirically approximated using nonparametric Parzen window estimation from a finite set of measurements (a form of training set)[13]. This approach is free from any assumption of a particular functional form, as the parameters of the model are determined directly from the training set. Thus, the GRNN learns and is able to generalize immediately. Cacoullos in [14] has shown the suitability of Parzen window estimation for multidimensional cases. The probability density of *X* at any sample point $x$ in a hypercube region $\mathcal{R}^D$ can be estimated [15]as:

$$f(\boldsymbol{x}) = \frac{1}{N\sigma^D} \sum_{n=1}^{N} k\left(\frac{x - X_n}{\sigma}\right) \tag{6.4}$$

where $\sigma$ is the side length of a hypercube, $\sigma^D$ is the volume of the hypercube and $k(x)$ is a statistical kernel or window function [15].

To estimate the joint pdf of $\boldsymbol{X}$ and $Y$, different kernel functions $k(x)$ such as rectangular or Gaussian kernels can be used. As the Gaussian function is simple to implement and has continuous derivatives, a multivariate Gaussian kernel is widely applied to obtain a smooth density model. Thus the Parzen window density function using a multivariate Gaussian kernel function with a covariance matrix $\Sigma$ [11] can be written as:

$$f(\boldsymbol{X},Y) = \frac{1}{N\sqrt{(2\pi)^D * |\Sigma|}} \sum_{n=1}^{N} exp\left(-\frac{(x-X_n)^T\Sigma^{-1}(x-X_n)}{2}\right) * exp\left(-\frac{(y-Y_n)^T\Sigma^{-1}(y-Y_n)}{2}\right) \quad (6.5)$$

If the Parzen window estimator of (6.4) is modified by the conditional mean of (6.5), then the basic equation for the GRNN function $g(x)$[16] can be written as:

$$g(x) = \frac{\sum_{n=1}^{N} Y_n exp\left(-\frac{{D_n}^2}{2}\right)}{\sum_{n=1}^{N} exp\left(-\frac{{D_n}^2}{2}\right)} \quad (6.6)$$

where $x$ is a new measurement used for testing and ${D_n}^2 = (x - X_n)^T\Sigma^{-1}(x - X_n)$ is the squared Mahalanobis distance [15] between the training data set and the point of prediction. (This is a generalization of the Euclidean distance to allow for the case where $\Sigma$ is non-diagonal). The exponential terms of (6.6) works as a weighting parameter that reflects the contribution of each known $Y_n$ to the output $g(x)$. Training points $X$ closest to a prediction point will contribute preferentially as the exponential term becomes bigger due to decreased distance.

The smoothness of the GRNN function depends on the multivariate standard deviation$\Sigma$. When the value of $\Sigma$ is large, the estimated density model is forced to become smoother. As a result, it ignores some features of the training samples but also attenuates any additive noise in the training examples [12]. If the value $\Sigma$ is too

small, the model will over-fit the training examples, trying to track every feature of training set, becoming sensitive to sparse and noisy data, and resulting in a loss of its generalization capability [17]. Therefore, a good choice of $\Sigma$ is imperative so that all useful features of the training set are taken into account since the prediction points closer to $X$get heavier weighting.If the actual distribution of measurements for any application field is unknown then the optimal value of $\Sigma$ for a given number of $N$ measurements is critical [11]. One way of computing the optimal value of $\Sigma$ is by an experimental search, such that the estimated value of any known $g(\boldsymbol{X_j})$based on the remaining $\boldsymbol{X_{n-1}}$ training measurements is as close as possible to its actual value. Therefore, $\Sigma$ is chosen such that the mean squared error between the estimated value and the actual value will be minimized. A detail procedure for calculation of $\Sigma$ is shown in [11].

## 6.3 Methodology

In this section, a GRNN is used to find the correlation between independent variables and a continuous dependent variable. The GRNN uses a statistical Gaussian kernel for exploring a best fitting model to predict the health index (HI) score of transformers using six independent variables. The calculated HI scores are finally used to assess the health condition of transformers. To present a fair comparison between the GRNN, Fuzzy Logic and BLR, the same six inputs are used here. However, the GRNN could be adapted to use more inputs when measurements are available. Different subsections of the methodology section are discussed below.

### 6.3.1 Input Selection

In the dissolved gas analysis (DGA) method, concentrations of different combustible dissolved gases such as Hydrogen ($H_2$), Methane ($CH_4$), Ethylene ($C_2H_4$), Ethane ($C_2H_6$), Acetylene ($C_2H_2$) and Carbon monoxide (CO) are measured to identify faults such as partial discharge, internal arcing, overheating and poor electrical contacts in

transformers [4,9,18]. As normal operation of transformers produces some gas, there is a chance of mis-diagnosis from DGA. Moreover, there are cases when DGA fails to provide sufficient information about the integrity of transformers [4]. Therefore, it is beneficial to use the summation of combustible gases and include additional measurements to improve the accuracy of overall assessment. In this research, a quantitative HI score based on total dissolved combustible gas (TDCG) and five additional measurements such as oil quality, dissipation factor, acidity, water in oil and insulation resistance has been used. The TDCG was calculated from the summation of combustible gases. The reasons for using six independent variables are discussed in the following paragraph.

In an oil filled transformer, both mineral oil and paper are used as insulators. During normal operation of transformers, due to unavoidable inefficiency, some power is always lost through the insulating oil as a form of heat energy. This dissipated power increases the overall temperature of a transformer and accelerates its aging rate. The ageing by-products contaminate oil and increase the conductivity and permittivity of this insulating liquid [19]. Therefore, oil resistance decreases, resulting in an increase in the dissipation factor. The amount of degradation due to the dissipated power and contamination is evaluated by the dissipation factor (DF) test [5,20]. Besides insulating, the solid paper/pressboard helps to hold the windings in position. Degradation of this paper insulation is considered to be a primary cause of a transformer's end-of-life [21]. Furan (2-Furfuraldehyde) is a chemical compound that is produced from the breakdown of cellulose chains with in the solid insulation and is usually used to assess the condition of paper ageing. The furan concentration has a conditional correlation with the degree of polymerization (DP) and increases with the ageing of paper insulation [8, 22]. If the conditions are satisfied, the furan concentration may be used to estimate the DP value of paper insulation. Generally, a DP value less than 200 is considered the end-of-life for paper insulation [7]. According to a recent research, the furan level for the normal and thermally upgraded paper (TUP) corresponding to DP of 200 is 7.337 ppm and 2.843 ppm (by weight)

respectively [7]. However, due to the maintenance activities, if the oil is reclaimed, replaced or topped-up the relation between furan and DP is not valid until the concentration has been given time to destabilize. Therefore, both furan and DF have been used in the proposed HI calculation. As there were only few transformers with TUP in the asset register of the utility and so this factor was not considered here.

Water is one of the most unexpected impurities in transformer oil. It can be produced locally from chemical processes such as ageing of paper and oxidation of oil [22]. The dipole momentum of water molecules make them polarized in an electric field thus affecting the dissipation factor [22]. Moreover, the contaminating particles and free water reduce the dielectric breakdown voltage (DBV) of oil [9, 23]. The water may also create bubbles at high temperature that can increase the probability of partial discharge inception and has an accelerated aging effect on the paper [24]. The DBV measures the strength of oil to withstand electrical stress without failure. Thus DBV and water content give an overall condition assessment of oil in transformers [5]. As these two measurements can provide valuable information about oil integrity, they have also been included in the HI calculation.

During a transformer's service life, acids are produced in its oil resulting from atmospheric contamination and oxidative degradation [25]. These acids degrade the properties of the oil and paper insulation. The concentration of acids provides an indication of the oxygenated products and solid contaminants of the insulation. Consequently, the acidity has also been adopted in the proposed HI calculation to indicate the condition of insulation.

### 6.3.2 Data Processing and Normalization

In this work, six dimensional measurements, specifically TDCG, dissipation factor, acidity, water content, furan and dielectric strength are used as the domain of the GRNN model. The upper and lower limits of each measurement have been

considered to create a four level quantization of each measurement. The ranges have been chosen based on the IEEE Std C57.106shown in Table 6.1. To develop a training set, the mid points of the four conditional limits for each test were used. A conditional score such as 0.25, 0.5, 0.75 and 1.0 respectively were set to the middle points of the Good, Fair, Poor, Very Poor ranges. A number of $X_n = 4^D (where\ D = 6\ is\ the\ number\ of\ inputs)$ independent variables for the training set were produced using the combination of these mid points. The dependent variable $Y_n$ for each combination was calculated by averaging their corresponding position scores. The 4096 training measurements (patterns) produced from the combination of six tests are used as an input to train the proposed GRNN. To ensure the same scaling of each dimension, each input of the test set is normalized dividing by 1.5 times of the lower limit value of the Very Poor category. (The scaling factor 1.5 ensures that outlying measurements are included in the chosen range specially when the Very Poor category upper limit boundary is missing). Due to this approach, the underlying pdf for a kernel has been estimated with the same width in each dimension.

**Table 6.1:**Grading of transformers based on six key measurements [1, 19]

| | U≤69 kV | 69 kV <U <230kV | 230kV≤U | Classification | Condition Score |
|---|---|---|---|---|---|
| Dielectric Strength kV (2mm gap) | ≥45 | ≥52 | ≥60 | Good | 1 |
| | 35-45 | 47-52 | 50-60 | Fair | 2 |
| | 30-35 | 35-47 | 40-50 | Poor | 3 |
| | ≤30 | ≤30 | ≤40 | Very Poor | 4 |
| Neutralization Number (Acidity) | ≤0.05 | ≤0.04 | ≤0.03 | Good | 1 |
| | 0.05-0.1 | 0.04-0.1 | 0.03-0.07 | Fair | 2 |
| | 0.1-0.2 | 0.1-0.15 | 0.07-0.1 | Poor | 3 |
| | ≥0.2 | ≥0.15 | ≥0.10 | Very Poor | 4 |
| Water content (ppm) | ≤30 | ≤20 | ≤15 | Good | 1 |
| | 30-35 | 20-25 | 15-20 | Fair | 2 |
| | 35-40 | 25-30 | 20-25 | Poor | 3 |
| | ≥40 | ≥30 | ≥25 | Very Poor | 4 |
| Dissipation factor (%) at 50 Hz 25˚C | ≤0.1 | | | Good | 1 |
| | 0.1-0.5 | | | Fair | 2 |
| | 0.5-1.0 | | | Poor | 3 |
| | ≥1.0 | | | Very Poor | 4 |
| Total dissolved combustible gas (TDCG) in ppm | 720 | | | Good | 1 |
| | 721-1920 | | | Fair | 2 |
| | 1921-4630 | | | Poor | 3 |
| | >4630 | | | Very Poor | 4 |
| Furan (ppm) | 0-0.1 | | | Good | 1 |
| | 0.1-1.0 | | | Fair | 2 |
| | 1.0-10 | | | Poor | 3 |
| | >10 | | | Very Poor | 4 |

***Note:*** *The boundaries of conditional scores for Dielectric Strength, Acidity and Water content are dependent on the voltage rating of transformers.*

### 6.3.3 Working Principle

To improve the accuracy of overall conditional assessment of power transformers, a continuously interpolated function has been proposed in this work. If IEEE Std. C57.106 is strictly applied, each measurement is quantised into four non-overlapping ranges. Therefore, after quantisation all the values within each range are indistinguishable and this throws away information could be useful in the later stage, forming a major drawback of this approach. To deal with this limitation, a continuous function has been developed using the GRNN interpolation technique, but still based on the limit values of the four conditional scores. The midpoint of the high and low

point of each limit has been assigned with a conditional score and used in the GRNN model.The GRNN interpolation technique based solely on the water concentration of the oil is shown in Figure 6.1.

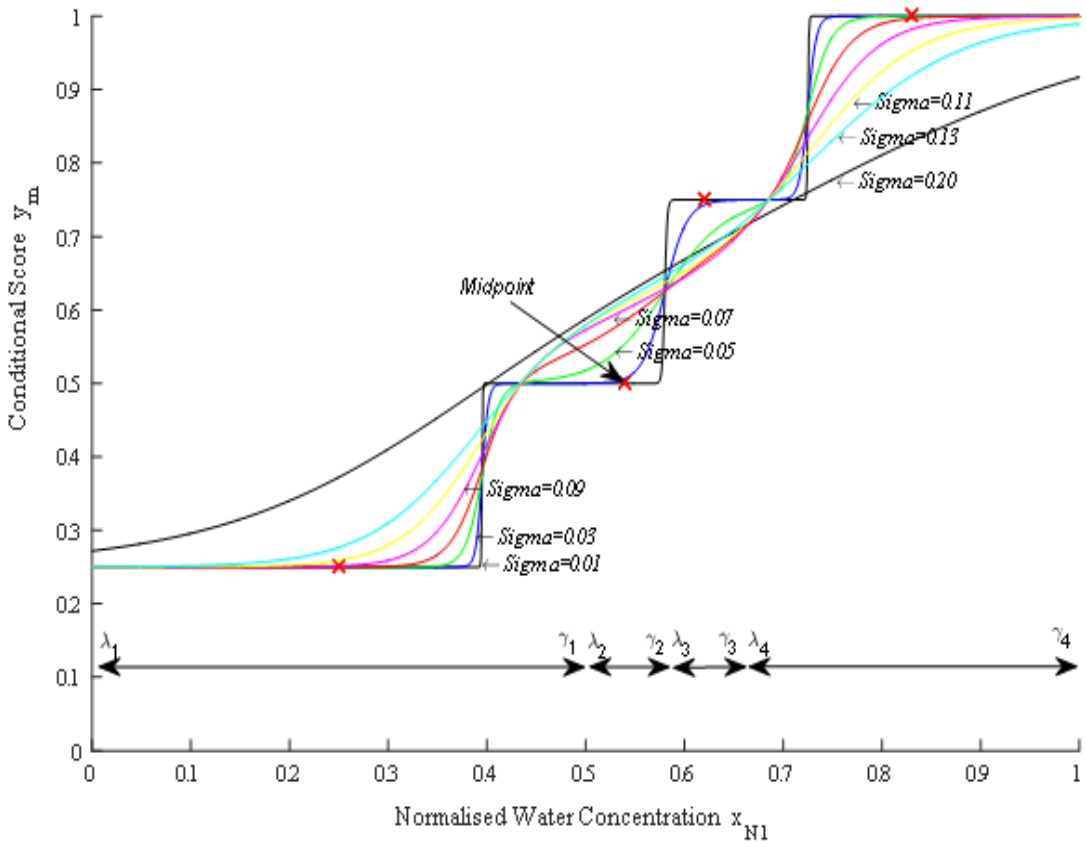


**Figure 6.1:** GRNN interpolation of normalised water content and conditional score.

In Figure 6.1. $\lambda$ and $\gamma$ represent the upper and lower limit of a Voronoi (quantisation) region respectively so the four ranges can be expressed using the following notation.

$$Limit\ values = \begin{bmatrix} \lambda_{1,D} & \gamma_{1,D} \\ \lambda_{2,D} & \gamma_{2,D} \\ \lambda_{3,D} & \gamma_{3,D} \\ \lambda_{4,D} & \gamma_{4,D} \end{bmatrix}$$

where $D$ is the dimension of the measurements and$\gamma_{i,D} = \lambda_{i+1,D}$ for the next band and so on (the ranges are non-overlapping and contiguous). The targeted midpoint (shown as a red cross in Figure 6.1) for each Voronoi region can be written as :

$$\emptyset_{n,D} = \frac{\lambda_{n,D} + \gamma_{n,D}}{2}\ where\ n = 1,2 \ldots,4\ and\ D = 1,2,..,6 \qquad (6.7)$$

It is apparent from Figure 6.1 that a small value of $\Sigma$ (0.01) instructs the GRNN to work as a step function. The GRNN gradually became a smooth interpolator with the increased values of $\Sigma$. A similar representation but for a two-dimensional domain comprising normalised water concentration and acidity and for small and large values of $\Sigma$ controlled by a variable multiplicative parameter $E$ is shown in Figure 6.2 (a) and (b) respectively.

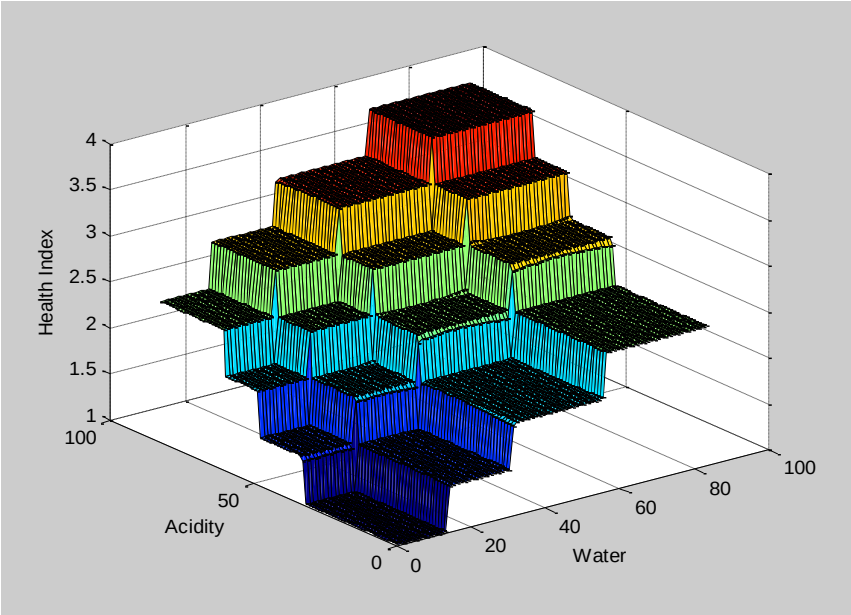


**Figure 6.2 (a):** Health Index at a Small Value of $E$.

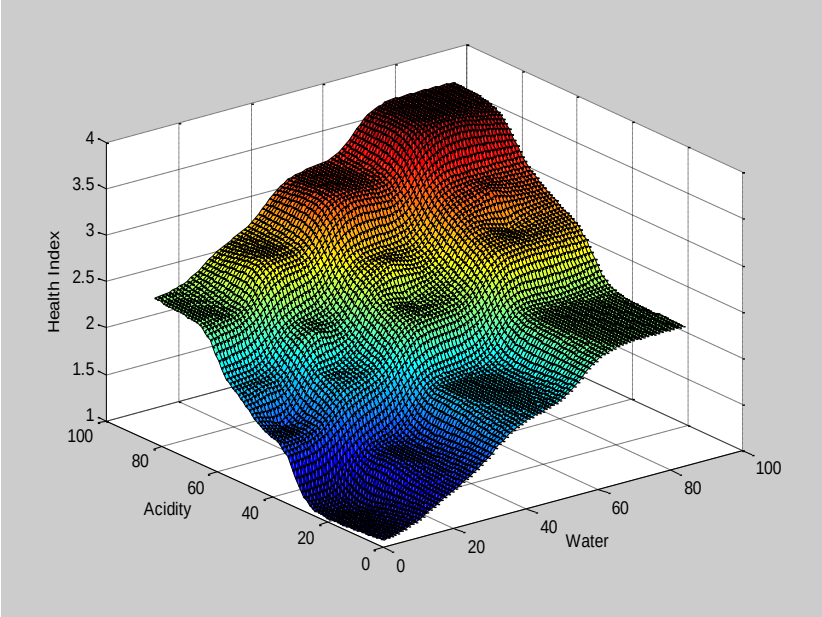


**Figure 6.2 (b):** Health Index at a Large Value of $E$.

Figure 6.1 and 6.2 shows a function in a one and two-dimensional domain respectively, but a similar approach may be applied to much higher dimensional measurements to calculate their respective conditional scores. As the method is based on the six-dimensional measurements, the actual algorithm is more complex than the graphical three-dimensional presentation shown in Figure 6.2 (a) and Figure 6.2 (b).

In this research, six dimensional measurements were used. Therefore, the midpoint of each Voronoi region (plateau) in six dimensional space can be expressed as follows.

$$X_{i,j,k,l,m,n} = \left[\emptyset_{i,1}\ \emptyset_{j,2}\ \ \emptyset_{k,3}\ \ \emptyset_{l,4}\ \emptyset_{m,5}\ \ \emptyset_{n,6}\right] \tag{6.8}$$

After selecting an optimal value of $\Sigma$, the conditional score for any higher dimensional measurements may be calculated by mapping with a continuous smooth interpolated function.

### 6.3.4 Proposed Model

In the proposed GRNN method, following equation (6.8) a set of 4096 measurements were produced using the boundaries of four conditional scores. The measurements were divided into training and test sets. The training set comprises 3996 measurements while the remaining 100 measurements were randomly selected as a test set. To estimate the probability distribution function (pdf) of the training set, a nonparametric Parzen window (PW) estimation technique was applied. In the PW approach, a multivariate Gaussian kernel function was centred on each of the 3996training vectors. The individual kernels were added together (equation 6.4) to determine a common width (smoothing parameter) to estimate the probability density of each measurement. The equation of the covariance matrix $\Sigma$ (smoothing parameter) for the proposed six-dimensional cases can be expressed by (6.9).

$$\Sigma = E\Sigma_S \tag{6.9}$$

where $\Sigma_S$ is the covariance matrix of the training samples and $E$ is a multiplicative factor chosen to provide an appropriate amount of smoothing (see Figure 6.1).

The estimation of $E$ is very important as the smoothness of the pdf depends on it, much as demonstrated in Figure 6.1. So, it has a great influence on the performance of GRNN. The optimal value of $\Sigma$will vary based on the size, mixture of noise and type of the training set [27]. Although, a larger value of $\Sigma$ will make the estimated pdf curve smoother, the estimated curve will also start to lose finer details. Conversely, a smaller value of $\Sigma$ may lead to false spikes in the pdf curve depending on the specific distribution of the training points and thus the interpolated function becomes prone to noise. Therefore, the optimal value $E$was estimated by linearly increasing the value of $E$with a step size 0.001in the range 0.001 to 1.0. With the increased value of$E$, the accuracy of the model was monitored for the 100 test cases chosen from 4096 measurements. It was found that with the increased value of $E$the

accuracy was increased up to a certain level. If the value of $E$ further increased, the accuracy started to drop. As a result, the value at which maximum accuracy found considered as a near-optimal point for this experiment which was 0.450.

After estimating the value of $E$, the actual health index of a transformer could be calculated by summing the general regression of separate measurements as shown in Figure 6.1.

$$g(x) = g_1(x_1) + g_2(x_2) + \ldots + g_D(x_D) \tag{6.10}$$

If the functions $g(x)$ are linear the solution degenerates into one such as equation (1), whereas if they are non-linear the solution is closer to that in equation (6.2). The drawback of this approach is that, the model only learns $4 \times 6 = 24$ regions (4 for each dimensional measurement). The model could not appraise any cross correlation of the measurements. To overcome this limitation, in this work, the regressions are combined in a multivariate way so that it can learn all the possible combinations ($4^D$=4096) and evaluate the cross correlation of the measurements to calculate the HI of a transformer. (For instance, in the two-dimensional (D=2) domain shown in Figure 6.2(a) there are $4^2$ = 16 plateaus.) This approach can be expressed using the following equation.

$$g(x) = g(x_1, x_2, \ldots, x_D) \tag{6.11}$$

Here the function $g(x)$ is implemented as a GRNN using a method described in equation (6.6). From (6.11), it can be said that for any combination such as one or two tests indicate poor condition of a transformer while other indicate fair or good, the GRNN and learn from it. This cross correlation exploring capability helps the proposed model to accurately calculate the HI of transformers. As can be seen from Figure 6.2 (a) the training data (equation (6.8)) derived from the IEEE Std. C57.106 does not show large scale correlation but the interpolation provided by Figure 6.2 (b)

allows localized correlation to be exploited. Methods for exploring larger scale correlation will form the basis for future work.

## 6.4 Results and Discussion

To analyze performance of the proposed GRNN model, data from power transformers rated less than 69 kV were collected from a utility company in Australia. As the boundary of conditional scores for Dielectric Strength, Acidity and Water content(shown in Table 6.1) changes with the increased voltage rating, only the 100 transformers having less than 69 kV rating were considered in this experiment. Out of them, 83 transformers were installed between 1965 and 1980 prior to the introduction of the thermally upgraded paper (TUP). In 1993, the utility started to use TUP in new transformers. Although this information has not been provided by the utility, the set of transformers made with TUP cannot comprise more than 17% of the total set. Therefore, the impact of 17% or less TUP transformers on their furan concentration is not considered in this work. The measurements from the transformers were made in 2013. The oil samples were collected without any exposure to the atmosphere and the winding, oil and ambient temperatures were recorded at the time of sampling. Therefore, the impact of ambient temperature on the samples was ignored. As most of the transformers had been in operation for over 30 years, their ageing is apparent in expert classifications. Only four transformers which are under 20 years old were found in the poor category and this could be the result of loading patterns, harmonics in load, different faults and their maintenance plans. The utility experts used 19 tests to determine the HI score of transformers. To calculate the HI scores following a linear approach, they divided the test results into five groups to assess the condition of different subsystems such as paper, oil, Tap changer, windings and bushings. Based on the calculated scores, transformers were classified into four groups such as Satisfactory, Fair, Poor and Severe. However, in the majority of the cases no significant degradation was found in the tap changers, windings and bushings. So these measurements were deemed to be of little diagnostic

value and have been omitted from these tests. A comparison between the proposed method and the expert classifications is summarized in Table 6.2, where VG, G, M, B and VB in proposed method indicate very good, good, moderate, bad and very bad condition respectively. Moreover, to facilitate the comparison, the VG and G conditions were considered the same as the satisfactory category of expert classifications.

**Table 6.2:** Comparative health condition between experts' classifications and proposed method.

| Conditions | Proposed method | | | | | Expert classifications |
|---|---|---|---|---|---|---|
| | VG | G | M | B | VB | |
| Satisfactory | **2** | **1** | | | | 3 |
| Fair | | 4 | **16** | 2 | | 22 |
| Poor | | | 6 | **31** | 3 | 40 |
| Severe | | | | 2 | **33** | 35 |
| Total | 2 | 5 | 22 | 35 | 36 | 100 |

***Note:*** *The matching cases are shown in bold*

From Table 6.2, it can be seen that in 17 cases the proposed method wrongly classified the fault category of transformers, which means the method showed an 83% match to the expert classifications. Several reasons could contribute to these misclassifications. One of the important reasons is that they assign weight to each test based on their experience, statistical analysis and the survey reports published by Omicron, Doble and CIGRE[28]. Moreover, the experts also used an additional 13 tests, not seen by the proposed method, that lead to them forming different conclusions in some complex cases.

## 6.5 Comparison with Other Methods

The proposed method was also compared with other published approaches such as asset-management and health assessment consulting company (AMHA)

classifications, Fuzzy Logic [5] and Binary Logistic Regression [9]. The AMHA classifications have been considered as a target value for the proposed method. A comparison between the proposed method and other published methods is summarised in Table 6.3, and the results of six diagnostic tests of 30 transformers are shown in appendix A of the report.

**Table 6.3:** Calculated health indices and corresponding conditions of transformers.

| Number | AMHA | | Fuzzy Logic | | Binary Logistic Regression | | Proposed GRNN | |
|---|---|---|---|---|---|---|---|---|
| 1 | 0.377 | G | 0.36 | G | 0.434 | M | 0.370 | G |
| 2 | 0.334 | G | 0.3 | G | 0.17 | G | 0.560 | M |
| 3 | 0.29 | G | 0.3 | G | 0.007 | G | 0.047 | VG |
| 4 | 0.7 | B | 0.78 | B | 0.826 | VB | 0.78 | B |
| 5 | 0.102 | G | 0.2 | VG | 0.002 | G | 0.03 | VG |
| 6 | 0.274 | G | 0.3 | G | 0.004 | G | 0.085 | VG |
| 7 | 0.316 | G | 0.3 | G | 0.023 | G | 0.316 | G |
| 8 | 0.29 | G | 0.3 | G | 0.006 | G | 0.133 | VG |
| 9 | 0.226 | G | 0.22 | VG | 0.003 | G | 0.04 | VG |
| 10 | 0.316 | G | 0.3 | G | 0.12 | G | 0.586 | M |
| 11 | 1 | B | 0.94 | VB | 0.973 | VB | 0.93 | VB |
| 12 | 0.931 | B | 0.93 | VB | 0.841 | VB | 0.69 | B |
| 13 | 1 | B | 0.94 | VB | 0.973 | VB | 0.83 | VB |
| 14 | 0.916 | B | 0.83 | B | 0.589 | B | 0.59 | B |
| 15 | 0.732 | B | 0.78 | B | 0.885 | VB | 0.70 | B |
| 16 | 0.354 | G | 0.3 | G | 0.03 | G | 0.399 | G |
| 17 | 0.45 | M | 0.53 | M | 0.594 | B | 0.45 | M |
| 18 | 0.291 | G | 0.3 | G | 0.37 | G | 0.406 | G |
| 19 | 1 | B | 0.94 | VB | 0.997 | VB | 0.79 | B |
| 20 | 0.347 | G | 0.3 | G | 0.005 | G | 0.119 | VG |
| 21 | 0.414 | M | 0.15 | VG | 0.077 | G | 0.36 | G |
| 22 | 0.241 | G | 0.11 | VG | 0.002 | G | 0.04 | VG |
| 23 | 0.953 | B | 0.94 | VB | 0.895 | VB | 0.85 | VB |
| 24 | 0.368 | G | 0.3 | G | 0.018 | G | 0.015 | VG |
| 25 | 0.45 | M | 0.51 | M | 0.181 | G | 0.55 | M |
| 26 | 0.072 | G | 0.11 | VG | 0.004 | G | 0.01 | VG |
| 27 | 0.371 | G | 0.42 | M | 0.045 | G | 0.61 | M |
| 28 | 0.225 | G | 0.3 | G | 0.006 | G | 0.314 | G |
| 29 | 0.241 | G | 0.3 | G | 0.015 | G | 0.238 | G |
| 30 | 0.45 | M | 0.48 | M | 0.2 | M | 0.79 | B |

***Note:*** *In GRNN, HI score between 0.0-2.0 is VG, 0.21-0.40 is G, 0.41-0.60 is M, 0.61-0.80 is B and 0.81-1.0 is VB*

From Table 6.3, it can be seen that the proposed method performed well with the published cases. In four cases (case number 2, 10, 27 and 30), it slightly deviated from the AMHA classification. The AMHA classified them as G, G, G and M which has been classified by the proposed GRNN as M, M, M and B respectively. The

Fuzzy Logic and Binary Logistic Regression also disagreed in three and four cases respectively. The root cause analysis of the misclassification revealed that the case number 2, 10 and 27 crossed the boundary of the good condition in three tests(results shown in bold in Table 6.4) out of six suggested by IEEE Std C57.106 and this lead the misclassification. Case number 30 crossed the good condition limit in five tests (results shown in bold in Table A.1 in Appendix Section) out of which two are in the poor condition region. Therefore, it has been classified as a bad transformer.

## 6.6 Conclusions

In this paper, a novel statistical kernel-based GRNN approach has been presented to calculate the health index of power transformers. Four conditional scores based on six important tests (TDCG, DBV, acidity, water, furan and dissipation factor) have been used to train the proposed model. The conditional score of each test measurement was calculated through a direct mapping using a smooth interpolated continuous function and the weight has been calculated based on the distance between the training data set and the point of prediction. The method was tested using measurements from 100 transformers collected from a utility company and compared with their experts' classifications. The comparative results show that in 83% of the cases the GRNN classification matches the expert classifications. Moreover, a comparative result with three published methods shown in Table 6.3 is also satisfactory. As the approach is free from any assumption, it can be used directly by utilities to compute the HI of their fleets of transformers. Therefore, it is expected that this method will help utilities to make the best technical and economic decisions on asset management and will play an important role to improve the long-term performance of transformers. The boundaries of different conditional scores available in the IEEE Std. C57.106 are not papameters for the proposed method. The accuracy of the proposed method may be improved by slight adjustment of the IEEE boundaries. Searching the improved boundaries based on a bigger training set could be a basis for future work.

## References

[1] M. Wang, A.J. Vandermaar and K.D. Srivastava, Review of condition assessment of power transformers in service, IEEE Electr Insul Mag, Vol.18, pp. 12-25, 2002.

[2] A.E.B. Abu-Elanien and M.M.A. Salama, Asset management techniques for transformers, Electric Power Systems Research, Vol. 80, pp. 456-464, 2010.

[3] J. Singh, Y.R. Sood and R.K. Jarial, Condition Monitoring of Power Transformers - Bibliography Survey, IEEE Electr Insul Mag, Vol. 24, pp.11-25, 2008.

[4] A. Jahromi, R. Piercy, S. Cress, J. Service and W. Fan, An approach to power transformer asset management using health index, IEEE Electr Insul Mag, Vol. 25, pp. 20-34, 2009.

[5] A.E.B. Abu-Elanien, M.M.A. Salama and M. Ibrahim, Calculation of a Health Index for Oil-Immersed Transformers Rated Under 69 kV Using Fuzzy Logic, IEEE Transactions on Power Delivery, Vol. 27, pp. 2029-2036, 2012.

[6] T. Hjartarson and S. Otal, Predicting Future Asset Condition Based on Current Health Index and Maintenance Level, in: ESMO 2006 - 2006 IEEE 11th International Conference on Transmission & Distribution Construction, Operation and Live-Line Maintenance, 2006, pp. 1.

[7] L. Cheim, D. Platts, T. Prevost and S. Xu, Furan analysis for liquid power transformers, IEEE Electr Insul Mag, Vol. 28, pp. 8-21, 2012.

[8] T. Leibfried, M. Jaya and N. Majer, Postmortem Investigation of Power Transformers-Profile of Degree of Polymerization and Correlation With Furan Concentration in the Oil, IEEE Transactions on Power Delivery, Vol. 28, pp. 886-893, 2013.

[9] W. Zuo, H. Yuan, Y. Shang, Y. Liu and T. Chen, Calculation of a Health Index of Oil-Paper Transformers Insulation with Binary Logistic Regression, Mathematical Problems in Engineering, 2016 (2016) 9.

[10] A. Barron, J. Rissanen and Y. Bin, The minimum description length principle in coding and modeling, IEEE Transactions on Information Theory, Vol. 44, pp. 2743-2760. 1998.

[11] D.F. Specht, A general regression neural network, IEEE Transactions on Neural Networks, Vol. 2, pp. 568-576,1991.

[12] O. Polat and T. Yıldırım, Hand geometry identification without feature extraction by general regression neural network, Expert Systems with Applications, Vol. 34, pp. 845-849, 2008.

[13] E. Parzen, On Estimation of a Probability Density Function and Mode, Annals of Math Statistics, Vol. 33, pp. 1065-1076, 1962.

[14] T. Cacoullos, Estimation of a multivariate density, Annals of Math Statistics, Vol. 18 pp. 179-189, 1966.

[15] Z. Hu, M. Xiao, L. Zhang and S. Liu and Y. Ge, Mahalanobis Distance Based Approach for Anomaly Detection of Analog Filters Using Frequency Features and Parzen Window Density Estimation, Journal of Electronic Testing, pp. 1-13, 2016

[16] J. Song, C.E. Romero, Z. Yao and B. He, A globally enhanced general regression neural network for on-line multiple emissions prediction of utility boiler, Knowledge-Based Systems, Vol. 118, pp. 4-14, 2017.

[17] I.M. Overton, G. Padovani, M.A. Girolami and G.J. Barton, ParCrys: a Parzen window density estimation approach to protein crystallization propensity prediction, Bioinformatics, Vol. 24, pp. 901-907, 2008.

[18] M.M. Islam, G. Lee and S.N. Hettiwatte, A review of condition monitoring techniques and diagnostic tests for lifetime estimation of power transformers, Electrical Engineering, pp. 1-25, 2017.

[19] I. Fofana and Y. Hadjadj, Electrical-Based Diagnostic Techniques for Assessing Insulation Condition in Aged Transformers, Energies, Vol. 9, pp. 679, 2016.

[20] J. Singh, Y. R. Sood and P. Verma, Experimental Investigation Using Accelerated Aging Factors on Dielectric Properties of Transformer Insulating Oil, Electric Power Components and Systems. Vol. 39, 2011.

[21] A.E.B. Abu-Elanien, M.M.A. Salama and M. Ibrahim, Determination of transformer health condition using artificial neural networks, In: 2011 International Symposium on Innovations in Intelligent Systems and Applications, 2011, pp. 1-5.

[22] V.G. Arakelian, Effective diagnostics for oil-filled equipment, IEEE Electr Insul Mag, Vol.18, pp. 26-38, 2002.

[23] B. Pahlavanpour, Characterisation of insulating oils, In: IEEE Colloquium on Characterisation of Dielectric Materials: a Review, 1994, pp. 1-8.

[24] T.V. Oommen and T.A. Prevost, Cellulose insulation in oil-filled power transformers: part II maintaining insulation integrity and life, IEEE Electr Insul Mag, Vol. 22, pp. 5-14, 2006.

[25] IEC, Insulating liquids - Determination of acidity - Part 1: Automatic potentiometric titration, IEC 62021-1, 2003.

[26] IEEE Guide for the Interpretation of Gases Generated in Oil-Immersed Transformers - Redline, IEEE Std C57.104-2008 (Revision of IEEE Std C57.104-1991) - Redline, 1-45, 2009.

[27] C. Archambeau, M. Valle and A. Assenza, M. Verleysen, Assessment of probability density estimation methods: Parzen window and finite Gaussian mixtures, In: 2006 IEEE International Symposium on Circuits and Systems, 2006, pp. 4 pp.

[28] M.R. Florian Predl, Case studies on Tap Changer Diagonostics Using Dynamic Winding Resistance Measurement. Omicron Seminar, Perth WA, 24 April 2015.

# Chapter 7: Calculating a Health Index for Power Transformers Using a Subsystem-based GRNN Approach

## Abstract

A power transformer is one of the most crucial items of equipment in the electricity supply chain. The reliability of this valuable asset is strongly dependent on the condition of its subsystems such as insulation, core, windings, bushings and tap changer. Integration of various measured parameters of these subsystems makes it possible to evaluate the overall health condition of an in-service transformer. This paper develops an artificially intelligent algorithm based on multiple General Regression Neural Networks (GRNN) to combine the operating condition of various subsystems of a transformer to form a quantitative health index (HI). The model is developed using a training set derived from four conditional boundaries based on IEEE standards, the literature and the knowledge of transformer experts. Performance of the proposed method is compared with expert classifications using a database of 345 power transformers. This shows that the proposed method is reliable and effective for condition assessment and is sensitive to poor condition of any single subsystem.

## 7.1 Introduction

Power transformers are one of the most important and expensive high voltage components in power transmission and distribution networks. The average designed life of a transformer is 25 to 40 years [1]. In this paper, the percentage of the 345 units investigated that were over 50 years was 9% and another 23% were between 40 and 50 years of age. Many of these transformers have not shown much evidence of aging that would indicate they are near end-of-life [2]. To avoid the catastrophic failure of these older transformers while managing the growing demand for electricity, significant changes are required to current operation and maintenance procedures. Therefore, actual condition assessment of transformers is gaining attention from power utility organizations to improve their technical and financial performance [3-6].

Over the past decade, to summarize various diagnostic test results, health index (HI) calculations have been proposed as a useful tool to assess the overall condition of transformers [1]. In a HI calculation, results from site and laboratory testing, field inspection and operator observations are combined into a single quantitative index that reflect the health condition of each transformer. The index value helps to identify the risky assets that need more attention than others and helps to prioritize the maintenance program based on the actual and changing condition of each device [7]. If the HI changes suddenly then it indicates one of the two possible situations, either deterioration of a transformer health or an indication of incorrect measurements. Hence the method also provides a way of highlighting misleading test results. All the methods currently reported in the literature for the HI calculation have some limitations. Most of them are linear approaches where the HI is calculated using the weighted average of different routine and diagnostic tests. The averages are calculated by quantizing against conditional ranges (each separated by a sharp boundary) for different measurements suggested by industry standards such as IEEE, IEC and CIGRE [1]. The quantization technique treats wide ranges of measurements

equally and also becomes very sensitive near the boundaries, since a small change of measurement at the boundary may result in a different quantization level. Moreover, the weighting of health indices in this method is subjective and usually decided by the utility experts. As a result, the calculated index may inconsistent between different utilities.

Over the past decade, beside conventional linear approaches, artificial intelligence methods such as Fuzzy Logic [8], Fuzzy C-Means [9], Support Vectors Machines [9] and Binary Logistic Regression [10] have also been used to combine the measurement of transformers into a quantitative HI. Most methods are based on the oil test data that ignore a transformer's ancillary components such as bushings and tap changer. As a result, these methods cannot provide a comprehensive assessment of transformer condition. According to an international survey conducted by CIGRE [11], the contribution of different subsystems to the failure of power transformers is shown in Figure 7.1. It is apparent from Figure 7.1 that the on-load tap changer (OLTC), winding and bushing make the most significant contribution to a transformer's probability of failure. Therefore, it is imperative to also include these components' operating condition as part of the HI calculation.

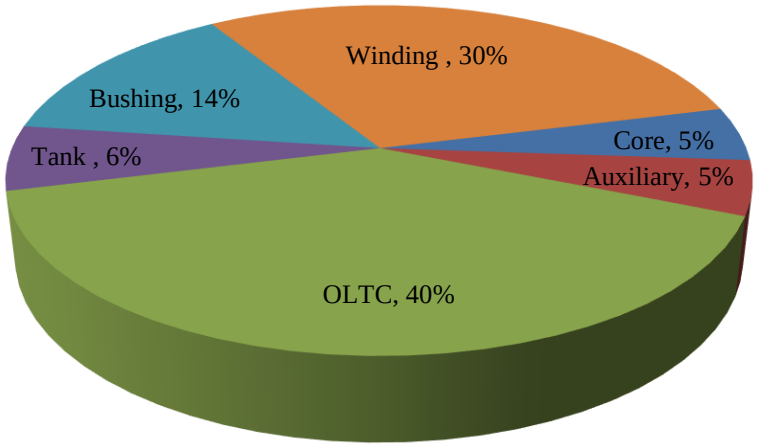


**Figure 7.1:**Power transformers failure statistics based on a CIGRE survey [11].

To partly overcome the limitations of existing methods, a general regression neural network (GRNN) based artificial intelligence technique is proposed in this paper. The GRNN offers a smooth interpolation property and can learn quickly the underlying function of high dimensional measurements from a limited set of training examples. It is largely nonparametric as most of the required parameters can be derived directly from the available measurements. To integrate the condition of different sections in the HI, the proposed method divided the measurements into groups associated with physical subsystems. The condition of each subsystem was evaluated by using a nonparametric GRNN function. Finally, they were combined in a multivariate way to compute a quantitative HI for assessing the health condition and predicting the failure probability of transformers over time.

## 7.2 Review

The diagnostic measurements of power transformers are not always linearly dependent. To combine these measurements into a quantified HI score, the available linear approaches are insufficient. Therefore, the introduction of artificial intelligence and machine learning techniques has become necessary. In recent years, different non-linear machine learning techniques such as Fuzzy Logic [8], Fuzzy C-Means [9] and Binary Logistic Regression [10] have been proposed by experts to analyze transformers' measurements. These new techniques have improved the accuracy of the HI calculation and helped utilities to better manage assets. In the Fuzzy Logic approach [8], membership functions are overlapped with each other such that a measurement can be a member of a single or multiple sets with a different degree of membership. This association is evaluated by using a number of expert rules derived from the order of measurements which are subjective and dependent on the expert's experience. Moreover, a large number of parameters such as the shape of boundary functions and their overlapping area with the adjacent boundaries are required to provide a consistent outcome. Therefore, the calculated HI based on Fuzzy rules may have a certain degree of inaccuracy. A similar approach was proposed in [9] with

measurements having a higher degree of membership to a set used to form clusters. The clusters were assigned with a health index level that was used to develop the training set. Another nonlinear HI calculation approach was proposed by Weijie in [10] using binary logistic regression (BLR). The regression model can be expressed by (7.1).

$$H(x;\beta) = \frac{1}{1+e^{-\left(\beta_0+\sum_{i=1}^{n}\beta_i x_i\right)}} \tag{7.1}$$

where $\beta_0$ is a constant and $\beta_i$ is a coefficient that reflects the contribution of each independent test measurement $x_i$ .

It is apparent from (7.1) that the accuracy of this method is always dependent on the estimation of $n+1$ parameters. All these machine learning methods are highly parametric and their estimation of parameters is therefore dependent on a sufficient number of training examples that, in practice, may not be available [12]. To overcome the problem of estimating large number of unknown parameters, a non-parametric GRNN technique has been proposed in this work. The required smoothing parameter of the GRNN can be derived directly from the finite set of training examples.

## 7.3 Parameters in Health Index Calculation

Various tests can be used to influence the health index of transformers. It is beneficial to include additional tests to get a more realistic assessment of a power transformer [1]. To compute a quantitative HI, 21 representative measurements of diagnosis were used in six groups shown in Figure 7.2 to assess the condition of individual subsystems. The condition parameters of each group are discussed below.

### 7.3.1 Insulation Condition

During operation, due to ageing and variable stresses, different types of gases, acid compounds, moisture and other contaminants may form in a transformer's insulating oil [13]. The compositions of the gases are correlated with distinct internal faults such as partial discharge, arcing and overheating [14]. As normal operation of transformers also produces some gases, it is not always possible to check the integrity of this valuable asset using dissolved gas analysis (DGA) alone. In fact, some transformers can operate throughout their useful life emitting a substantial amount of gas. Moreover, it is difficult to combine all gases in a HI calculation. Therefore, summation of just the combustible gases is used in this method to improve the calculation efficiency. To assess the thermal decomposition of cellulose paper, sometimes the ratio of $CO_2/CO$ is also used. The typical ratio of $CO_2$ to $CO$ for healthy cellulose insulation should be between 3 and 10 [14]. According to [15], this ratio is normally more than seven and only applicable if the respective concentrations of $CO_2$ and $CO$ exceed 5000 ppm and 500 ppm respectively. Under high temperature overheating conditions (such as arcing), $CO$ forms more rapidly than $CO_2$ and the ratio approaches unity. A ratio below 3 indicates degrading insulation by arcing while above 10 it indicates cellulose ageing from thermal heating. To include the condition of paper insulation in HI calculation, this ratio is used in the proposed method.

Besides DGA, there are other chemical oil tests such as acidity, furan and interfacial tension measurement used to assess the condition of oil and paper insulation. In a transformer, acid is mainly produced from oxidation of insulation [16]. However, it can also be produced from atmospheric contamination and changes to the properties of oil-paper insulation that greatly reduce the service life of transformers [17, 18]. Concentration of furan, a by-product of cellulose, can be used to measure the degradation of paper. Furan is inversely correlated with the degree of polymerization (DP) up to a certain temperature which is considered as a primary indicator of transformers' end-of-life [19]. As the measurement of DP from direct paper sampling

is difficult to undertake, it is indirectly estimated from the conditional correlation of the furan concentration in oil [13, 20]. The chemical formula of cellulose can be written as $[C_6H_{10}O_5]_l$ where $l$ the length of glucose rings that comprise the polymer and so $l$ is used as the DP value. Due to ageing and chemical reactions, the glucose rings gradually split into smaller fragments and furanoid compounds are produced as a by-product. The compounds are partially soluble in oil. The production rate of the furanoid compounds increases with the presence of high temperatures and catalytic ageing by-products such as moisture, acids and oxygen. Therefore, the paper loses its mechanical strength and eventually threatens the electrical integrity of a transformer. The damaged paper cannot provide sufficient mechanical support against magnetic forces caused by short circuit and magnetic inrush current and this may lead to premature failure. Moreover, furan concentration can also be used to validate the $CO_2$ to $CO$ ratio approach that are used to identify cellulose degradation. If the ratio is less than three and furan concentration atypically is high then it indicates the gases are produced from the degradation of paper insulation. Another way of estimating the deterioration of insulating fluid is to measure the interfacial tension (IFT) between the fluid and water. Generally, the insulating oil of transformers is a non-polar saturated hydrocarbon. However, with the oxidative degradation of paper and oil, hydrophilic carboxylic acids are produced that can affect the chemical (acidity) and physical (interfacial tension) properties of the fluid. In an IFT test, the surface tension between oil and water is measured as this decrease with an increase of hydrophilic materials in the insulating oil. Since the condition of transformer insulation is a very important aspect of HI calculations, the acidity, furan and interfacial tension are also adopted to reflect the condition of oil and paper insulation.

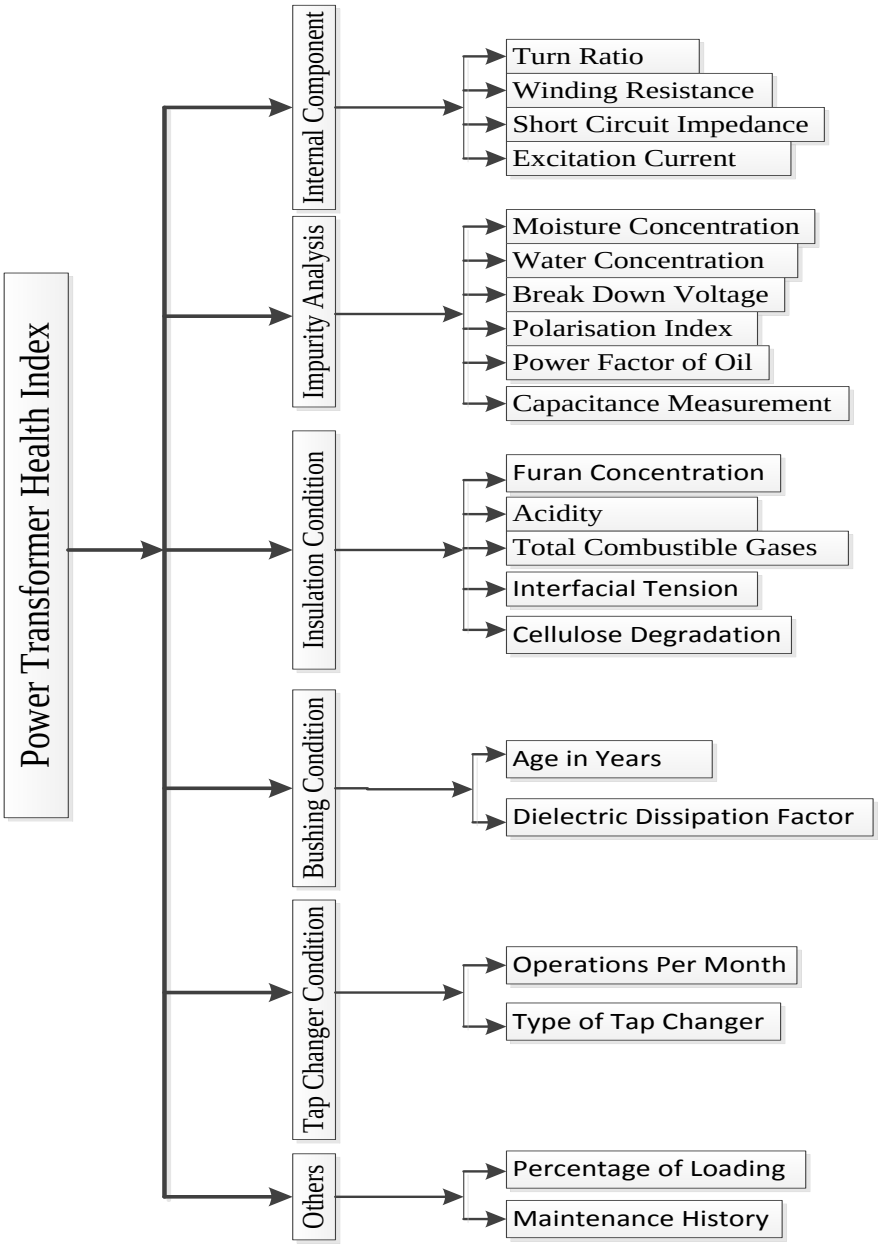


**Figure 7.2:** Subsystem-based measurements for HI calculation of transformers.

### 7.3.2 Impurity Analysis

Moisture is the most harmful impurity in transformer insulation that is produced from the degradation of paper insulation. It reduces the dielectric strength of oil and paper insulation and increases their ageing rate. In a power transformer, the moisture

content comes from several sources such as the surrounding atmosphere, leaky seals and the drying process, or it may be produced internally from the degradation of solid insulation [21]. Moisture dynamics between insulating oil and paper are quite complex and greatly dependent on the temperature [21]. With the increase of winding temperature, moisture starts migrating from paper to oil and vice versa. A sudden temperature raised from emergency overloading or initial energization releases moisture in the form of bubbles that float up into the oil [22]. The dielectric strength of bubbles is very low. Therefore, flash-over may occur between the electrodes in the area having strong electric stress. If the moisture increases beyond the saturation level of oil, free water starts to form and further decrease the dielectric strength of the oil [17]. This water also increases the ageing rate of the cellulose hence reducing the service life of transformers.

A power factor test may also be used to evaluate the ageing of oil [23]. The test is very sensitive to the ageing by-products and soluble polar contaminants like water [17]. A higher value of power factor is a good indicator of contaminated oil. The power factor is also known as dielectric dissipation factor (DDF) and can also be used to determine the dryness of insulating system (windings and oil). In the DDF test, an alternating voltage is applied to insulation and the dielectric loss (dissipated as heat energy) across the insulating liquid is measured [24]. Capacitance measurements between inter-windings and windings to main tank body are also carried out at the same time to check the ageing of insulation or mechanical deformation of windings. The break down voltage (DBV) measures the dielectric strength of oil to withstand electrical stress without failure [25]. It is always necessary to have a significantly higher DBV value of oil than the operating voltage to prevent premature dielectric failure. The DBV value decreases with increased water and contaminants in the oil. The polarization index (PI) is another common method to assess the dryness and cleanness of solid insulation [26]. In the PI test, the ratio of 10 minute resistance to 1 minute resistance of insulation is calculated after applying a test voltage. The polarization index value decreases with the increase of

moisture and impurity in the insulation. As these test results are greatly influenced by the moisture content and contaminants, they are kept as part of the same subsystem group.

### 7.3.3 Internal Components

To check the integrity of a transformer's internal components, a number of electrical tests such as excitation current, sweep frequency response analysis (SFRA), windings ratio, windings resistance and short circuit impedance are used [1]. The excitation current test is used to detect short circuit turns, core delamination shorts, tap changer problems and multiple groundings. During the test, magnetization current is measured by energizing the high voltage side while keeping the low voltage neutral grounded. Any short circuit incident in the core, windings and grounding changes the magnetization current that will be picked up by this test [2]. The turn ratio tests can detect any shorts between turns of the same winding including the tap changer. The winding resistance is measured to detect poor electrical connection in windings and the tap changer. Short circuit impedance can identify the winding movement and structural problems. In any transformer, most of the flux passes through the core rather than the spaces between windings and core. This test measures the leakage reactance of the flux passing through these spaces. With any distortion of windings, the size of the spaces varies and that changes its leakage reactance. The SFRA technique is a very sensitive method that is used to check the mechanical condition of core and windings. Deformation could take place in windings (axial and radial) and core (delamination) due to fault currents and large mechanical forces resulting from transportation and relocation. As no mechanical deformation was found in any SFRA test report of transformers collected from the utility, it was excluded from this group.

### 7.3.4 Bushing Condition

The average expected life of a bushing is 30 to 40 years. It is the third highest contributor to transformer failures [11]. Moisture may enter into bushings through leaky gaskets and other openings, and degrades the quality of a bushing. According to [18], 90 % of bushing failures occur due to moisture ingress. Deposition of dirt and conductive contaminants such as salts on the outer surface of a bushing may cause flashover. Therefore, it is imperative to appraise all bushings carefully to ensure reliable operation of transformers. To assess their actual condition, besides operating age, diagnostic tests like dielectric dissipation factor (DDF) and capacitance measurement are commonly used. In the capacitance test, the capacitance $C_1$ between the centre conductor and outer layer of the foil is measured by accessing the DDF tap. Moreover, the capacitance $C_2$ between the DDF tap and ground is also measured. If the foil becomes degraded by cracks and moisture ingress, the capacitance value will be changed. Consequently, the measured capacitance and DDF value can be used to diagnose the bushing condition and contamination of its insulation respectively.

### 7.3.5 Tap Changer Condition

Statistically the tap changer makes the single highest contribution to any transformer's failure risk [11]. As a result, special care should be taken with this device to avoid unexpected failures. Several distinct types of tap changers are used in transformers. Based on their construction, a range of insulating materials such as oil, epoxy resin, fiberglass and cardboard are used. To assess the condition of a tap changer, beside various tests like DGA, oil quality and contact resistance, some statistical information such as the number of previous operations, maintenance history and construction type are commonly used by utilities. Unlike DGA of the main tank, a certain level of combustible gases is quite normal in a tap changer due to the operational arcing. Therefore, the interpretation of its DGA is slightly different from that of the main tank. Due to poor availability of DGA and oil analysis data, the

construction type and the number of operation are used in this work to assess the condition of a tap changer.

### 7.3.6 Other Parameters

Beside the conventional condition assessment approaches, loading information and maintenance history are also considered in this work to improve the accuracy of health index calculation. The recorded peak load of a particular month was applied to calculate the historical load contribution on health index calculation. Moreover, the last five years' maintenance work orders for each transformer are also analysed to find the past condition of individual transformers.

## 7.4 Methodology

In this section, the general regression neural network (GRNN), a kind of probabilistic model, was used to calculate the health index (HI) for each subsystem of transformers. The GRNN has a nice interpolation property and the capability to learn high dimensional mappings very quickly. It is non-parametric, as all the required parameters in the GRNN can be derived directly from the finite set of training measurements. In the GRNN, a dependent variable $Y = \{Y_n\}$ is predicted using a number of given *D*-dimensional independent measurements $\boldsymbol{X} = \{X_n\}$ where $X_n \in \mathcal{R}^D$. The prediction is the most probable value of $Y$ for each value of $X$ based on a finite set of $n$measurements and their associated $Y$ values. Thus, the GRNN learns a mapping from an input domain containing $X$ to an output codomain containing $Y$, where either space can be multidimensional. If a GRNN is trained with a finite number of available measurements, it can estimate a linear or nonlinear regression surface to predict the most probable value of $Y$ for any new measurement of $x$. According to [27], the basic equation for the GRNN function $g(x)$ based on a multivariate Gaussian kernel can be written as:

$$g(x) = \frac{\sum_{n=1}^{N} Y_n exp\left(-\frac{{D_n}^2}{2}\right)}{\sum_{n=1}^{N} exp\left(-\frac{{D_n}^2}{2}\right)} \quad (7.2)$$

where in this application $x$ is a multidimensional new measurement used for testing, $Y_n$ is the HI score for the training set and ${D_n}^2 = (x - X_n)^T \Sigma^{-1}(x - X_n)$ is the Mahalanobis distance between the training set and the point of prediction. The exponential terms of (7.2) reflect the contribution of each of the training points to the HI score of $x$.

The challenge of this approach is to find an optimal value of the multivariate standard deviation$\Sigma$ for the training set, also known as the smoothing parameter. A large value of $\Sigma$ forces the model to become smoother and ignores some features of the training samples [28]. Conversely, if the value of $\Sigma$ is too small, the model will overfit the training examples and try to track every feature of the training set [29]. Overfitting makes the model very sensitive to noise and damages its generalization capability. Therefore, a reasonable estimation of $\Sigma$ is very important so that all useful features of the training set are taken into account since the prediction points closer to training sample will get heavier weighting. One way of deterring the optimal value of $\Sigma$ is via the "holdout" method [30]. In this approach, one sample from the training set is removed at a time and a network is constructed using all of the other samples. A presentation on holdout method is available in [30]. An implementation of this method is presented in section 7.3. Different subsections of the GRNN approach are discussed below.

### 7.4.1 Data Processing and Normalization

In this work, measurements of 345 power transformers[1] were collected from a large utility company in Australia. The transformers assessed comprised of 28% at 72kV, 65% at 154kV and the remainder at 245 kV and 345kV. The company uses 21 tests to

[1]This work used only 345 transformer measurements out of 376 collected from the utility company as only 345 transformers provided the full set of 21 measurements.

evaluate their large population of transformers. The measurements were collected into six groups (Figure 7.2) following their cross correlation to assess the individual subsystem of transformers such as insulation, windings, bushing and tap changer. The upper and lower limits of each measurement have been considered to create a four-level quantization of each measurement. The ranges have been chosen from the combination of IEEE Standards, manufacturer guidelines and utility practices. To develop a number of $X_n = 4^D$(where $D$ is the number of tests) independent variables of a training set (patterns) for a subsystem, the mid points of the four conditional ranges for each test related to it were used. For instance, if the number of tests in a subsystem is six than total number of training patterns will be $4^6 = 4096$. To calculate the dependent variable $Y_n$ corresponding to a pattern, a conditional score value such as 0.25, 0.5, 0.75 and 1.0 respectively was set at the mid-points of the Good, Fair, Poor, Very Poor ranges for each test (the stepped line in Figure 7.3). Finally, the dependent variable $Y_n$ for each pattern was calculated by averaging their corresponding position scores. The patterns of the training set was normalised by dividing their corresponding upper limit of the Very Poor condition to ensure the scaling between zero and unity. This approach ensured the same scaling of each dimension. In the case of a missing upper limit (which could be infinity), 1.5 times the lower limit of the Very Poor condition was used as a normalisation factor.

### 7.4.2 GRNN Model

To develop the GRNN model, a Gaussian kernel was used in this work. As the Gaussian function is simple to implement and has continuous derivatives, it has been adopted here to obtain a smooth probability density model. According to IEEE Std. C57.106, each test is quantized into four non-overlapping ranges using sharp boundaries. The Standard treats all values equally within a range. Quantization throws away valuable information that could be useful at a later stage, forming a major drawback of this approach. Moreover, near the boundary of two adjacent ranges, the quantization is very sensitive to the measured value. A small change at

this region may lead to a completely different condition. To overcome these limitations, a continuous function has been developed using the GRNN interpolation technique but using the same limit values of the four conditional scores. The midpoint of the high and low point of each limit has been assigned with a conditional score and used in the GRNN model. The GRNN interpolation technique based on the water concentration of the insulating oil is shown in Figure 7.3.

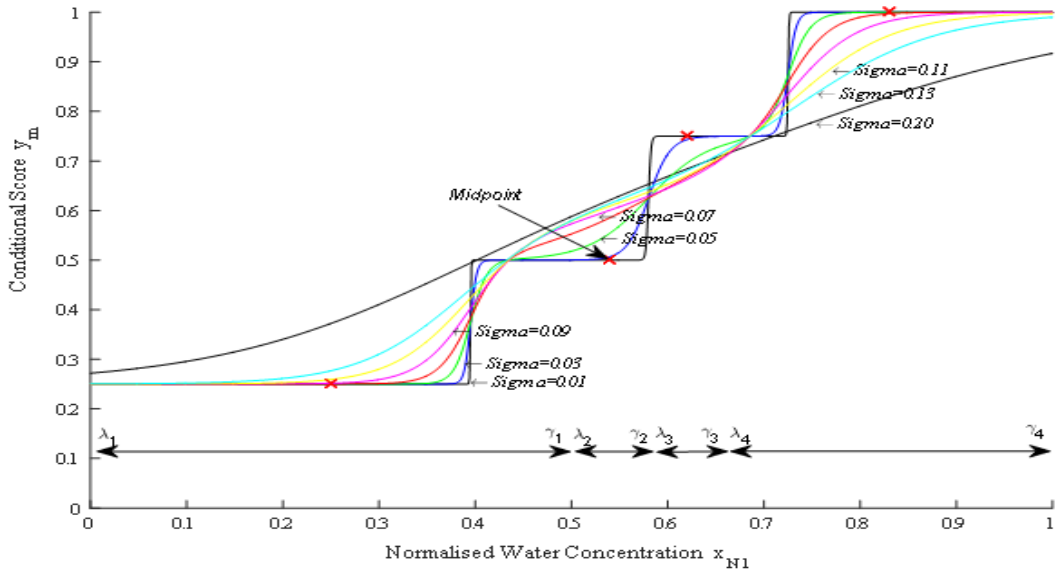


**Figure 7.3:** GRNN interpolation of normalized water content and conditional scores.

In Figure 7.3. $\lambda$ and $\gamma$ represent the lower and upper limits of each quantisation region respectively so the four ranges can be expressed using the following notation.

$$Limit\ values = \begin{bmatrix} \lambda_{1,D} & \gamma_{1,D} \\ \lambda_{2,D} & \gamma_{2,D} \\ \lambda_{3,D} & \gamma_{3,D} \\ \lambda_{4,D} & \gamma_{4,D} \end{bmatrix}$$

where $D$ is the dimension of the measurements and$\gamma_{i,D} = \lambda_{i+1,D}$ for the next range and so on. The targeted midpoint (shown as a red cross in Figure 7.3.) for each quantisation region can be written as

$$\emptyset_{m,D} = \frac{\lambda_{m,D} + \gamma_{m,D}}{2} \; where \; m = 1,2 \ldots ,4 \qquad (7.3)$$

It can be seen from Figure 7.3 that the GRNN works like a step function given a small value of $\Sigma = 0.01$. It gradually becomes a smooth interpolator with the increasing values of $\Sigma$. Therefore, a small change of water concentration does not impact much on the conditional score near the boundary regions resulting in almost identical scores. A similar multivariate approach has been applied to higher dimensional measurements to calculate the conditional scores of each individual subsystem. The detail procedure of this multivariate approach is available from previous published work [31].

### 7.4.3 Feature Extraction for the Health Index Calculation

In the proposed GRNN model, initially the mid points of the four conditional limits for each test of a subsystem were calculated following equation (7.3). The points were assigned with a score of *0.25, 0.5, 0.75 and 1.00* respectively based on their position in the middle of Good, Fair, Poor and Very Poor ranges. The combination of the points was used to produce a set containing $4^D$ independent variables $X_n$ used as the training set. The dependent variable $Y_n$ (HI score for a subsystem) for each combination of $X_n$ was calculated by averaging their corresponding position scores. For instance, if a subsystem is assessed by three tests and the scores are the midpoints of a Good, Fair and Very Poor limits respectively, then the HI score will be the average of 0.25, 0.5, and 1.0 which is 0.58. After computing $X_n$ and $Y_n$, they were used to train the GRNN model. To estimate the smoothing of the model, the covariance ($\Sigma_S$) of $X_n$ was calculated and the holdout method was applied. To vary the value of $\Sigma_S$, a multiplicative factor $E$ was added in front of it. Therefore, the new equation of $\Sigma_S$ can be written as

$$\Sigma = E\Sigma_S \tag{7.4}$$

where $E$ is a multiplicative factor chosen to provide an appropriate amount of smoothing (see Figure 7.3) and $\Sigma$ is the smoothing value used for the distance metric $D_n$ of (7.2).

In the holdout approach, one sample from the training set was removed at a time and a network was constructed using all of the other samples. The network is used to estimate the HI score of the missing sample at a small value (0.001) of $E$. The process is repeated for all samples and the mean-squared error is estimated and stored. Then the value of $E$ is increased linearly up to 1 with a small incremental step and the whole process is repeated. The mean-squared error for all values of E was plotted. Finally, the value of $E$ giving the smallest error was selected for the proposed model. The mean-squared error at different values of $E$ for the moisture analysis subsystem is shown in Figure 7.4.

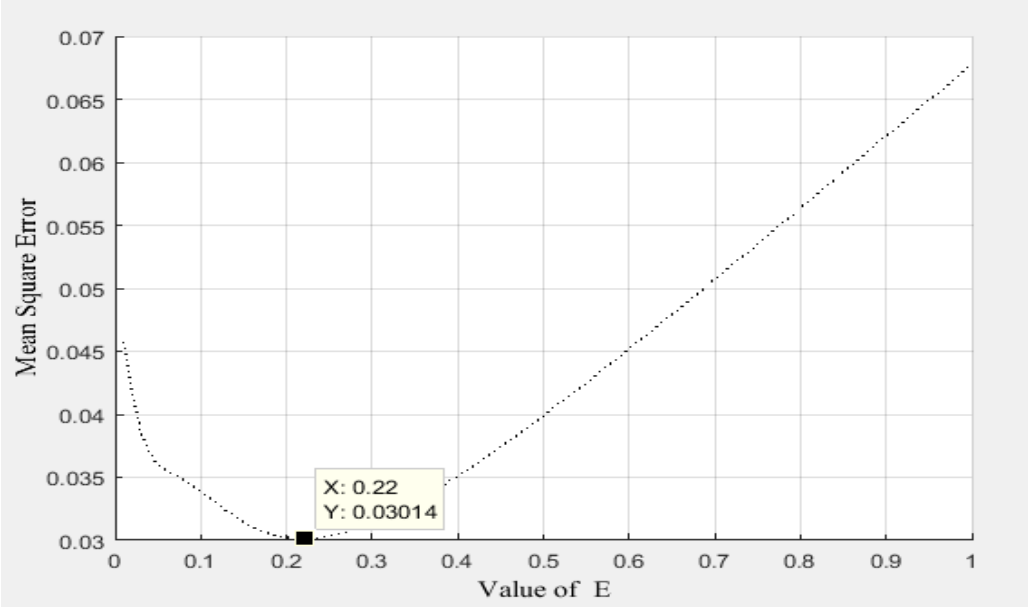


**Figure 7.4:** Mean-squared error at different values of smoothing control parameter$E$.

In Figure 7.4, it is apparent that the mean-squared error at small values of $E$ is high and decreases with the increasing value of $E$. After a certain point ($E = 0.2208$), the error again starts to increase. Therefore, the value 0.2208 was chosen as the optimal solution of $E$ for the subsystem. Similarly, the smoothing parameters $E$ for the other five groups/subsystems were also calculated. These values were used as a multiplicative factor for $\Sigma_S$ (equation 7.4) to ensure the optimal smoothing to the GRNN interpolated function for each subsystem of the training set. Finally, the HI score for each subsystem of the 345 transformer measurements collected from the utility was calculated using GRNN interpolation following the equation (7.1). To compute the overall HI score of transformers, the general regression (equation 7.2) of the individual subsystems were combined using arithmetic and geometric mean. In the arithmetic approach, the regressions were added together and normalised in the range 0 to 100. The equation of the approach can be written as follows.

$$g(x) = \frac{1}{k}\left(g_1(s_1) + g_2(s_2) + \cdots + g_k(s_k)\right) \tag{7.5}$$

where $k$ is the number of subsystems considered and $g_k(s)$ is the HI score of the $k_{th}$ subsystem.

In the multiplicative approach, the resultant HI score was calculated from the $k_{th}$root of the product of $k$regressions. This approach was chosen so that, if one or more subsystems of a transformer are unhealthy, then the overall HI score of the transformer will also be very unhealthy. It is based on the assumption that, to work correctly, each of the independent subsystems that comprise a transformer must be healthy. The equation of the multiplicative approach can be expressed using the following equation.

$$g(x) = \sqrt[k]{g_1(s_1)g_2(s_2)\ldots g_k(s_k)} \tag{7.6}$$

where $k$ and $g_k(s)$ have the same meaning as in equation (5.5).

From equation (7.6), it can be seen that the overall HI score of a transformer was calculated from the geometric mean of the subsystem scores. Therefore, if one or more subsystem is unhealthy (close to zero), it will dominate the product to strongly influence the overall HI (it behaves much like a logical AND function). However, the arithmetic mean (7.5) considers all subsystems equally and is much less sensitive to an individual unhealthy subsystem condition (it behaves more like a logical OR).

## 7.5 Results and Analysis

In the previous work [1], the HI was created as a weighted average of individual measurement. They were not following a subsystem-based approach, where weighted scores of each measurement were combined linearly to compute an overall HI of a transformer. This made the approach insensitive to any single measurement. Moreover, in most of the previous work, a high degree of quantization was applied that throws away information and treated wide ranges of measured values equally. To overcome these limitations, the proposed method has preserved all the available information up to the end stage to produce an effective HI as a percentage between 0 and 100 where 100 implies totally unhealthy and 0 means very healthy (note this scale is opposite to that discussed in section 7.4.3). Therefore, comparing the proposed method with the linear approach the experts have followed is not sufficient, as at best the model will learn only to be as good as the experts. The proposed method has the potential to do better than the experts. Consequently, to explore the secondary evidence, the conventional linear approach and the GRNN (Additive and Multiplicative) HI scores based on 345 transformers measurements collected from a utility company were analysed. The comparative results are shown in Figure 7.5 (a) and (b) respectively.

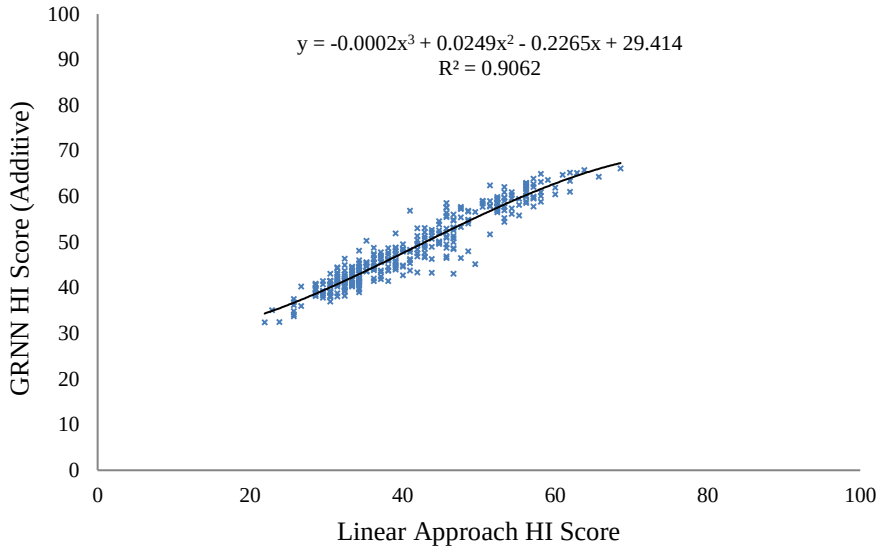


**Figure 7.5 (a):** Linear versus additive approaches.

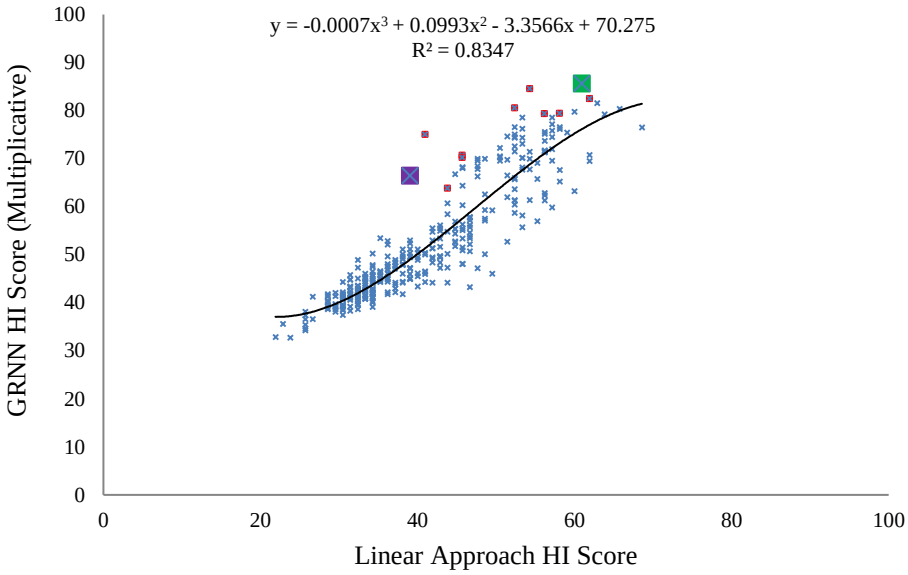


**Figure 7.5 (b):** Linear versus multiplicative approaches.

It can be seen from Figure 7.5 (a) that there is reasonable agreement between the additive approach (equation 7.5) and the conventional linear technique ($R^2 =$

0.9062). The variance above and below the line of best fitting is almost constant throughout the range and the discrepancy came from the interpolation of measurements (as per Figure 7.3). As both methods rely on arithmetic averaging, neither occupies the entire HI range of 0-100. However, the multiplicative approach Figure 7.5(b) only agreed closely with the linear approach at lower values ($overall\ R^2 = 0.8347$). At higher values, in some cases the multiplicative approach became disassociated (highlighted as coloured squares) from the linear approach. After analysis, it was found that one or more transformer's subsystems of these cases were in critical condition which increased the HI significantly (equation 7.6). For instance, a transformer (Green Square at the top right corner of Figure 7.5 (b)) was assigned with a much higher (82) HI score by the multiplicative method than the linear approach, which assigned 61 due to the very unhealthy condition of its Bushing and Tap changer subsystems. Likewise, the purple transformer assigned with smaller (healthier) score than the green one as only its Bushing was very unhealthy but its Tap changer was relatively healthier. Therefore, these cases suggest that the multiplicative approach is performing better than the additive and linear approaches by focusing on individual subsystems that may compromise operation of a transformer.

To offer a deeper understanding, the GRNN and linear approach HI scores are also plotted against the operating age of transformers in Figure 7.6 (a) and (b) respectively.

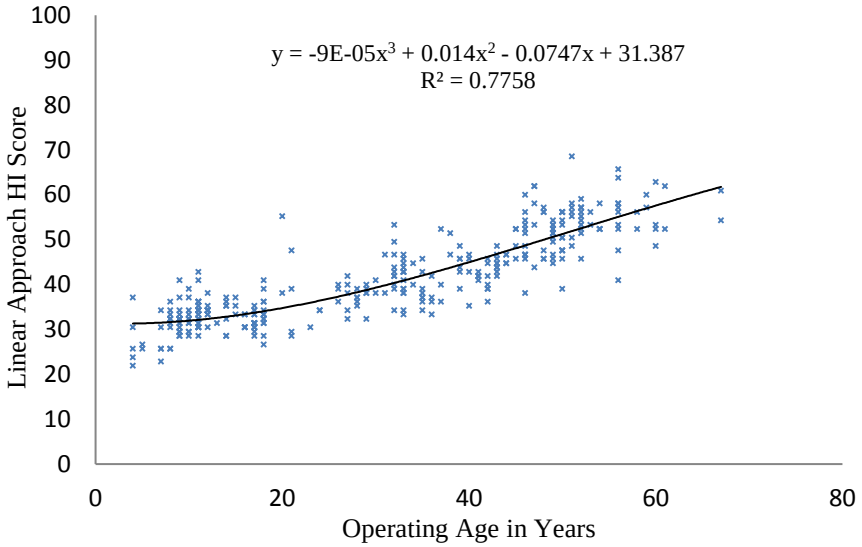


**Figure 7.6 (a):** Relationship between age and linear HI.

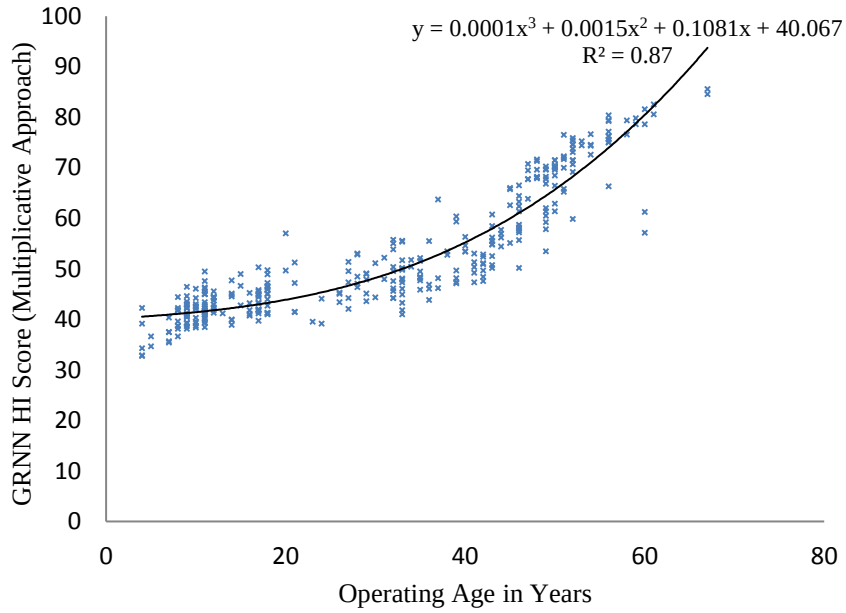


**Figure 7.6 (b):** Relationship between age and GRNN HI.

It is clear from Figure 7.6(a) that the average HI score of transformers monotonically increases with operating age. It has been shown in the literature that the average expected life of transformers is around 40-50 years and its failure pattern follows typical bathtub curve [3]. However, in this case the infant failure of transformers due

to manufacturing defects may be ignored since devices are strictly factory tested prior to installation. Hence the curve starts with a constant failure rate and it can be expected that the HI score will increase gradually up to a certain age with a limited number of failure incidents. After the average age (40-50 years), the failure rate will increase rapidly. The best fit curve of the linear approach does not show these expected properties. Given that, the HI scores increase in a relatively linear way from delivery age zero. However, the GRNN score in Figure 7.6(b) gradually increased up to 40 years of service. After the age, it increased more rapidly as would be expected by the experts. Therefore, the GRNN in Figure 7.6(b) appears to model the expected failure rate better than the conventional linear approach shown in Figure 7.6(a).

To directly compare the utility experts' classification with the proposed method, a candlestick chart is shown in Figure 7.7. In this chart, the midpoint is the mean HI score of a class and the coloured body shows one standard deviation either side of the mean. The maximum and minimum score of a class are used to calculate the upper and lower outlier/error of the sticks.

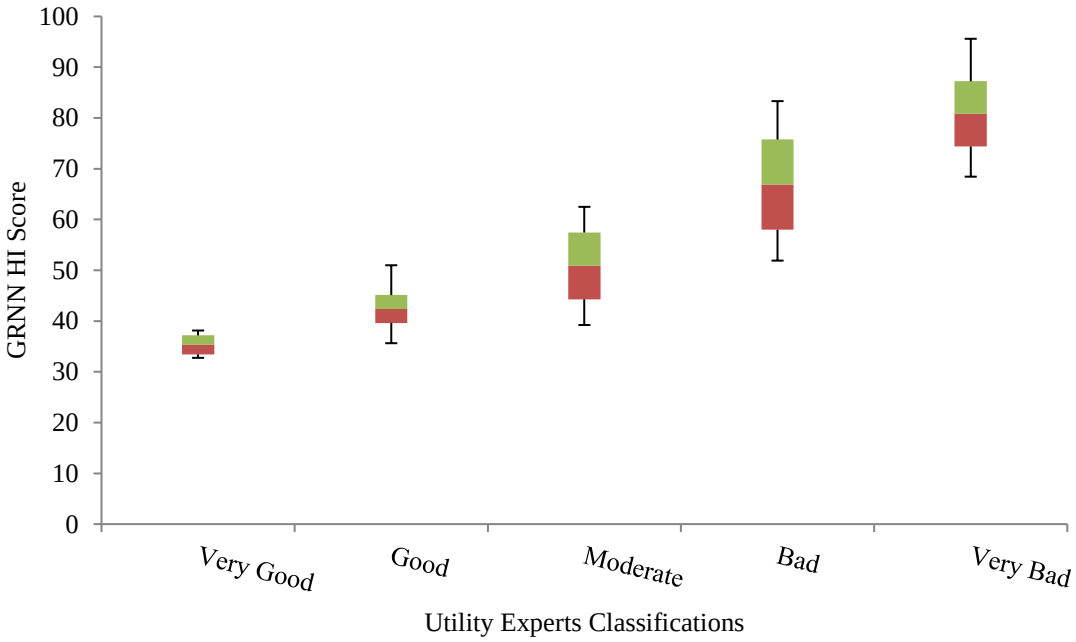


**Figure 7.7:** Comparison between the GRNN score and expert classifications.

Expert classification is normally presented in a quantised way as one of five categories [1]: Very Good, Good, Moderate, Bad and Very Bad. These categories were compared with the multiplicative GRNN HI scores using a candlestick chart shown in Figure 7.7. From the chart, it can be seen that there is a strong agreement between the GRNN and expert classification for the Very Good transformers. However, the disagreement starts from the Good condition with outliers that gradually increase with the degradation of transformers. This GRNN method is much more sensitive to one dysfunctional subsystem than the expert's typically linear approach. Therefore, the unhealthiest transformers in the good category having some moderate class measurements in their subsystems were assigned with a higher HI score. Conversely, the healthiest transformers in the moderate class were allocated a lower HI score as some of their measurements were near the region of different quantization boundaries. Unlike the linear approach, the GRNN does not apply any quantization to the intermediate results. Moreover, the GRNN is less sensitive to the exact placement of the quantisation boundaries as it works based on a continuous smooth interpolated function rather than a step function. Therefore, it picked up the boundary cases and assigned with appropriate scores which may be overlooked by the utility experts.

## 7.6 Probability of Failure Analysis

In this section, the Weibull distribution has been applied to estimate the actual failure probability of power transformers. It is one of the most commonly used lifetime distributions that can model the failure rate function of populations of complex systems [33] such as those with bathtub curve-like hazard functions. It provides a flexible modelling technique as the corresponding failure rate function can be adjusted by using a variable shape parameter. The function of a two parametric Weibull distribution can be expressed as follows:

$$f(x) = \begin{cases} \frac{k}{\lambda}\left(\frac{x}{\lambda}\right)^{k-1} e^{-(x/\lambda)^k}, & x \geq 0 \\ 0 \quad , & x < 0 \end{cases} \tag{7.7}$$

where, in this application, $x$ is the age of transformers(in years), $k$ and $\lambda$ are the shape and scale parameter respectively.

It is assumed that the median life expectancy of power transformer is 50 years and that no transformers will be in operation beyond 80 years [1]. Therefore, using the Weibull function, the failure probability density function of transformers versus operating age has been calculated. A Weibull probability distribution of transformers is shown in Figure 7.8(a).

Using a similar approach to that in [32], the value of $k$ is assumed to be 4 implying that the mean time to failure decreases with the cube of operating age. (The mean time to failure is an averge length of time a device is expected to be operational based on the finite number of observations). The scale parameter $\lambda = 54.503$ is estimated from the function so that 50 % of transformers in operation have failed before the age of 50 years. The ratio of failed transformers is shown in Figure 7.8(b) and the cummulative density function is derived from Figure 7.8 (a).

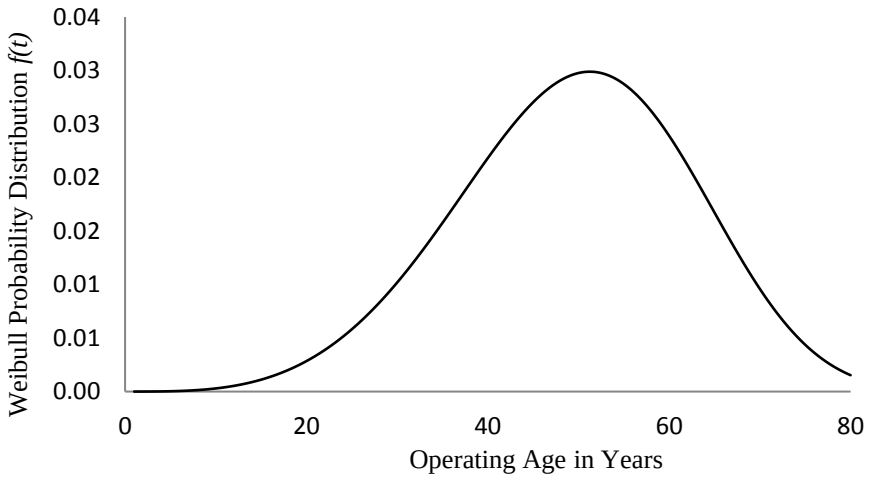


**Figure 7.8 (a):** Weibull distribution over time.

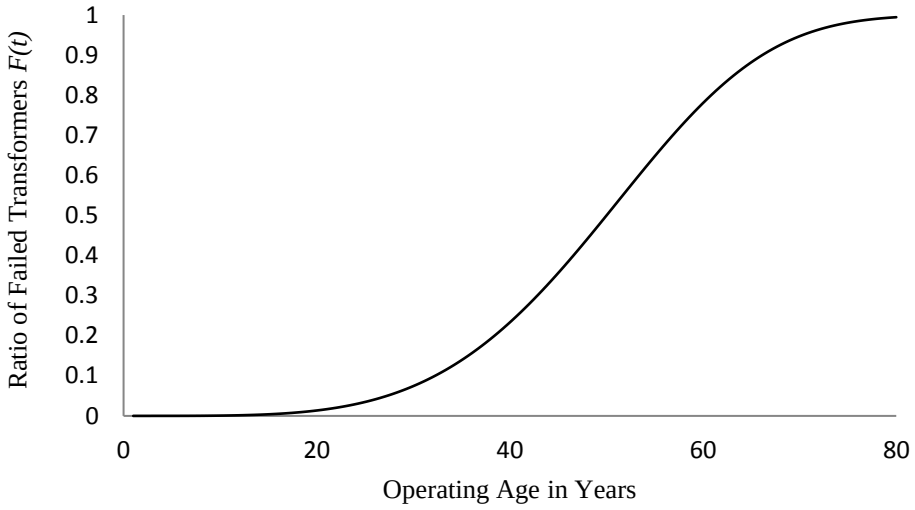


**Figure 7.8 (b):** Ratio of failed over time.

As the ratio of failure is known from Figure 7.8 (b), the failure rate per year can be calculated using the following equation [33].

$$h(t) = \frac{f(t)}{1-F(t)} \tag{7.8}$$

where $f(x)$ is a failure density function and $F(t)$ is a cumulative failure distribution function (as in Figure 7.8 (b)).

The relation between the failure rate $h(t)$ and operating age of transformers is shown in Figure 7.9(a). Now mapping the best fitting curve of the HI score over operating age from Figure 7.6(b) to the failure rate per year curve shown in Figure 7.9(a), the failure rate over HI score has been calculated. A relationship between failure rate and HI score is shown in Figure 7.9(b)

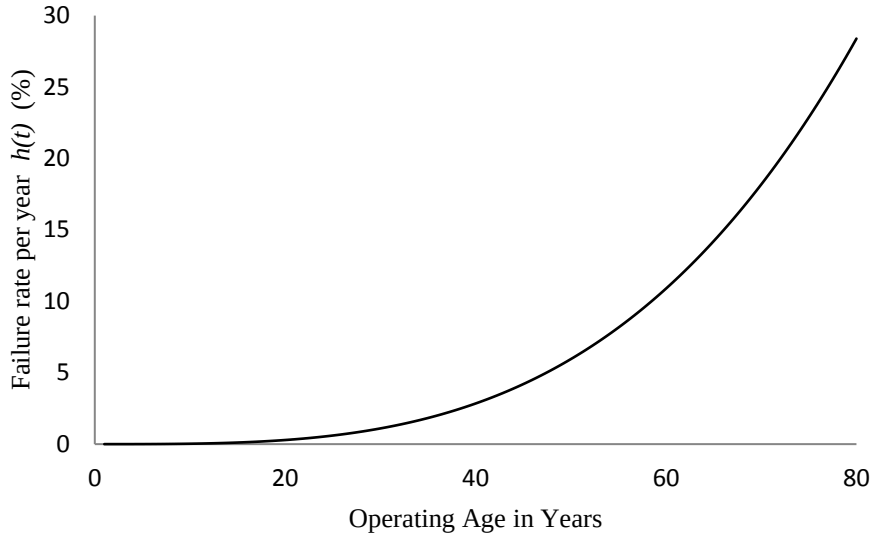


**Figure 7.9 (a):** Failure rate over time.

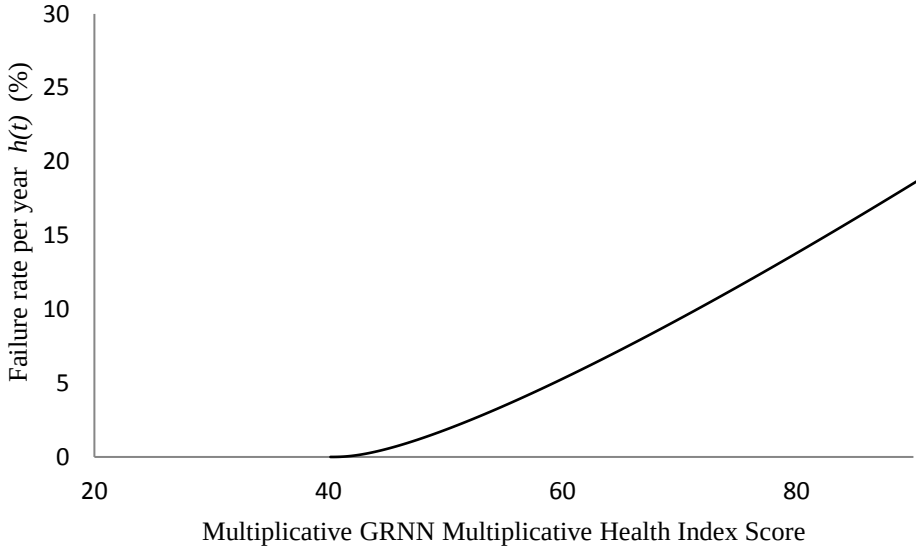


**Figure 7.9 (b):** Failure rate over HI score.

If the initial failure due to manufacturing defects is ignored, then from Figure 7.9 (b), it is clear that for values below the 40 HI score, the failure rate is very insignificant. With increasing HI score, the failure rate increases in a relative linear fashion. It represents the estimated failure probability of individual transformers rather than an average probability of failure for a large fleet of transformers. As a result, at any HI

score, the probability of failure for individual transformer can be estimated. For ++-instance, if the HI score of a transformer is 80, then its probability of failure in next year will be approximately 14 %. Therefore, the calculated HI can be calibrated to justify the plan of assets replacement at the end-of-life.

## 7.7 Conclusions

In this work, a HI score for a power transformer has been estimated by non-linear combination of condition scores for each of its subsystems. The condition of each subsystem is estimated from diagnostic measurements using a non-parametric GRNN regression model. The model assessed the long term degradation of different subsystems such as insulation, windings, core, bushing and tap changers of transformers and combined them into a condition-based HI score. Beside the conventional routine and diagnostic tests, the maintenance history and loading information is also evaluated in this work. It was found that the proposed method was sensitive enough to detect a single degraded subsystem of transformers (resulting in an increase in the HI score). The system is performing at least as well as experts for most of the transformers with some evidence provided for unusual cases such that the proposed method is doing better than existing techniques. Moreover, the calculated HI has been mapped to the probability of failure over time. Therefore, it is expected that the proposed HI method will be a useful tool for utilities to manage their large fleets of transformers and will provide them methodical justification for asset replacement at the end-of-life.

## References

[1] A. Jahromi, R. Piercy, S. Cress, J. Service and W. Fan, An approach to power transformer asset management using health index, IEEE Electr Insul Mag, Vol.25, pp. 20-34, 2009.

[2] M.M. Islam, G. Lee and S.N. Hettiwatte, A review of condition monitoring techniques and diagnostic tests for lifetime estimation of power transformers, Electrical Engineering, pp.1-25, 2017, DOI: 10.1007/s00202-017-0532-4.

[3] M. Wang, A.J. Vandermaar and K.D. Srivastava, Review of condition assessment of power transformers in service, IEEE Electr Insul Mag, Vol. 18, pp. 12-25, 2002.

[4] T.K. Saha, "Review of modern diagnostic techniques for assessing insulation condition in aged transformers, IEEE Trans Dielectr Electr Insul, Vol. 10, pp. 903-917, 2003.

[5] ABB Service Handbook for Transformers, 2nd ed., Zurich, Switzerland: ABB Management Service, Ltd., 2007.

[6] M.M. Islam, G. Lee and S.N. Hettiwatte, A nearest neighbour clustering approach for incipient fault diagnosis of power transformers, Electrical Engineering, pp.1-11, 2016, DOI:10.1007/s00202-016-0481-3.

[7] A. Naderian, S. Cress, R. Piercy, F. Wang and J. Service (2008, July), An Approach to Determine the Health Index of Power Transformers, IEEE International Symposium on Electrical Insulation, pp. 192-196.

[8] A.E.B. Abu-Elanien, M.M.A. Salama and M. Ibrahim, Calculation of a Health Index for Oil-Immersed Transformers Rated Under 69 kV Using Fuzzy Logic, IEEE Transactions on Power Delivery, Vol.27, pp. 2029-2036, 2012.

[9] A.D. Ashkezari, H. Ma, T.K. Saha and C. Ekanayake, Application of fuzzy support vector machine for determining the health index of the insulation system of in-service power transformers, IEEE Trans Dielectr Electr Insul, Vol. 20, pp. 965-973, 2013.

[10] W. Zuo, H. Yuan, Y. Shang, Y. Liu and T. Chen, Calculation of a Health Index of Oil-Paper Transformers Insulation with Binary Logistic Regression, Mathematical Problems in Engineering, Vol. 2016, pp. 9, 2016.

[11] I.A. Metwally, Failures Monitoring and New Trends of Power Transformers, IEEE Potentials, Vol. 30, pp. 36-43, 2011.

[12] A. Barron, J. Rissanen and Y. Bin, The minimum description length principle in coding and modeling, IEEE Transactions on Information Theory, Vol. 44, pp. 2743-2760, 1998.

[13] V.G. Arakelian, Effective diagnostics for oil-filled equipment, IEEE Electr Insul Mag, Vol. 18, pp. 26-38, 2002.

[14] IEC60599, International Standard for Mineral oil-impregnated electrical equipment in service – guide to the interpretation of dissolved and free gas analysis, Edition 2, 1999.

[15] IEEE.StdC57.104, Guide for the Interpretation of Gases Generated in Oil-Immersed Transformers, February 2009

[16] IEC62021-1, Determination of acidity by automatic potentiometric titration, 2003.

[17] B. Pahlavanpour, Characterisation of insulating oils, in: IEEE Colloquium on Characterisation of Dielectric Materials: a Review, pp. 1-8, 1994.

[18] X. Zhang and E. Gockenbach, Asset-management of transformers based on condition monitoring and standard diagnosis [feature article], IEEE Electrical Insulation Magazine, Vol. 24, pp. 26-40, 2008.

[19] X. Zhang, E. Gockenbach, V. Wasserberg and H. Borsi, Estimation of the Lifetime of the Electrical Components in Distribution Networks, IEEE Transactions on Power Delivery, Vol. 22, pp. 515-522, 2007.

[20] T. Leibfried, M. Jaya and N. Majer, Postmortem Investigation of Power Transformers-Profile of Degree of Polymerization and Correlation With Furan Concentration in the Oil, IEEE Transactions on Power Delivery, Vol. 28, pp. 886-893, 2013.

[21] T.V. Oommen and T.A. Prevost, Cellulose insulation in oil-filled power transformers: part II maintaining insulation integrity and life, IEEE Electr Insul Mag, Vol. 22, pp. 5-14, 2006.

[22] C.Y. Perkasa, N. Lelekakis, T. Czaszejko, J. Wijaya and D. Martin, A comparison of the formation of bubbles and water droplets in vegetable and mineral oil impregnated transformer paper, IEEE Trans Dielectr Electr Insul, Vol. 21, pp. 2111-2118, 2014.

[23] T. K. Saha, H.Ma, C. Ekanayake and D. Martin, Pattern recognition technique for determining the health index of oil-paper insulation pattern recognition technique for determining the health index of oil-paper insulation CIGRE, Paris Session, Vol. 59, pp. 75, 2014.

[24] J. Singh, Y. R. Sood and P. Verma, Experimental Investigation Using Accelerated Aging Factors on Dielectric Properties of Transformer Insulating Oil, Electric Power Components and Systems, Vol. 39, 2011.

[25] IEC60156, Insulating liquids - Determination of the breakdown voltage at power frequency - Test method, 1995.

[26] H. Torkaman and F. Karimi, Measurement variations of insulation resistance/polarization index during utilizing time in HV electrical machines – A survey, Measurement, Vol. 59, pp. 21-29, 2015.

[27] J. Song, C.E. Romero, Z. Yao and B. He, A globally enhanced general regression neural network for on-line multiple emissions prediction of utility boiler, Knowledge-Based Systems, Vol. 118, pp. 4-14, 2017.

[28] O. Polat and T. Yıldırım, Hand geometry identification without feature extraction by general regression neural network, Expert Systems with Applications, Vol. 34, pp. 845-849, 2008.

[29] I.M. Overton, G. Padovani, M.A. Girolami and G.J. Barton, ParCrys: a Parzen window density estimation approach to protein crystallization propensity prediction, Bioinformatics, Vol. 24 , pp. 901-907, 2008.

[30] D.F. Specht, A general regression neural network, IEEE Transactions on Neural Networks, Vol. 2, pp. 568-576, 1991.

[31] M.M. Islam, G. Lee and S.N. Hettiwatte, Application of a General Regression Neural Network for Health Index Calculation of Power Transformers, International Journal of Electrical Power and Energy Systems, Vol. 93, pp. 308-315, 2017.

[32] M. Xie, Y. Tang and T.N. Goh, A modified Weibull extension with bathtub-shaped failure rate function," Reliability Engineering & System Safety, Vol. 76, pp. 279-285, 2002.

[33] R. Jiang and D.N.P. Murthy, A study of Weibull shape parameter: Properties and significance, Reliability Engineering & System Safety, Vol. 96, pp. 1619-1626, 201.

[34] H. Pham and C.D. Lai, On Recent Generalizations of the Weibull Distribution, IEEE Transactions on Reliability, Vol. 56, pp. 454-458, 2007.

# Chapter 8: Summary and Future Directions

## 8.1 Summary

Power transformers are working at the heart of transmission networks to deliver power to end users. To manage the growing demand for electricity, besides other electrical infrastructure, the number of transformers in utility networks is continuously increasing over time. The reliability of the power system is strongly dependent on the maintenance pattern and the operating condition of this expensive device. To prevent an unexpected outage of a network and avoid time-consuming, costly repair or replacement, improvement in the fault diagnosis and condition monitoring techniques is always desirable. These improvements provide the fundamental research questions of this thesis. To address these issues, one of the objectives of the research was to develop a hybrid clustering approach that can improve transformer diagnosis accuracy and fault classifications. This work also quantified the operating condition of transformers using a set of routine and diagnosis measurements that can evaluate their subsystems such as insulation, core, windings, bushings and tap changers. Therefore, operators can identify the assets that need more attention than others by looking at their condition score. Moreover, the detected correlation between the condition score and failure probability of transformers as a function of operating age can provide decision support to the asset managers to plan the repair or replacement of the expensive assets.

It is always beneficial to detect faults in a transformer at an incipient stage. To identify defects and improve their classification accuracy, besides conventional methods such as the family of Duval Triangles and ratio approaches, the application of artificial intelligence (AI) has become commercially viable. The intelligence methods look for the secondary evidence using the measured concentration of variable performance indicative byproducts such as dissolved gases, furan, acid and moisture. To track down their changing rate over time, oil samples from on service

transformers are periodically collected. Utility expert's use these findings to make maintenance decisions and judge the necessity for further off-line investigations. However, due to unavoidable situations, such as a problem with a sensor, faulty communication devices, a laboratory defect, financial constraints and utility practices, some measurements may be missed out. Therefore, experts have to take the decision based on the available dimensions (known measurements) of each vector. To deal with the missing dimensions in the measured vectors, a General Regression Neural Network was used in this research. The model can estimate the missing value using the knowledge of a complete set of vectors with a reasonable error.

It has been shown in many recent studies that a single method is insufficient to classify the fault category of transformers accurately. Especially, if the measured gas ratios fall outside the predefined limits of available ratio approaches, they cannot give any diagnosis. Also, most of the methods only provide a valid diagnosis if the concentrations of gases exceed certain minimum thresholds. Moreover, if the measured vector of a faulty transformer is located at the boundary between two or more faulty classes they cannot distinguish the fault's cause with any confidence. Therefore, understanding the actual correlation between different measured quantities and the introduction of more sophisticated analysis techniques like AI became necessary.

Although there is an extensive body of literature available on different aspects of fault diagnosis of power transformers, relatively few relevant scientific studies were found dealing with health index (HI) calculation of a transformer. In a HI calculation, the condition of different primary and supplementary components is summarized to reflect the overall operating condition of each transformer. In practice, there is typically a scarcity of information and knowledge to allow the combination of various measurable quantities into a quantitative health index in an appropriate manner. Most of the available methods are dependent on a linearly weighted score of measurements. Therefore, they are insensitive to the condition of a single but critical primary or auxiliary component that can potentially cause a catastrophic failure of

transformers. Over the last decade, researchers started to use some nonlinear artificial machine learning techniques based on the oil test data to quantify the health condition of transformers. However, their approaches are insufficient to give an overall assessment of a transformer as oil test data can only evaluate the status of the oil and paper insulation of transformers. They mostly ignore the condition of the bushings, tap changer, maintenance history and past operating load information. Therefore, the focus of this research was to integrate the status of all subsystems including loading pattern and maintenance history to find unified assessment of transformer condition.

In Chapter 2, a comprehensive literature review was carried out to underline the limitations of existing fault diagnostic techniques and explore the scope of improvement to overcome some of the constraints. As part of the review process, a comparative analysis of different fault diagnosis methods has been presented here. It also covered the methodology and application of various electrical, dialectic and chemical tests, and their dependency on multiple factors. A summary of existing ageing and remaining life estimation procedures based on the hot spot temperature, DP value, and concentration of furan is also discussed in this section. Finally, different health index calculation techniques and their correlation with operating age have been included in this chapter.

Chapter 3 presented a fault diagnostic technique for transformers based on a supervised hybrid k-means algorithm. It was found in the literature that some of the existing methods struggle to distinguish critical faults when they are overlapping with each other. Many of the ratio approaches cannot always provide diagnosis and are only valid when gas concentrations exceed certain limits. To overcome the limitations, a hybrid algorithm was developed to form the desired number of clusters based on the vector of five combustible gas concentrations collected from 376 power transformers owned by a large utility company in Australia. The clusters were representative of a single or multiple fault classes with different distinguishable percentages. The center of each cluster was calculated from the mean of associated vectors belonging to it. It was proven from the initial output of the k-means algorithm that the performance of the method varied with the initial positioning of the cluster

centers. The limitation was partially overcome by integrating the Linde-Buzo-Gray (LBG) algorithm with the k-means. The LBG algorithm was used to better supervise the splitting and relocation of cluster centers during the training process. In each iteration, a center with associated with an empty set of measurements was removed or occasionally relocated until the number of cluster centers reached the desired value. The hybrid method helped to reduce the clustering error that results from the local convergence. Additionally, a novel three nearest-neighbour concept was developed allowing cumulative voting, based on the distances of measured vectors from three closest centers. The performance of the approach was compared with other published methods and expert's classifications of the same set of data resulting in an accuracy of 93%, which is much higher than the ratio approaches such as IEC ratio (74%) and Roger's ratio (76%) respectively. Nevertheless, the identification of global centers for different faults, based on the finite set of vector measurements, was quite complex and dependent on a significant number of supervising iteration techniques developed in this work. So, this was found to be a comparatively slow process and a computationally expensive method. Furthermore, the outcome of the approach suggests that there may be value in exploring a relatively non-parametric approach that can increase the accuracy of fault diagnosis that will reduce the number of unknown parameters.

Chapter 4 presented an extended version of the clustering diagnosis technique based on a probabilistic Parzen Window (PW) method. The method was established to deal with critical cases where conventional approaches fail to provide a definitive fault diagnosis. To develop the process, the same five gas concentrations of the previous hybrid clustering method were used. The gas concentrations were divided into groups to classify the seven standard fault categories of transformers. The members of each fault group were assigned based on the combination of expert's classification and other established methods. The PW method initially estimated the joint probability distribution function (PDF) of the five-dimensional training measurements in different fault groups. To enable this, multivariate Gaussian kernels were centered on top of each training vector and superimposed. The performance of the method was

improved by selecting an optimal smoothing (width) parameter for the PDF. The function was then used to estimate the probability of each transformer in different fault groups. As the PW method provides a kind of soft clustering, a transformer could be a member of various fault groups with a distinct percentage of probability. Therefore, a transformer having maximum probability in a defective group was used to classify its fault category. Unlike hybrid clustering, the method only considers the possibility of defects in different target groups, not on the location of their centers. Therefore, it is free from the problem of local convergence. It was evident from the comparative analysis that this PW method can accurately classify over 94% critical test cases and performed much better than the conventional ratio-based diagnostic strategies. As the accuracy of the method is dependent on the number of training data, it can further be improved if a large training set is available.

Chapter 5 attempted to estimate the missing values in multidimensional measurements of power transformers to facilitate the maintenance decision. To assess the condition and take maintenance decisions for a transformer, experts normally group the discrete measurements of it into a vector to observe the variation of different measurements over time. Often technical issues and limited operational budget cause utilities to omit some of the measurements rendering the vectors incomplete and hence unusable. However, some of the dimensions in the measured vectors are often inter-related and partially duplicate the missing information necessary for decision making. Therefore, to estimate missing values, the interpolation property of a General Regression Neural Network (GRNN) was used. The GRNN determined the missing values based on the knowledge of other complete sets of vector measurements. The performance of the model was verified against a set of vectors by deliberately leaving off some of their dimensions to mimic actual missing values. From a comparative analysis of the deliberately obscured data, it was found that the GRNN model was capable of estimating missing values with less than 7% average error. Only in a few cases, did the errors exceeded 10%, due to the discontinuity of the training examples in the high dimensional space where they were located. The performance of the model can be improved by using well-distributed

training examples that can help to develop a smooth continuous GRNN function. By estimating missing values, incomplete vectors can be rectified allowing them to be utilized for fault diagnosis and health index methods (as discussed in other chapters). Although the estimated missing values of a vector do not provide any new information to the model, the other complete dimensions, based on real measurements, can be used to improve the performance of models. Moreover, it can help transformer experts to make better maintenance decisions by looking at the complete vector measurement.

Chapter 6 aimed to address the research objective related to a quantitative health index (HI) of power transformers from the correlation of oil characteristic measurements. In the existing linear approaches, the health index score is calculated using the weighted average of different measurements. Therefore, they are insensitive to any single measurement but critical to the operating condition of transformers. To overcome this drawback and quantify the operating condition of transformers using diagnostic measurements, the interpolation property of a GRNN was applied. The approach used the insulating oil test data to calculate a quantitative index. Four conditional categories of 30 transformers and their associated indices supplied by an asset-management and health assessment consulting company (AMHA) were used as a target value for this method. A training set of 4096 conditional scores was developed using the four conditional limit values of six oil test data following the IEEE Standard C57.106. Finally, the HI score was calculated by mapping the oil test vectors with 4096 combinations using an interpolated multivariate GRNN mapping. The single bandwidth parameter of the model was estimated using an experimental search such that the mean square error between the target and estimated value was minimized. The performance of the model was compared with three other methods: AMHA, Fuzzy Logic, and Binary Logistic Regression and it was found to out-perform the other methods in condition assessment of transformers. Moreover, the new method was used to calculate the HI core of 345 power transformers operated by an Australian utility company. A comparative study against the utility expert's health index was also presented in this section. The method agreed in 83% of cases with the

expert's decision to classify the conditional category of transformers. However, experts used an additional 13 measurements that were not seen by the proposed method, resulting in disagreement with them in some cases. As a faulty bushing or tap changer can lead to the catastrophic failure of a transformer, it is also important to include their condition in any HI calculation. Therefore, the results highlighted the necessity of further investigation to improve the performance of the model.

Finally, Chapter 7 presented as an extended method for calculating a quantitative health index to characterize the condition of operating power transformers. The objective of this section was to assess the individual subsystem and explore the correlation between quantified health index and the probability of failure as a function of operating age in years. The proposed method was based on analysis of multiple (possibly correlated) test measurements associated with each subsystem of the device and was shown to be very sensitive to a poor performance, even of a single subsystem. For proper function, all the subsystems of a transformer must simultaneously operate correctly. To calculate the HI, initially the condition of each subsystem was assessed using a GRNN mapping derived from a training set, which is the novelty of this approach never applied by others. The training set was developed from the combination of IEEE, IEC and CIGRE guidelines on measurements that classify the four conditional categories of transformer subsystems. The calculated HI score for each subsystem were then combined in a sensitive "multiplicative" way, such that if any one of its subsystems was found to be faulty, then the whole transformer would be considered as unhealthy. Unlike the conventional linear approach, this method did not apply any premature quantization that could throw away valuable information at an early stage of processing. Additionally, compared to other nonlinear artificial intelligence directions, the method avoided the estimation of large sets of model parameters, following a largely non-parametric approach. Moreover, the method used the Weibull distribution to estimate the failure probability of any individual transformer. The primary outcome of the integration of Weibull distribution was the expected percentage failure rate of each transformer over the coming year. As the utility experts are very cautious allowing suspect

transformers to remain in service to avoid possible catastrophic failure and subsequent consequences, there is huge scarcity of faulty transformer data. Therefore, the performance of the method was validated by systematically exploring the statistical evidence. The secondary evidence proved that the method performs better than established approaches on more challenging cases. Therefore, it is expected that this approach will provide a valuable tool for utilities to manage fleets of transformers while providing a methodical justification for asset replacement.

The objectives of the research were to resolve the asset management problem of power transformers and develop a decision support mechanism that can help experts in decision making. Relevant literature of this area has been critically reviewed to achieve the goals and underlined the strength and weakness of existing fault diagnosis and condition monitoring techniques. A comparative analysis of them is presented in the second chapter of this report. The proposed hybrid clustering approach introduced in the third section improved the fault detection and classification of transformers significantly. However, the method was found computationally expensive and was not suitable for online fault detection. To overcome the limitations, a non-parametric Parzen Window function was applied and found to offer a satisfactory solution. The quantified health index calculation approach forming chapters six and seven is capable of providing a valuable condition summary beyond what is readily detectable by using diagnostic measurements alone. The failure probability estimation for an individual power transformer based on its condition score is the core contribution of this research. Therefore, it is expected that the outcome of this study will contribute to the power transformer asset management and could be a source of reference point for future works.

## 8.2 Future Directions

The findings of this research suggest that the condition of each subsystem of a transformer shows distinctive performance characteristics before failure. These properties can be correlated with different operating conditions of transformers

including their loading pattern to estimate the degradation rate of their service life. In future, we plan to develop a model based on artificial intelligence that can predict the remaining service life of transformers at variable operational stresses and loads. I would also like to explore the influence of manufacturers and their design specifications on operating condition of transformers. Therefore, it would be possible to increase the service life of this valuable asset by adjusting its loading and reducing stress by introducing proper maintenance plan. Also, there are scopes to adjust the conditional boundaries (Very Good, Good, Moderate, Bad, Very Bad) of different diagnostic measurements as the IEEE, IEC and CIGRE standards are not always absolute, and there is some contradiction between each other. The boundary range can be adjusted with a large number of statistical evidence. Moreover, we would also like to validate our percentage of failure probability statistics (Chapter 7) against the historically recorded measurements of failed transformers.

# Appendix A

The results of six diagnostic tests of 30 arbitrarily numbered transformers used in section 6.5 are shown in Table A.1. Although this section was a part of Chapter 6 in the original published paper, to ensure a better flow of this thesis report, it has been relocated to the final appendix section.

**Table A.1:** Results of six diagnostic tests.

| Number | Water (ppm) | Acidity (mgKOH/g) | DBV (kV) | Dissipation Factor (%) | TDCG (ppm) | Furan (ppm) |
|---|---|---|---|---|---|---|
| 1 | 21.7 | 0.024 | 32.5 | 0.075 | 483 | 0.86 |
| 2 | 26.9 | 0.098 | **40.5** | **0.894** | 254 | **0.65** |
| 3 | 14.5 | 0.033 | 58 | 0.14 | 78 | 0.26 |
| 4 | 21.2 | 0.226 | 48.7 | 0.424 | 215 | 5.53 |
| 5 | 10 | 0.01 | 75 | 0.111 | 126 | 0.06 |
| 6 | 15.5 | 0.075 | 71 | 0.143 | 38 | 0.53 |
| 7 | 16.8 | 0.167 | 70.1 | 0.255 | 149 | 0.78 |
| 8 | 15 | 0.092 | 67.8 | 0.211 | 28 | 0.69 |
| 9 | 17 | 0.035 | 62.7 | 0.113 | 9 | 0.21 |
| 10 | 30 | 0.088 | **37.6** | **0.353** | 197 | **0.31** |
| 11 | 16.2 | 0.181 | 25.5 | 0.201 | 35 | 8.76 |
| 12 | 15 | 0.155 | 37.5 | 0.182 | 53 | 7.29 |
| 13 | 16.8 | 0.115 | 25.6 | 0.174 | 78 | 9.6 |
| 14 | 15 | 0.21 | 57 | 0.22 | 53 | 6.69 |
| 15 | 27.6 | 0.089 | 30.4 | 0.128 | 336 | 5.12 |
| 16 | 23.5 | 0.106 | 45.8 | 0.207 | 30 | 0.24 |
| 17 | 24.8 | 0.012 | 29.9 | 0.068 | 504 | 1.68 |
| 18 | 23.6 | 0.07 | 39.2 | 0.203 | 22 | 0.5 |
| 19 | 30.5 | 0.073 | 28.7 | 67 | 30 | 1.7 |
| 20 | 18.4 | 0.063 | 64.5 | 0.243 | 69 | 0.15 |
| 21 | 21.1 | 0.019 | 28.4 | 0.025 | 144 | 0.02 |
| 22 | 8.1 | 0.01 | 66.9 | 0.042 | 71 | 0.05 |
| 23 | 19.6 | 0.216 | 41.1 | 0.264 | 48 | 7.54 |
| 24 | 6 | 0.01 | 67.6 | 0.126 | 427 | 0.08 |
| 25 | 18.4 | 0.152 | 37.2 | 0.299 | 81 | 1.14 |
| 26 | 11.1 | 0.032 | 67.2 | 0.089 | 119 | 0.04 |
| 27 | 21.5 | **0.147** | 60.8 | **0.938** | 168 | **0.92** |
| 28 | 7.5 | 0.16 | 70.1 | 0.448 | 10 | 0.06 |
| 29 | 13 | 0.091 | 51.6 | 0.369 | 8 | 0.32 |
| 30 | **35.7** | **0.229** | **41.4** | **0.639** | 24 | **1.07** |